NASA CR-145034

TECHNICAL AND ECONOMIC

ASSESSMENT OF SPAN-DISTRIBUTED

LOADING CARGO AIRCRAFT CONCEPTS

By

William M. Johnston
John C. Muehlbauer
Roy R. Eudaily
Ben T. Farmer
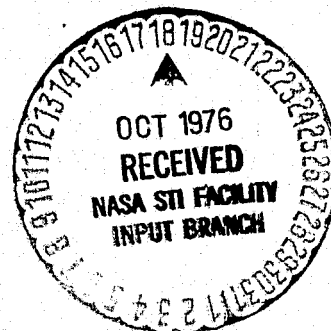John F. Honrath
Sterling G. Thompson

August 1976

By

THE LOCKHEED-GEORGIA COMPANY
A Division of the Lockheed Aircraft Corporation
Marietta, Georgia

For

NASA

National Aeronautics and
Space Administration

1. Report No. NASA CR-145034	2. Government Accession No.	3. Recipient's Catalog No.
4. Title and Subtitle Technical and Economic Assessment of Span-Distributed Loading Cargo Aircraft Concepts		5. Report Date August 1976
		6. Performing Organization Code
7. Author(s) William M. Johnston, John C. Muehlbauer, Roy R. Eudaily, Ben T. Farmer, John F. Honrath, Sterling G. Thompson		8. Performing Organization Report No. LG76ER0013
		10. Work Unit No.
9. Performing Organization Name and Address Lockheed-Georgia Company 86 South Cobb Drive Marietta, Georgia 30063		11. Contract or Grant No. NAS1-14383
		13. Type of Report and Period Covered Contractor Report – Final 26 March to 16 August 1976
12. Sponsoring Agency Name and Address National Aeronautics & Space Administration Washington, DC 20546		14. Sponsoring Agency Code

15. Supplementary Notes

16. Abstract

Studies were conducted to assess the technical feasibility and to evaluate the economics of a span-distributed loading aircraft relative to a conventional aircraft. A 700 000 kg (1 540 000-lb) aircraft with a cruise Mach number of 0.75 was found to be optimum for the specified mission parameters of a 272 155-kg (600 000-lb) payload, a 5560-km (3000-n.mi.) range, and an annual productivity of 113 billion revenue-ton km (67 billion revenue-ton n. mi.). The optimum 1990 technology level spanloader aircraft exhibited the minimum 15-year life-cycle costs, direct operating costs, and fuel consumption of all candidate versions.

Parametric variations of wing sweep angle, thickness ratio, rows of cargo, and cargo density were investigated. The optimum aircraft had two parallel rows of 2.44 x 2.44-m (8 x 8-ft) containerized cargo with a density of 160 kg/m^3 (10 lb/ft^3) carried throughout the entire 101-m (331-ft) span of the constant chord, 22-percent thick, supercritical wing. Additional containers or outsized equipment were carried in the 24.4-m (80-ft) long fuselage compartment preceding the wing. Six 284 000-N (64 000-lb) thrust engines were mounted beneath the 0.7-rad (40-deg) swept wing. Flight control was provided by a 36.6-m (120-ft) span canard surface mounted atop the forward fuselage, by rudders on the wingtip verticals and by outboard wing flaperons.

Benefits of the spanloaded aircraft relative to a conventional aircraft with identical mission capability are: 11.7-percent lower direct operating and 15-year life-cycle costs, 8.2-percent less fuel consumption, 20.8-percent lighter operating weight, and 10.4-percent smaller gross weight. Cargo loading and the 66.5-m (218-ft) main landing gear tread will pose potential airport compatibility problems.

17. Key Words (Suggested by Author(s)) Span-Distributed Loading Aircraft Spanloader Aircraft Innovative Aircraft Concepts Flying Wing Aircraft	18. Distribution Statement Unclassified – Unlimited		
19. Security Classif. (of this report) Unclassified	20. Security Classif. (of this page) Unclassified	21. No. of Pages 126	22. Price* $5.75

Page intentionally left blank

FOREWORD

The Lockheed-Georgia Company conducted a technical and economic assessment of span-distributed loading cargo aircraft concepts as part of its Independent Development Program. The approach, guidelines, and requirements outlined in NASA Request for Proposal 1-16-5603 provided the basis for the general plan followed in the Lockheed study. Several minor changes were made to the suggested guidelines, and some additional study tasks were undertaken.

Monthly reports were submitted to Allen H. Whitehead, Jr., NASA's Span-Distributed Loading Aircraft Studies Coordinator, to keep him informed of the latest progress on the Lockheed study. Several conferences, including mid-term and final presentations at the NASA-Langley facility on 23 October 1975 and 5 February 1976, respectively, were held to assure compatibility with the NASA efforts. Toward the end of the study, Lockheed and NASA agreed to make the results available in a NASA report to the general public. Funding to underwrite part of the cost of this publication was provided through Contract NAS1-14383.

William M. Johnston, the Study Manager, and his Deputy, John C. Muehlbauer, were responsible for the overall direction of this study which was performed as part of a continuing preliminary design investigation of new aircraft concepts by the Transport Design Department - Roy H. Lange, Manager. Roy R. Eudaily coordinated the overall structures effort; specific responsibilities were as follows: Michael C. Campion - Loads, Charles M. Jenness - Flutter, Lewis B. Lineberger - Stress, and R. Earnest Stephens - Weights. Ben T. Farmer fulfilled the design requirements, Sterling G. Thompson performed the economic analysis, and John F. Honrath directed the aerodynamic performance and parametric activities. Other contributors to this study included: S. R. Anthony, J. A. Bennett, D. N. Byrne, B. N. Crenshaw, H. V. Davis, Jr., R. S. Ferrill, O. M. Hayes, J. G. Hewell, Jr., J. D. Sowers, V. L. Turner, and F. M. Wilson, Jr.

Numbers contained in this report are in both SI and customary units, with the former stated first and the latter in parentheses. The principal dimensions and calculations were made in the customary system of units.

TABLE OF CONTENTS

LIST OF FIGURES

LIST OF FIGURES (Cont'd)

LIST OF FIGURES (Cont'd)

LIST OF TABLES

LIST OF TABLES (Cont'd)

SYMBOLS

AR	wing geometric aspect ratio
AR_{eff}	wing effective aspect ratio
b	wing span, m(ft)
C_D	drag coefficient
C_L	lift coefficient
C_l	section lift coefficient
DOC	direct operating cost ¢/T-km (¢/T-n.mi.)
E	modulus of elasticity, N/m^2 (psi)
EAS	equivalent air speed, m/s (kts)
EPNdB	effective perceived noise level, decibels
G	shear modulus of elasticity, N/m^2 (psi)
h	height of vertical end plate, m(ft)
I	moment of inertia, m^4 (in^4)
J	polar moment of inertia, m^4(in^4)
M	Mach number
M_C	cruise Mach number
M_D	dive Mach number
MAC	mean aerodynamic chord, m(ft)
OWE	operating weight empty, kg(lb)
SFC	specific fuel consumption, kg/N-hr(lb/lb-hr)
T/C	streamwise thickness-to-chord ratio
T/C_n	thickness-to-chord ratio normal to leading edge
$\bar{t}$	average equivalent wing cover thickness, m (in)
V_C	cruise speed, m/s(kts)
V_D	dive speed, m/s(kts)
W_u	wing weight, kg/m^2(lb/ft^2)
W/S	wing loading, N/m^2(psf)
X/C	chord position
Λ	sweep angle, rad (deg)
ξ	damping ratio
ω_n	frequency, rad/s

SUMMARY

Parametric analyses and design refinement studies were conducted to assess the technical feasibility of a span-distributed loading aircraft concept and to evaluate the performance and economics of this concept relative to a competitive fuselage-loaded conventional aircraft. The design mission for both aircraft was to carry a 272 155 kg (600 000 lb) payload over a range of 5560 km (3000 n.mi.) and to provide an annual fleet productivity of 113 billion revenue-ton km (67 billion revenue-ton n.mi.). Additional items of commonality between the two aircraft included equal cruise speeds and altitudes, identical economic operating factors, and the same 1990 technology levels of 60-percent composite materials, supercritical airfoils, and large-thrust engines.

Parametric variations considered to define the optimum span-loaded configuration included: 1 to 4 parallel rows of containerized cargo in the wing; wing sweep angles between 0 and 1.05 rad (60 deg); streamwise wing thickness-to-chord ratios of 15,20, and 25 percent; and cargo densities of 80, 160, and 240 kg/m^3 (5, 10, and 15 lb/ft^3). In addition to meeting the selection criterion of minimum 15-year life-cycle cost, the optimum configuration had the minimum direct operating cost and minimum fuel consumption of all candidate versions.

The refined optimum span-loaded aircraft is a 0.7 million kg (1.54 million lb) gross weight aircraft with a cruise Mach number of 0.75 and a wing sweep angle of 0.70 rad (40 deg). The aircraft carries two parallel rows of containerized cargo with a density of 160 kg/m^3 (10 lb/ft^3) throughout the entire 101 m (331 ft) span of the constant chord, 22-percent thick wing. Additional containers or outsized equipment are carried in the 24.4 m (80 ft) long fuselage cargo compartment which precedes the wing. Flight control is provided by a 36.6 m (120 ft) span canard surface mounted atop the forward fuselage, by rudders on the wingtip-mounted verticals, and by the outboard-wing flaperons. Six 284 000 N (64 000 lb) thrust engines and four 8-wheel main landing gears are mounted beneath the wing.

Benefits of the span-loaded aircraft relative to the conventional aircraft are: 11.7 percent lower direct operating cost and 15-year life-cycle cost, 8.2 percent less fuel consumption, 20.8 percent lighter operating weight, and 10.4 percent smaller gross weight. Cargo loading and the 66.5 m (218 ft) main landing gear tread width pose potential airport compatibility problems.

1.0 INTRODUCTION

Air cargo commands only that small portion of the total cargo transportation market for which the cost can be justified because of the value or perishability of the goods. To increase its share of the market, air freight must become cost-competitive with ground-based transportation systems.

Increased productivity, improved performance, and better economics have been the characteristics associated with the historical introduction of new cargo transports which have been responsible for achieving the present status of air freight. Several studies (Refs. 1, 2, and 3) have been made which indicate that further gains can accrue as aircraft grow in size and incorporate the latest advances in technology. However, Cleveland (Ref. 4) suggests that further improvements are likely to be attained in increasingly smaller increments until the next historical quantum jump occurs in aircraft capabilities, similar to that experienced with the introduction of the jet engine in the late 1950s.

Innovative design concepts may produce the quantum jump in aircraft characteristics required to increase substantially the share of the cargo market for air freight. Since 1966, the Lockheed-Georgia Company has maintained a continuing in-house effort in the conceptual and preliminary design of advanced transport configurations with the overall objective of improving the efficiency of aircraft as cargo carriers. In 1969 Lockheed developed its initial version of the Spanloaded aircraft (Refs. 5 and 6) which is named for the characteristic feature of having cargo loaded throughout the entire wing span. An artist's rendition of this concept is illustrated in Figure 1.
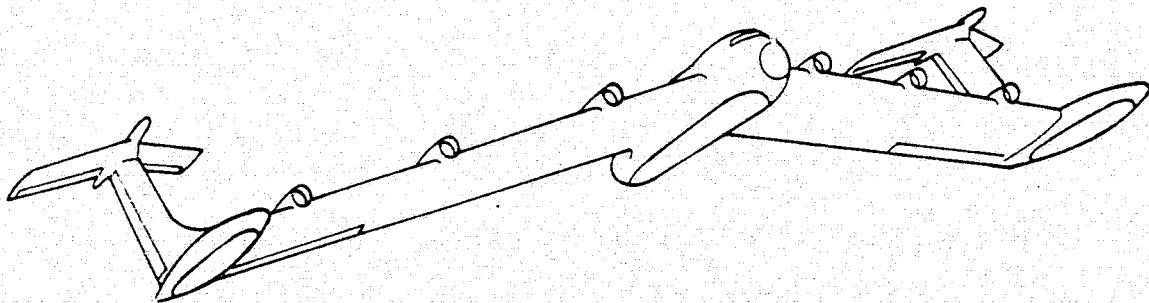
Figure 1. Original Spanloader Concept

The original point-design version of the Spanloader was envisioned as a 21st Century aircraft complete with an air cushion landing system and an integrated propulsion system imbedded in the wing. A simplified version of the Spanloader with conventional landing gear and pylon-mounted propulsion systems could conceivably attain operational status in the 1990s. The technical and economic merits of such an aircraft were investigated, as a part of the Lockheed-Georgia Company's Independent Research and Development Program and are reported herein. The NASA Span-Distributed Loading Aircraft Study Program (Ref. 7) served as a guideline for this Lockheed study, which included a parametric

analysis of various wing geometries and design refinements for the optimum configuration geometry. Economic and performance data for the span-loaded aircraft and for a competitive fuselage-loaded conventional aircraft provided the basis for the concluding assessments and recommendations presented in this report.

2.0 STUDY APPROACH

Contained in this section are the purpose and initial study guidelines for performing the subject study. Also, the overall study plan followed to achieve the objective is discussed.

2.1 STUDY OBJECTIVE

The objective of the study reported herein was to assess the technical feasibility of a span-distributed loading aircraft concept for future commercial air cargo operations and to evaluate the fuel and dollar economics relative to a competitive fuselage-loaded conventional aircraft.

2.2 STUDY GUIDELINES

Guidelines for this study were patterned after those of the NASA program (Ref. 7). Several changes were made to the guidelines during the study and are so noted, although the reasons for each change are reserved for later sections of the report. Assumptions were made, as required, to give quantitative definitions to general qualitative guidelines.

Initial study guidelines were the following:

Mission Constraints

o   Annual Productivity: 113 billion revenue-ton km
                         (67 billion revenue-ton m. mi.)

o   Range: 5560 km (3000 n.mi.)

o   Payload: 272 155 kg (600 000 lb)

Configuration Constraints

o   Payload to be containerized and non-bulk

o   Cargo containers: 2.44 m x 2.44 m (8 ft x 8 ft) cross-section

o   Oversized cargo carried in fuselage only

o   Fuselage cargo compartment dimensions: 4.1 m (13.5 ft) high by 5.2 m (17 ft)
                                            wide by 24.4 m (80 ft) long

o   Cargo compartment pressurization: 56 500 N/m^2 (8.2 psi)

3

o   Technology status: 1990 availability

o   Airport performance: 3660 m (12 000 ft) runway compatibility

Economic Constraints

o   Cost base: January 1, 1975

o   Annual utilization: 3000 hr. Changed to 4200 hr at study mid-point.

o   Load factor: 65 percent

o   Revenue tonnage: 91.8 percent of gross payload

o   Fuel price: 6.6 ¢/1 (25 ¢/gal). Changed to 9.8 ¢/1 (37 ¢/gal).

o   Crew size: 2 people. Changed to 3 people.

o   Production run: 350 aircraft. Ignored due to incompatibility with
                      productivity constraint.

Technologies projected to reach state-of-the-art status by 1990, and hence
available for application to the Spanloader aircraft, include supercritical airfoils,
advanced materials, and higher-thrust engines. Sufficient advances were assumed in
aerodynamic technology to produce an adequate data base for supercritical airfoils with
thickness-to-chord ratios up to 30 percent and with critical Mach numbers between
0.05 and 0.07 higher than for conventional airfoils.

The level of advanced material usage attainable by 1990 was assumed to represent
60 percent of the weight of an aircraft. Estimated values are shown in Table 1 for the
percentage of composites required for the various major components of an aircraft to
achieve the 60-percent overall value. Corresponding weight factors for the components
are expressed as a percentage of the weight of an all-aluminum aircraft.

Modified Pratt and Whitney STF-429 engines were assumed to have grown to a
310 000 N (70 000 lb) thrust level by 1990. Versions of these engines with a bypass
ratio of 4.5 were projected to have a specific fuel consumption value of 0.064 kg/N-hr
(0.63 lb/lb-hr) during cruise at 10 670 m (35 000 ft) altitude.

A listing of the established ranges of values for wing geometry and economic
variables has been relegated to Sections 3.1 and 5.0, respectively, to enhance the
continuity of those sections in which the parametric and sensitivity studies are discussed.

4

TABLE I. ADVANCED MATERIALS FACTORS

Component	Composite Weight, percent	Weight Factor, percent
Wing	70	80
Fuselage	60	78
Horizontal Tail	70	82
Vertical Tail	70	82
Nacelles	30	90
Landing Gear	0	100
Weighted Average	60	85

2.3 STUDY PLAN

The general approach followed in this study to accomplish the overall objective is illustrated in Figure 2. Numbers in the lower right-hand corner of each activity block on the study plan correspond to section numbers of this report.

Based on the study guidelines, a parametric analysis was conducted to evaluate the effect of variations in wing geometry on performance and costs of a span-loaded aircraft. The results of this analysis were used to select the optimum aircraft geometry for subsequent configuration refinement studies. Structural refinement studies included analyses of several load cases, a weight and balance check, and the solution of a critical flutter problem. In the area of aerodynamics, refinement studies were conducted to verify the drag estimate, to determine airport performance, and to investigate the stability and control of the aircraft. Design refinements studies included investigations of cargo loading, fuel tank volume and location in the wing, and landing gear placement and stowage.

Upon completion of the refinement studies and configuration evolution, economic studies were conducted to estimate the manufacturing and direct operating costs of the span-loaded aircraft concept. Cost sensitivities were determined for variations in purchase, maintenance, crew and fuel prices, as part of the economic analysis.

A conventional fuselage-loaded aircraft was designed consistent with the study guidelines to serve as a basis for comparing the technical and economic competitiveness of the span-loaded aircraft. Results from the comparison of the two aircraft concepts were responsible for many of the future study recommendations. Other recommendations were identified as a direct output from the various investigations performed during the parametric analysis and configuration refinement studies.

5
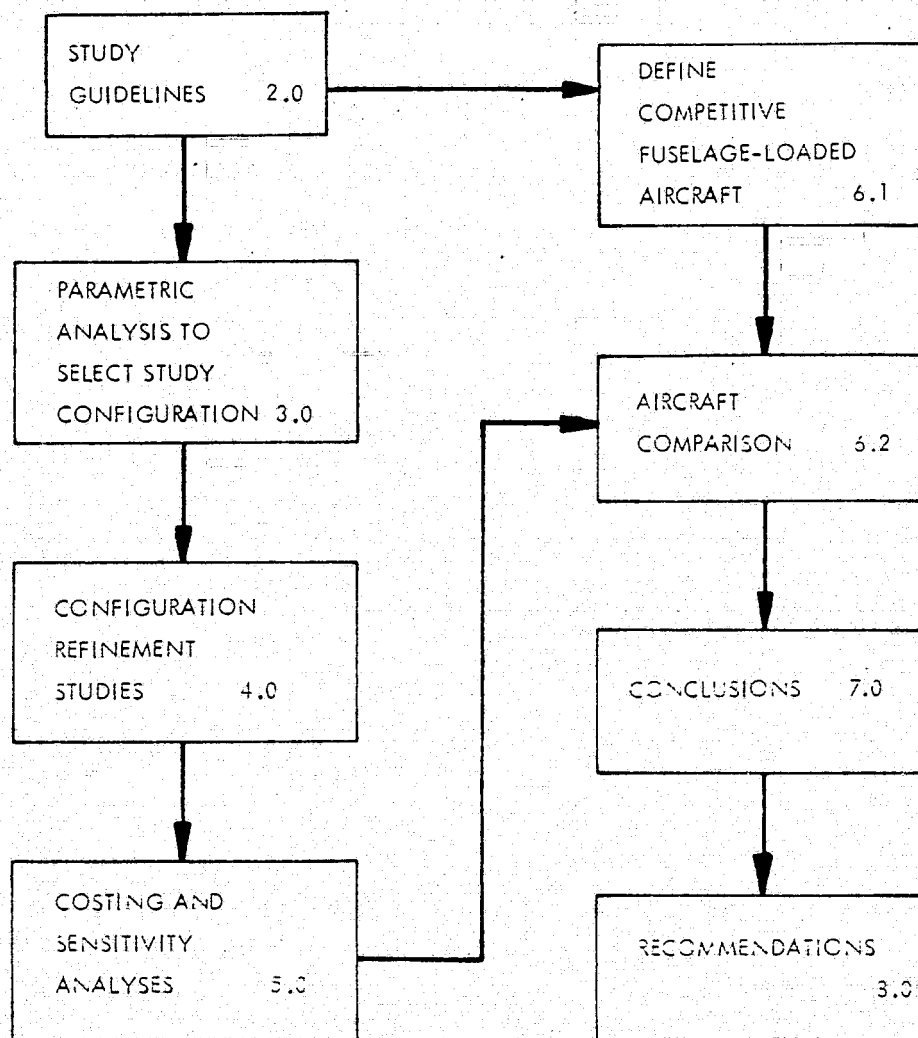
Figure 2. Study Plan

3.0 CONFIGURATION SELECTION ANALYSES

Optimum wing geometry characteristics for a span-loaded aircraft were selected based on the results of parametric design analyses. These analyses included a preliminary investigation of configuration layouts to establish and reduce the parametric matrix of candidate wing geometries. In addition, several baseline aircraft were developed, consistent with the design requirements for diverse points in the matrix, and analyzed to derive relationships for predicting weights and performance data for all of the candidate configurations in the parametric study. The approach followed in these analytical investigations and the rationale for selecting the optimum configuration for further refinement are described in this section.

3.1 PRELIMINARY CONFIGURATION ANALYSES

Initial analyses were directed toward defining the matrix of candidate geometries from which the optimum span-loaded aircraft was selected. Ranges of values are listed in Table II for the parametric variables that were considered to generate the study matrix. For each combination of parametric variable values, the minimum cargo compartment and wing sizes to accommodate the specified payload of 272 155 kg (600 000 lb) were fixed. Some of these candidate wing geometries proved to be impractical and were eliminated from further consideration. Detailed explanations are presented subsequently on the methodology used to generate the initial matrix of parametric study cases. Also, the rationale is discussed for the practical limitations adopted to reduce the parametric matrix.

TABLE II. PARAMETRIC STUDY VARIABLES

Payload Density	80, 160, 240 kg/m^3 (5, 10, 15 lb. ft^3)
Parallel Rows of Cargo in Wing	1, 2, 3, 4
Wing Sweep Angle	0, 0.35, 0.52, (0, 20, 30, 40, 0.70, 0.87, 50, 60 deg) 1.05 rad
Wing Thickness/Chord Ratio	15, 20, 25 percent

3.1.1 General Layout of Initial Study Configuration

Figure 3 shows the initial layout of the span-loaded aircraft concept analyzed in this study. This concept features the combination of a fuselage and a thick super-critical wing to accommodate the mission payload. Containerized and outsized cargo are transportable in the fuselage, but only containerized cargo, arranged in parallel rows extending for the entire span length of the wing, is carried inside the constant-chord, swept wing. Cargo loading is accomplished through doors located at each wing tip and through a nose visor door.
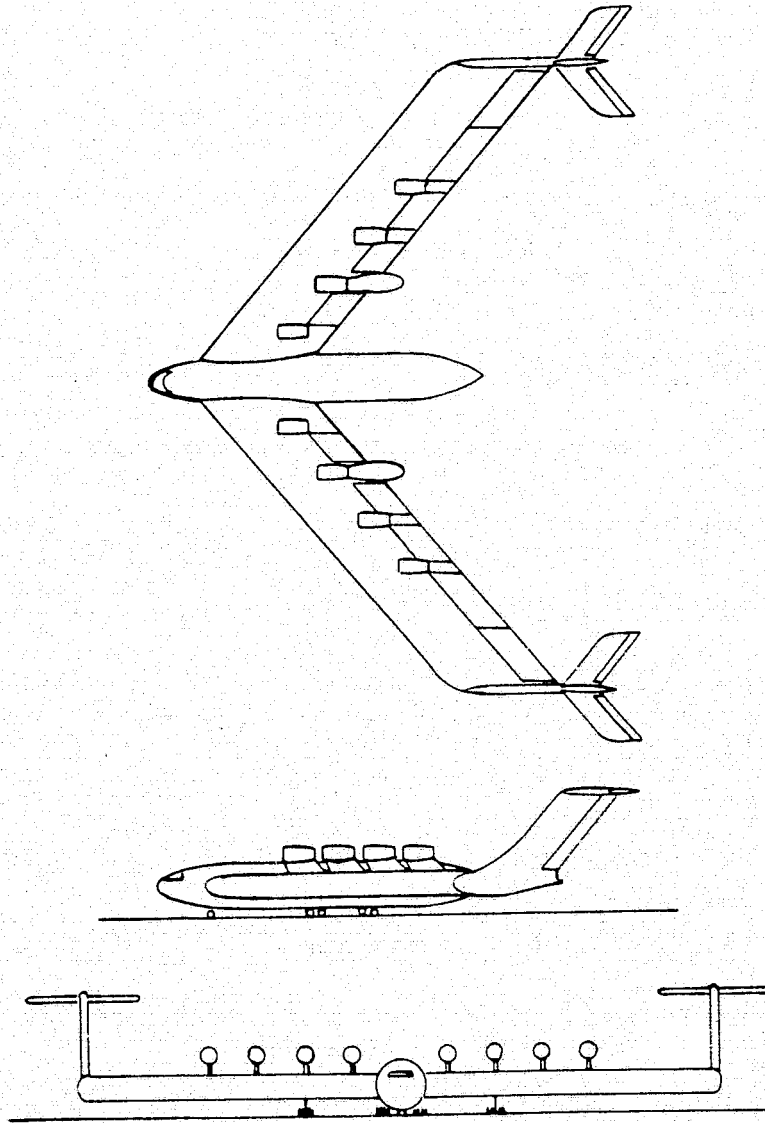
Figure 3. Initial Study Span-Loaded Aircraft

Other pertinent features of this initial configuration include conventional landing gear and eight modified Pratt & Whitney STF-429 engines mounted on pylons above the wing. Flight control is provided by the T-tail empennages mounted on each wing tip. The vertical portion of the empennage provides a secondary benefit by acting as a winglet which increases the effective aspect ratio of the wing and improves the overall aerodynamic performance.

3.1.2 Fuselage Sizing

Within the scope of this study, the intent was to investigate an aircraft configuration capable of satisfying both the civilian requirement to carry containerized cargo and the military need to transport some outsized equipment. Familiarity with military operations resulted in the decision to devise a cargo compartment design that would permit approximately 20 percent of the payload weight to be in the form of outsized equipment.

Candidate air-transportable items of large equipment from the military inventory are identified in Table III. Weights, overall dimensions, axle loads, and floor support running load requirements are presented for each item. The bridge launcher is the single item of equipment that established the maximum height requirement of 4.1 m (13.5 ft) and the maximum width requirement of 4.3 m (14.0 ft) for a cargo compartment cross-section to accommodate the entire inventory of air eligible equipment. The maximum running and axle loads of the equipment require a cargo floor and support structural weight of approximatey 34.2 kg/m^2 (7 lb/ft^2) per unit of floor area - about twice the floor structural weight for containerized cargo operation only.

A fuselage cargo compartment was deemed the best approach for accommodating the large overall dimensions and concentrated load distributions of the outsized equipment with the minimum weight penalty. Dimensions used throughout this study for the fuselage cargo compartment are shown on Figure 4.

Maximum commercial utilization of the fuselage cargo compartment dictated that the width be 5.2 m (17 ft) to provide minimal clearance while handling two rows of containers with 2.44 m by 2.44 m (8 ft by 8 ft) cross-sections. This width is more than adequate for the maximum outsized equipment width of 4.3 m (14 ft).

The cargo compartment length of 24.4 m (80 ft) was selected as a compromise to satisfy the requirements to carry both outsized equipment and containers. This length provides the capability to transport multiple numbers, or combinations, of 3.05, 6.1 or 12.2 m (10, 20 or 40 ft) long containers. Furthermore, this compartment length is consistent with the intent to transport approximately 20 percent of the payload weight in the fuselage, as suggested by military operations.

External dimensions of the fuselage enveloping the cargo compartment are defined by an upper radius of 3.4 m (11.1 ft) and a lower radius of 5.8 m (19.1 ft),

providing adequate depth for the cargo compartment floor and substructure and for the wing carry-through structure. At least 25.4 cm (10 in) are allotted at each corner of the cargo compartment to allow for fuselage structure.

TABLE III. AIR-TRANSPORTABLE MILITARY OUTSIZED EQUIPMENT CHARACTERISTICS

Heaviest Individual Load, kg (lb)	Recommended Minimum Dimensions, m (ft)		Running Load, kg/m (lb/ft)	Axle Load, No Shoring, kg (lb)
	Height	Width		
16 300 (36 000)	3.5 (11.5) Shopvan Truck	3.2 (10.5) Bridge Transport Truck	2 980 (2 000) Armored Personnel Carrier	⁻5 900 (13 000) 5T Wrecker
22 000 (48 500)	3.5 (11.5) Shopvan Truck	3.5 (11.5) M109 SP Howitzer	⁻7 450 (5 000) Light Tank Recon Vehicle	8 350 (18 400) 5T Fork Lift
50 000 (110 000)	3.5 (11.5) Shopvan Truck	⁻4.0 (13.0) M60 Tank	11 480 (7 700) M60 Tank	8 350 (18 400) 5T Forklift
55 500 (122 000)	⁻4.1 (13.5) Bridge Launcher	4.3 (14.0) Bridge Launcher	12 500 (8 400) Bridge Launcher	⁻15 250 (33 600) 20T Crane

⁻ Indicates item with heaviest load in each row.
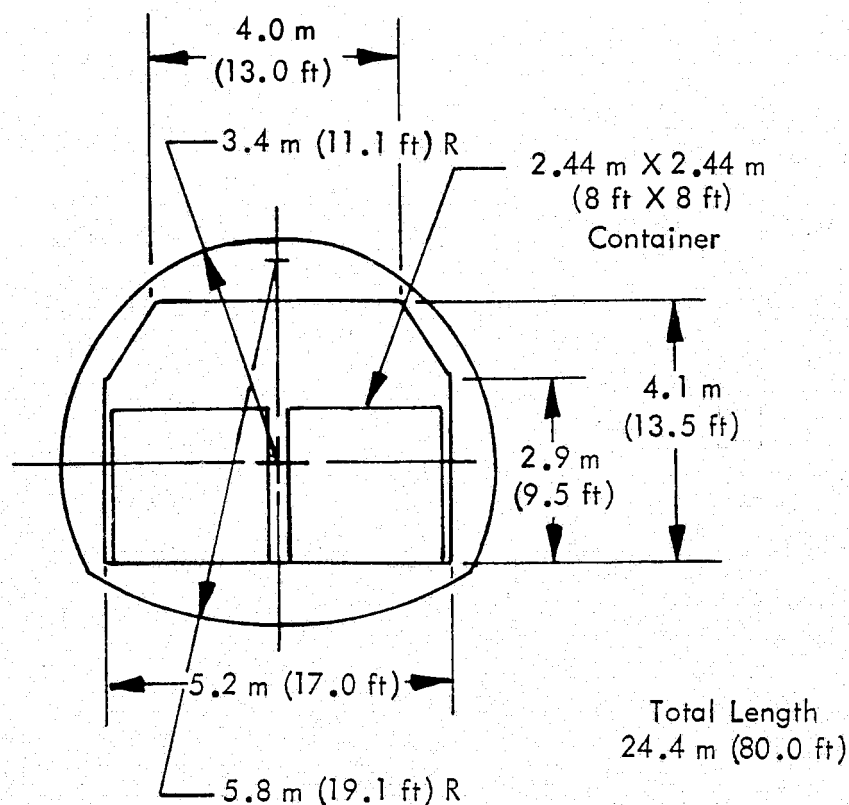
Figure 4. Fuselage Cargo Compartment Size

3.1.3 Wing Cargo-Box Sizing

All of the cargo carried in the wing of the aircraft is enclosed in containers with a cross-sectional area of 2.44 m by 2.44 m (8 ft by 8 ft). For commercial operations, the cargo in the fuselage is similarly containerized. Since the fuselage was sized, as discussed previously, for two 24.4 m (80 ft) rows of containers, the payload weight in the fuselage was fixed for a particular payload density value. Distributions of the 272 155 kg (600 000 lb) total payload between the fuselage and wing are itemized in Table IV for three density values of 80, 160, and 240 kg/m^3 (5, 10, and 15 lb/ft^3) considered in this study. Cargo boxes sized for the wing payload values derived in Table IV vary in cross-sectional areas and lengths as a function of the parametric study variables.

Derivation of the cross-sectional area allotted for each row of cargo containers in the wing was based on the arrangement depicted (not to scale) in Figure 5. Two 2.44 m by 2.44 m (8 ft by 8 ft) container cross-sections are shown with a minimal clearance of 7.6 cm (3 in) between each container and the adjacent structure. Including 7.6 cm (3 in) for the width of structure on each side of the containers, gives a total width of 2.74 m (9 ft) for each cargo row. The total width allotted for the wing cargo compartment is merely a multiple, equal to the number of cargo rows, of 2.74 m (9 ft). Thus,

11

TABLE IV. DETERMINATION OF WING PAYLOAD

Payload Density, kg/m^3 (lb/ft^3)	80 (5)	160 (10)	240 (15)
Total Payload, kg	272 155	272 155	272 155
lb	600 000	600 000	600 000
Fuselage Payload, kg	23 200	46 500	69 600
lb	51 200	102 400	153 600
Wing Payload, kg	249 000	226 000	202 500
lb	548 800	497 600	446 400
Wing Payload Length, m	523	237	142
ft	1 715.0	777.5	465.0

the wing cargo compartment is 11 m (36 ft) wide for four rows of cargo.

Minimum height of the wing cargo compartment is 2.6 m (8.5 ft). This value represents the sum of the 2.44 m (8 ft) container height and a minimal overhead clearance of 15.2 cm (6 in).

Length of the wing cargo compartment varies as a function of the payload density, the number of rows of cargo, the length of the individual containers, and the wing sweep angle. Table V shows the effect of the first three variables on the minimum length occupied by parallel rows of containers which satisfy the length requirement derived in Table IV for the wing payload. The lengths in Table V are based on an even number of containers per row. This recognizes that a balanced distribution of containers must be maintained about the fuselage centerline for a swept-wing aircraft, and that the center of a container cannot be located on the fuselage centerline.

Many of the sets of data in the matrix of Table V exhibit increases in total container row lengths as the individual container length increases from 3.05 to 6.1 or 12.2 m (10 to 20 or 40 ft). No attempt was made to investigate all of the ramifications concerning the potential desirability or beneficiality of the additional length of the larger containers. Instead, the decision was made to use only the smallest length for each case. A quick scan of Table V reveals that the 3.05 m (10 ft) long container exhibits the minimum total length per row realized in all cases for the three container lengths. Selection of the length derived for the 3.05 m (10 ft) container does not imply that the wing cargo box is limited to only 3.05 m (10 ft) containers. Both

12
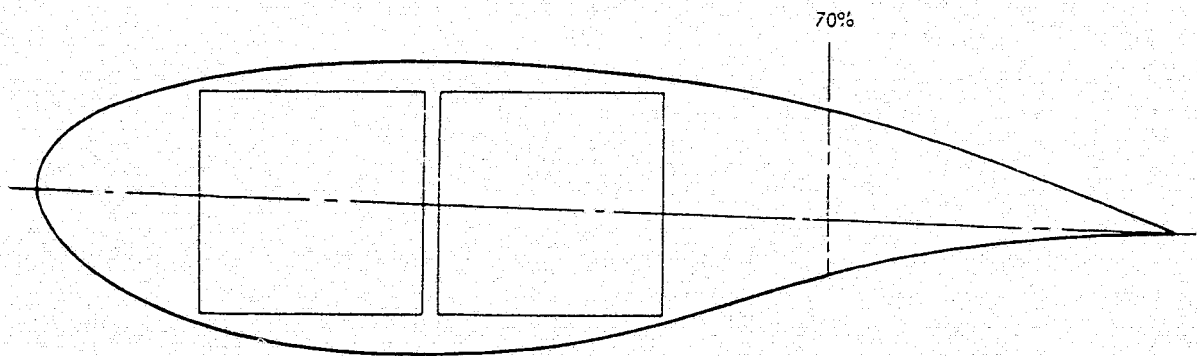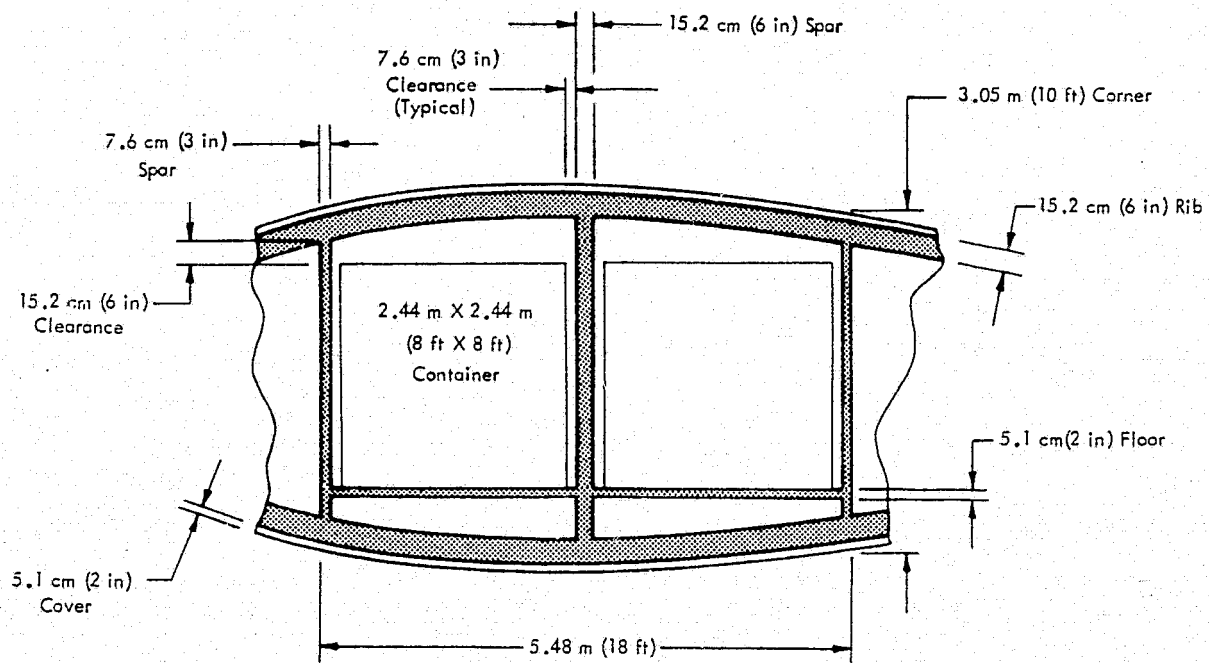
Figure 5. Wing Cargo Compartment Profile with Structural Allowances

TABLE V. MINIMUM LENGTHS OF WING CARGO ROWS

Cargo carried in 2.44 m by 2.44 m (8 ft by 8 ft) containers with lengths of 3.05/6.1/12.2 m (10/20/40 ft). Values in m (ft).

Number of Cargo Rows	Payload Density, kg/m^3 (lb/ft^3)		
	80 (5)	160 (10)	240 (15)
1	525/525/537 (1720/1720/1760)	238/244/244 (780/800/800)	146/146/146 (480/480/480)
2	262/268/268 (860/880/880)	122/122/122 (400/400/400)	73/73/73 (240/240/240)
3	177/183/195 (580/600/640)	79/85/98 (260/280/320)	49/49/49 (160/160/160)
4	134/134/146 (440/440/480)	61/61/73 (200/200/240)	37/37/49 (120/120/160)

6.1 and 12.2 m (20 and 40 ft) containers can also be transported. However, in some cases a mixture of containers with different length dimensions will be required to carry the total wing payload.

Additional space allowances were added to the wing cargo-box length as part of the wing span determination, which is discussed in Section 3.1.4. These allowances accounted for necessary clearances at the wing-tip cargo doors and for the effect of wing sweep.

3.1.4 Wing Sizing

Wings of conventional aircraft are characteristically sized by fuel volume requirements and aerodynamic considerations. For a span-distributed loading aircraft, the wing is sized by the cargo to be carried in it.

Each combination of parametric values considered in this study required that the wing airfoil be scaled to a size that would encompass the cross-sectional area of the wing cargo box. Similarly, the wing span in each case was sized to accommodate the length of the wing cargo box. In performing these sizing calculations, the intent was to determine the minimum acceptable chord and span dimensions of the wing for utilization in the remainder of this study. The wing aspect ratio, determined by combining these two dimensions, permitted the effects on wing geometry to be assessed for variations of all of the parametric variables.

14

All of the aircraft designed for specific points in the parametric matrix used scaled versions of a 21-percent-thick supercritical airfoil section designated LG5-621. This baseline airfoil has been defined and wind-tunnel-tested by Lockheed.

Each case in the parametric matrix required some scaling of the baseline airfoil to achieve both particular thickness-ratio values and sufficient size to enclose the wing cargo-box cross-section. In every case, the height of the airfoil at the corners of the cargo box was 3.05 m (10 ft). This value was the sum of the overall height of 2.6 m (8.5 ft), determined in Section 3.1.3, for the cargo box and the thicknesses shown on Figure 5 for the wing structures.

Minimum chord dimensions of scaled airfoils are presented in Figure 6 for all of the applicable parametric cases. Cargo density, which is the only study parametric variable not shown, does not affect the wing chord dimensions.

In addition to the chord length, the span length is the other significant dimension for describing wing geometry. With reference to Figure 7, observe that the minimum structural semi-span length exceeds one-half of the wing cargo-box length by the lengths allotted for the center walkway and wingtip cargo doors and by the length of unusable space resulting from the wing sweep angle. Lengths of 0.3 m (1 ft) and 1.83 m (6 ft) were allowed, respectively, for the center walkway and for each wingtip cargo door. By staggering the clearance spaces between containers, the total common length of unused space for all rows per side of the aircraft was computed as the product of the unit cargo compartment width of 2.74 m (9 ft) (see Section 3.1.3) and the tangent of the wing sweep angle.

As shown on Figure 7, the geometric span is a projection of the structural span, taking into account the wing sweep angle. Geometric span data for all applicable parametric cases are presented in Figure 8. Wing thickness-to-chord ratio, which is the only parametric variable not shown, does not affect the calculation of the minimum wing span.

3.1.5 Parametric Study Initial Matrix

Data on the minimum chord and span dimensions of the wing can be combined into a single descriptive parameter - aspect ratio - which shows the effects of variations in all of the parametric study variables. The resulting ratios of span-to-chord dimensions from Figures 8 and 6, respectively, are shown on Figure 9. This figure depicts the entire matrix of parametric study cases.

Cursory analysis of the candidate wing geometry data on Figures 6, 8, and 9 reveals the need for some practical limitations on wing dimensions. For example, wing spans up to 550 m (1800 ft) in length are unreasonable candidates. The span value that represents the upper practical limit is the subject of Section 3.1.6. Other limitations on wing geometries are discussed in Section 3.1.7.
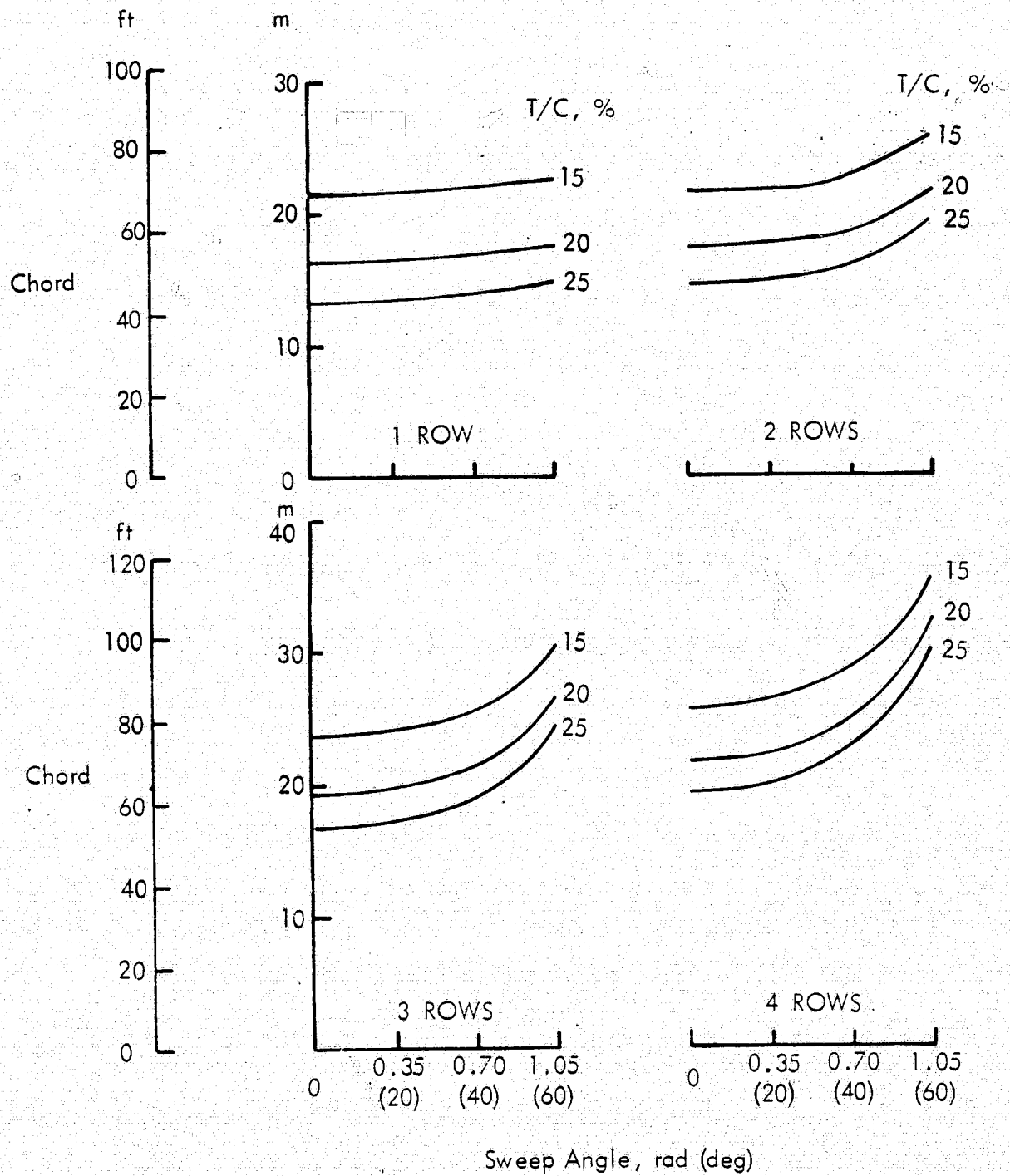
Figure 6. Parametric Study Cases - Chord Dimensions
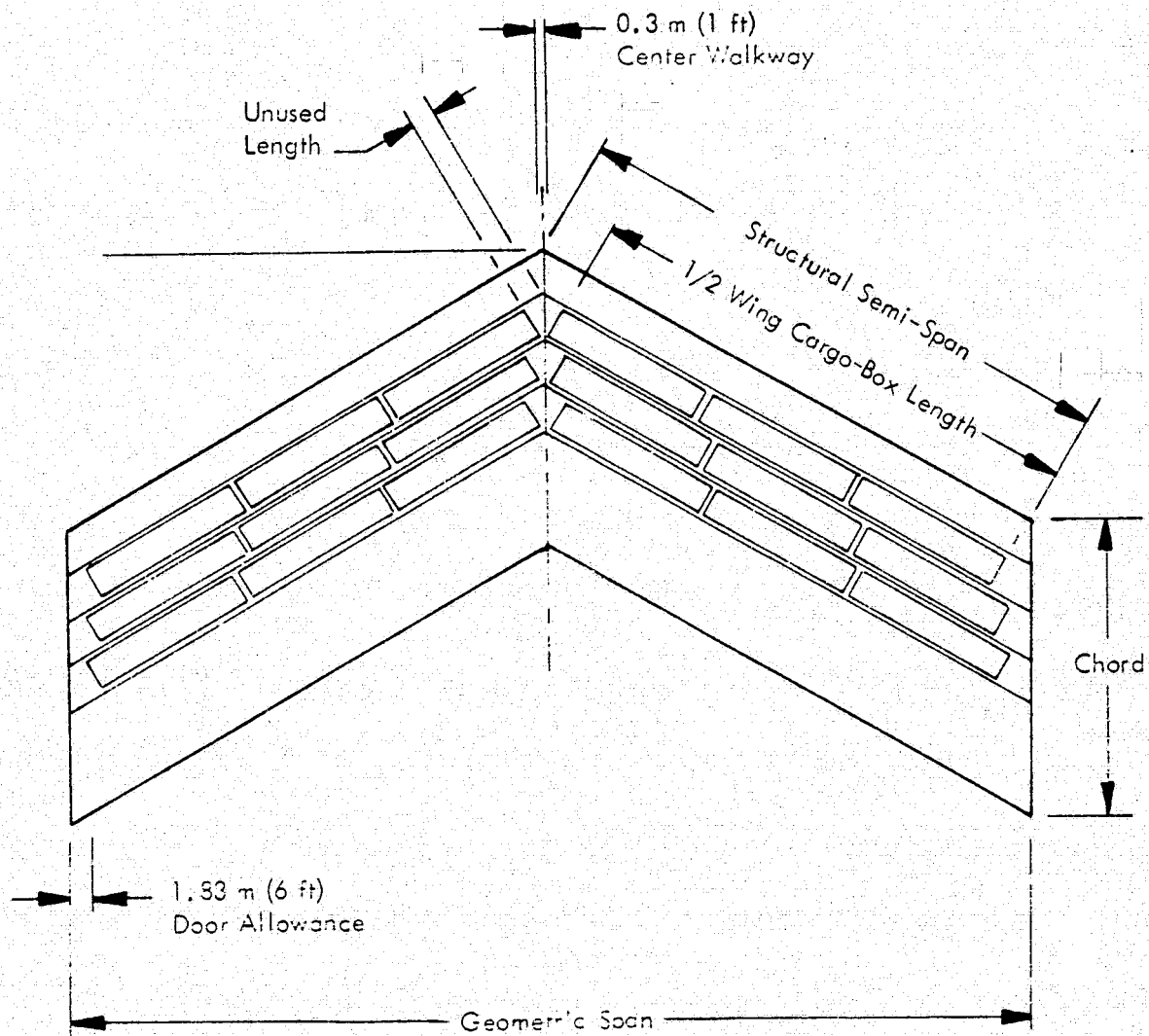
Figure 7. Minimum Span Determination Layout

3.1.6 Airport Constraints on Configuration Geometry

An important consideration in designing a new aircraft is its interface with existing and future airports. Major independent elements of an airport are runways, passenger and cargo facilities, and aircraft storage and servicing areas. These separate and distinct airport components are tied together by a taxiway system.

In this study, two of these elements - passenger and cargo facilities and aircraft storage and servicing areas - are not factors in the aircraft design. However, cargo facility compatibility is discussed in Sections 4.2.4 and 8.0. One of the guidelines in Section 2.2 requires the aircraft to operate from runways not exceeding 3660 m
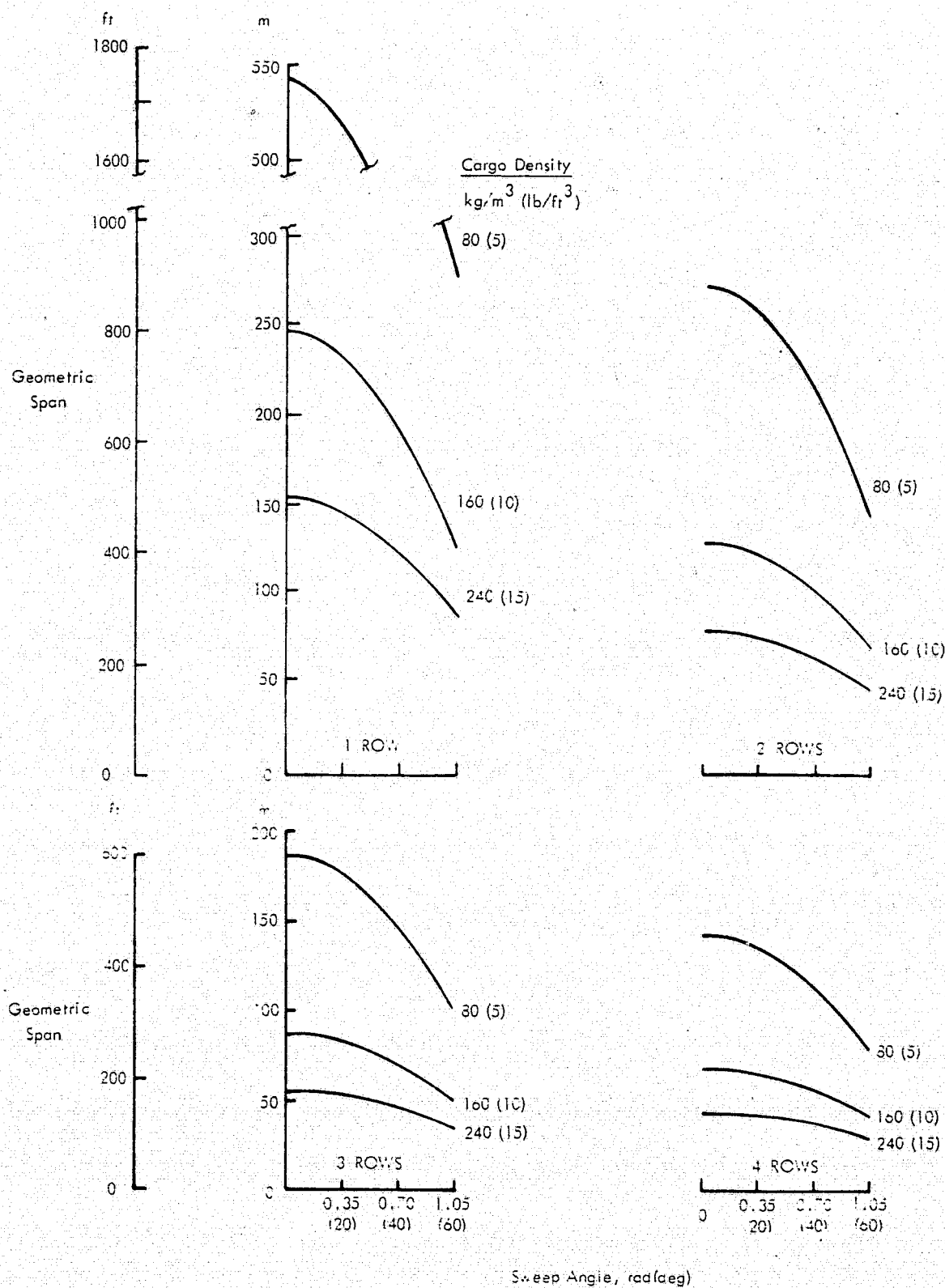
Figure 8. Parametric Study Cases - Span Dimensions
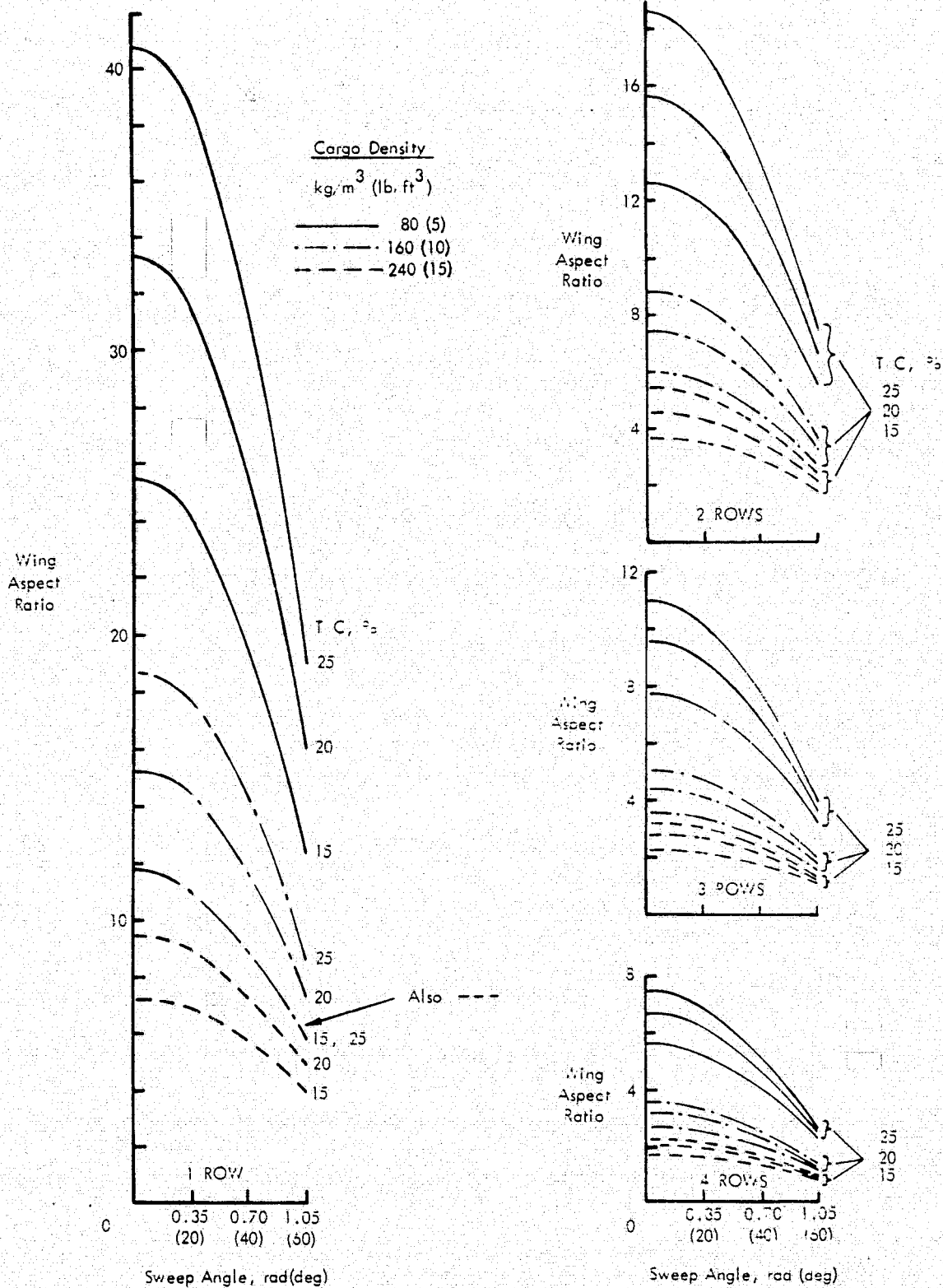
Figure 9. Parametric Study Matrix

(12 000 ft) in length. The 45.8 m (150 ft) runway width of most major airports does not impose any design constraint as long as existing and future taxiways widths remain in the range of 30.5 m to 38.2 m (100 to 125 ft). If increases in taxiway widths cannot be economically justified, then runway width becomes a constraining factor. As indicated by the data in the Appendix, a limited number of airports handling commercial traffic in the U. S. have runways exceeding 45.8 m (150 ft) in width. Both runway and taxiway dimensions of potential user airports impact span-loaded aircraft designs.

Analysis of airport taxiway design standards, prepared by the Federal Aviation Administration (Ref. 8), reveals limiting values which constrain the length of the wing span and the width of the landing gear tread. The derived wing span limitation for this study is based on the data listed in Table VI, as abstracted from Ref. 8. Some of the terminology used in the table is defined in Figure 10.

TABLE VI. TAXIWAY DIMENSIONAL CRITERIA

Design Item	Dimensional Criteria in m (ft) for Aircraft Taxiway Design Group	
	(B-747, L-500)	(Future)
1. Taxiway Structural Pavement Width on Straightaways	30.5 (100)	38.2 (125)
2. Taxiway Structural Pavement Width on Turns	35.2 (115)	42.8 (140)
3. Taxiway Shoulder Width	10.7 (35)	12.2 (40)
4. Safety Area Width	67.2 (220)	94.7 (310)
5. Taxiway Obstacle Free Area Width	111 (365)	143 (470)
6. Terminal Taxilane Obstacle Free Area Width	90.0 (295)	119 (390)
7. Recommended Wingtip to Obstacle Clearance	21.4 (70)	24.4 (80)
8. Wingspan	68.7 (225)	94.7 (310)
9. Landing Gear Pavement Edge Clearance	6.1 (20)	7.6 (25)
10. Undercarriage Width	18.3 (60)	22.9 (75)
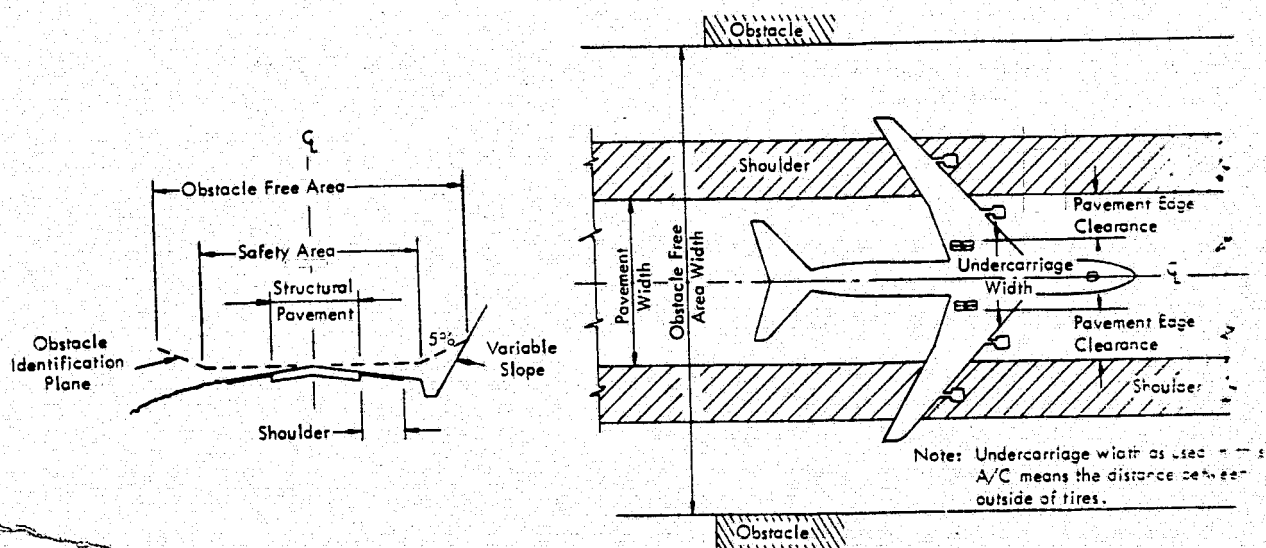
DEFINITIONS:

TAXIWAY - A defined path over which airplanes can taxi from one part of an airport to another. It includes the structural pavement, shoulder, taxiway safety area, and the obstacle free area. The taxiway drainage system, lighting, and marking are integral parts of the taxiway.

SHOULDER - An area abutting the edge of the taxiway structural pavement especially prepared to resist jet blast erosion and/or to accommodate maintenance equipment.

TAXIWAY SAFETY AREA - An area symmetrical about the taxiway centerline which includes the taxiway structural pavement and shoulders. The portion abutting the edges of the shoulder are cleared, drained, graded, and usually turfed and should be capable of supporting fire, crash, and snow removal equipment under normal conditions.

OBSTACLE FREE AREA - An area symmetrical about the taxiway centerline of specified width free of obstacles.

OBSTACLE IDENTIFICATION PLANE - An imaginary surface extending outward at zero slope from the centerline of the taxiway to the outer edge of the safety area and then continuing outward and upward at a slope of 5 percent.

OBSTACLE - Any fixed object, natural or man-made, including earth and rock, excluding visual and navigational aids, that protrudes through the obstacle identification plane.

Figure 10. Taxiway Layout and Terminology

21

Design item 8 from the table specifies a maximum wing span of 94.7 m (310 ft) for future aircraft. This dimension is derived from the guidelines suggested in design items 5 and 7. The taxiway obstacle-free area width of 143 m (470 ft) is reduced by twice the recommended wingtip-to-obstacle clearance of 24.4 m (80 ft) to achieve the 94.7 (310 ft) limit.

The recommended wingtip clearance of 24.4 m (80 ft) was deemed excessive for an aircraft concept that uses large wing spans to carry cargo efficiently. While there are no data to substantiate any alternate recommendation value, the following logic is offered as the basis for reducing the wingtip clearance.

It is anticipated that the pilot could maintain a large span-loaded aircraft within ± 3.05 m (10 ft) of the taxiway centerline during taxi maneuvers. Thus, a minimum wingtip clearance of 3.05 m (10 ft) is possible. In marginal cases, ground support personnel could accompany the aircraft to the runway and direct the pilot if any obstructions might be encountered which would damage the wing tip. By adopting 3.05 m (10 ft) for the wingtip-clearance value, wing spans up to 137 m (450 ft) are possible. This gives greater latitude in the number of cases that can be considered in the parametric study.

Design item 6 in Table VI specifies a terminal taxilane obstacle-free area width of 119 m (390 ft). This criterion was not implemented as a critical limitation for the wing span since special operating procedures could be adoped so that large aircraft are brought to the terminal area and are not taxied in most of the terminal area. Additional items noted in Table VI have applicability in establishing the landing gear tread-width limitation

The concept of span-distributed loading aircraft is to achieve a lighter weight vehicle by balancing the inertia loads of the cargo, fuel, and structure with the aerodynamic loads during cruise and with distributed landing gear loads during ground maneuvers. Limitations on the extent of landing gear spacing are imposed by the taxiway pavement width. As a result, balanced loads required by the span-distributed loading concept are not realized for large-span vehicles.

Criteria listed on Table VI provided the basis for establishing a landing gear width limitation. Specifically, design items 1, 9, and 10 from the table are pertinent. Item 10 recommends a maximum undercarriage width of 22.9 m (75 ft) for large aircraft of the future. This width was derived for the 38.2 m (125 ft) taxiway structural pavement width by providing 7.6 m (25 ft) of clearance from the landing gear wheels to the edge of the pavement on each side of the aircraft.

Following the logic expounded previously concering a pilot's ability to keep an aircraft close to the taxiway centerline during taxi operations, there is a basis for reducing the recommended 7.6 m (25 ft) of clearance. An undercarriage width

22

of 30.5 m (100 ft) is suggested as an alternate limit. This value provides a clearance of 3.8 m (12.5 ft) from the outer landing gear wheels to the edge of the pavement.

3.1.7 Aerodynamic Constraints on Configuration Geometry

Previous experience has shown that significant degradations in aerodynamic performance occur, and aircraft designs result that are far from optimum for some ranges of values for wing geometric characteristics. Two such characteristics are the wing aspect ratio and the wing thickness-to-chord ratio. Limitations have been placed on both of these ratios for this study.

Typically, subsonic aircraft today exhibit aspect-ratio values of five and higher. Designs with lower aspect-ratio values characteristically exhibit such a high induced drag that the configurations are unacceptable when evaluated by any of the usual standards of operating or life-cycle costs, fuel consumption, or weight. The very poor design cases in this study were eliminated by constraining the aspect ratio with a minimum value of three. Analysis of the remaining candidate designs in Section 3.3.3 confirmed that those cases with aspect ratios near the minimum constraint are not competitive with the selected configuration.

Another constraint imposed for this study was that the maximum thickness ratio normal to the leading edge, T/C_n, for the wing be limited to 30 percent. The thickness ratio normal to the leading edge is equivalent to the streamwise thickness-to-chord ratio divided by the cosine of the wing sweep angle. The reason for this constraint may be explained with the aid of Figure 11, taken from Ref. 9, which illustrates that large thickness-ratio values significantly increase the profile drag. At the 30-percent limit, the pressure drag produced by the high thickness-ratio value has increased the profile drag by 25 percent over the drag contribution from friction. With such increase in drag, performance levels are so poor as to be unacceptable. Analysis of the candidate designs in Section 3.3.3 confirmed that those cases with thickness ratios near the limit are not competitive with the selected configuration.

3.1.8 Parametric Study Matrix Reduction

Of the four constraints discussed in the preceding sections, three can be used to reduce the size of the parametric study matrix depicted in Section 3.1.5. These three constraints are itemized in Table VII. The fourth constraint on gear tread width is not applicable until individual aircraft designs are developed for each of the candidate points in the parametric matrix.

The initial matrix of parametric cases, shown previously on Figure 9, is repeated

23
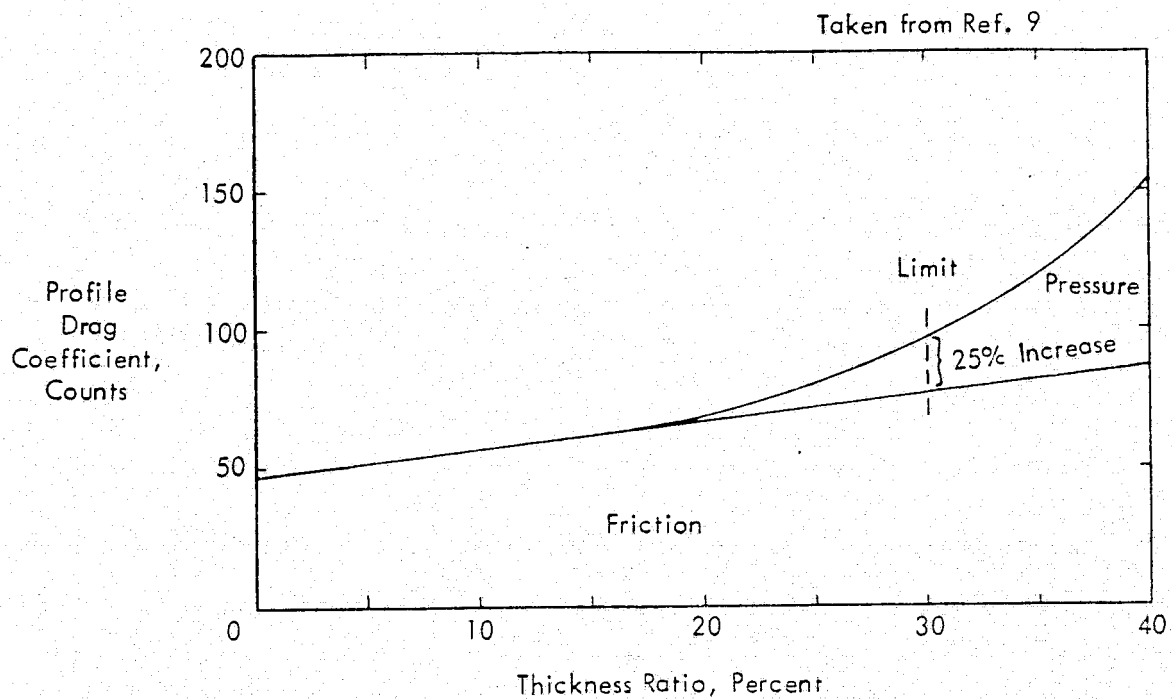
Figure 11. Thickness Ratio Limitation

TABLE VII. PARAMETRIC STUDY MATRIX GEOMETRIC LIMITATIONS

Maximum Wing Span	137 m (450 ft)
Minimum Geometric Aspect Ratio	3
Maximum Thickness Ratio Normal to Leading Edge	30°≥

in Figure 12 with the constraints of Table VII depicted. Points marked with an "x" were eliminated because the wing span exceeded 137 m (450 ft). The horizontal line across the figure shows the effect of the minimum aspect-ratio limitation of three. Triangles designate points which were eliminated as a result of the 30-percent maximum effective thickness-ratio limitation.

The reduced parametric matrix was composed of the remaining unmarked areas. Thus, the original matrix of 216 points was reduced to 68 points.

3.2 BASELINE CONFIGURATIONS AND ANALYSES

Prior to developing an aircraft design for each point in the reduced parametric matrix of Section 3.1.8, special design methodology was derived to handle the unique characteristics of a span-loaded aircraft. Simplified design approaches were used to produce several baseline configurations for further study. Subsequent analysis of these baseline configurations provided the necessary insight to enhance the sophistication of the design methodology.

3.2.1 Basic Data for Baseline Designs

Standard design criteria and data were used in the development of the baseline span-loaded aircraft. The data base and the pertinent criteria in the areas of structures and materials, aerodynamics, propulsion systems, and flight controls are reviewed under these area headings.

3.2.1.1 Structures and Materials

Basic structural design criteria were selected for use in determining the weights of the aircraft and in computing the structural loads, rigidity requirements, and sizes for each point-design case. Federal Aviation Regulations, Part 25, (FAR 25) (Ref. 10) served as a guide for the structural design criteria. The predominate requirements used in the structural analyses are listed in Table VIII.

In addition to the design criteria, certain assumptions were made concerning permissible stress levels in the structural materials. Aluminum alloys used in the wing box covers were 7475-T76 sheets and 7050-T76 extrusions. A maximum design stress level of 275.8 MN/m^2 (40 000 psi) was selected for these alloys to provide the necessary amount of damage tolerance and fatigue endurance. Composite materials used in the airframe structure were graphite-epoxy, type A, medium strength. Since composite materials have exhibited higher fatigue endurance stress levels than aluminum alloys, ultimate stress levels up to 413.7 MN/m^2 (60 000 psi) were assumed for the composite materials.

Pressurized shells were limited to 8.27 MN/m^2 (12 000 psi) stress level in both composite and aluminum materials at the operating cabin pressure of 56 500 N/m^2
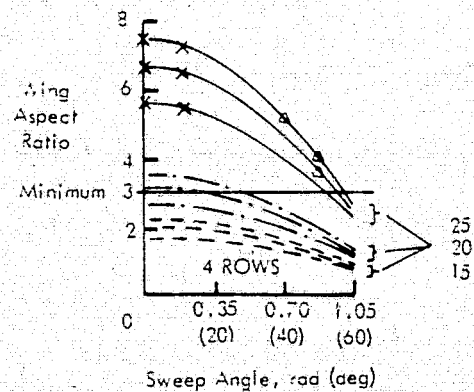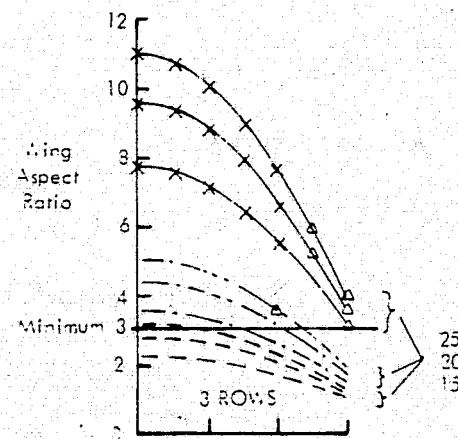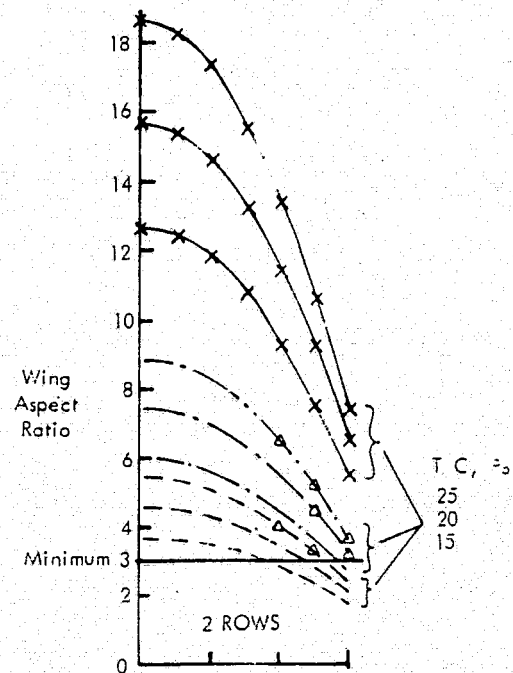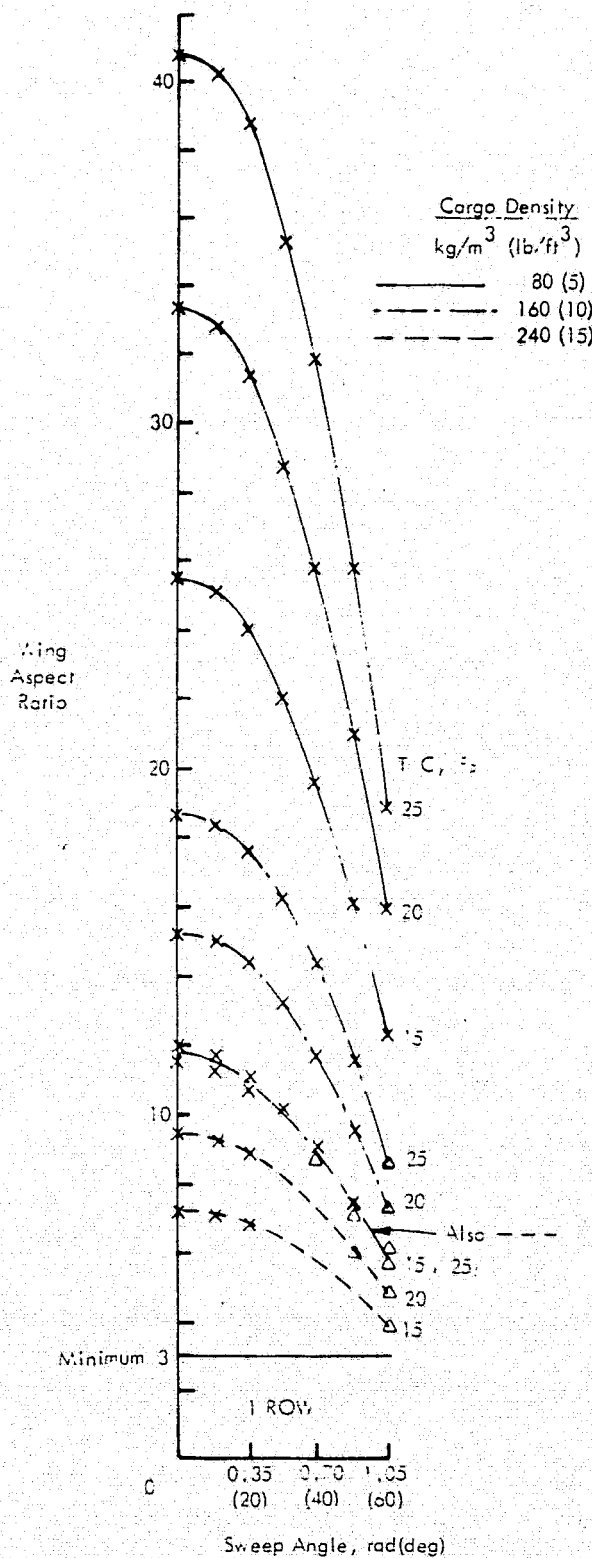
Figure 12. Reduction of Parametric Study Matrix

TABLE VIII. STRUCTURAL DESIGN CRITERIA

DESIGN SPEEDS

    o   Cruise, V_C/M_C 179 m/s (350 kts)/0.8

    o   Dive, V_D/M_D 210 m/s (410 kts)/0.9

LIMIT LOAD FACTORS

    o   Maneuver   -2.5 to -1.0 g's

    o   Landing & Taxi   ±1.5 g's

PAYLOAD DISTRIBUTION

    o   Wing   80 Percent

    o   Fuselage   20 Percent

CENTER OF GRAVITY RANGE

    20 to 30 Percent of MAC

CERTIFY TO FAR 25 WHERE APPLICABLE

(8.2 psi). This stress level has proven satisfactory for pressurized and compartment designs in numerous large transports. The derivation of this stress level value for aluminum materials was based on both fatigue and damage tolerant considerations. Use of the same stress level for composite materials may be conservative, but such an approach was dictated by the limited data base for designing damage tolerant shell structures with composite materials. While the results of the minimal number of tests conducted to date indicate that the crack propagation in composites is comparable with that in aluminum, a broader data base is required for picking a higher stress level.

3.2.1.2 Aerodynamics

The basic airfoil used in this study was previously defined and wind-tunnel-tested by Lockheed. The total thickness-ratio distribution for this 21-percent thick, cambered, supercritical airfoil is shown in Figure 13. Versions of the basic airfoil were scaled, as discussed in Section 3.1.4, to satisfy the parametric values for each design point in the matrix of candidate cases.

Variations in cruise Mach number and lift coefficient for the basic airfoil are shown in Figure 14 for two of the scaling variables - sweep angle and thickness ratio. These curves were derived to give maximum thickness ratio at a drag

27
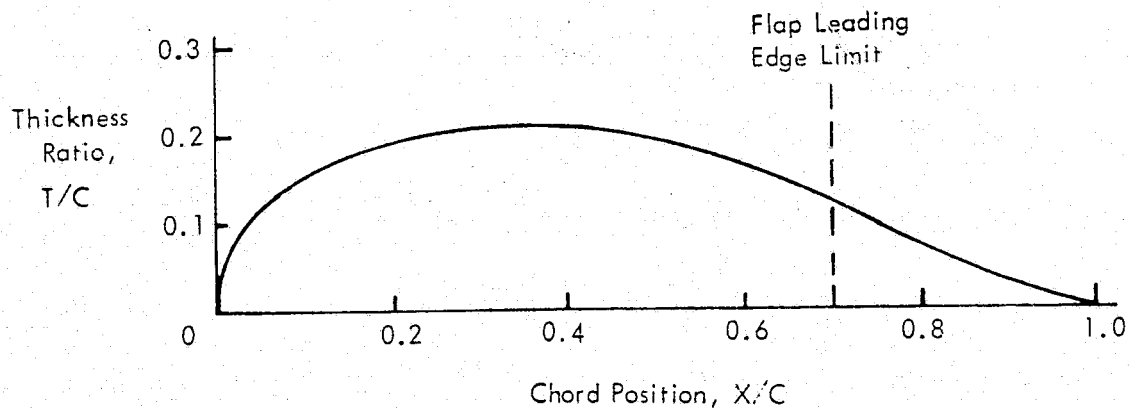
Figure 13. Thickness Ratio Distribution for Lockheed 21-Percent
Thick Supercritical Airfoil

rise of 10 counts. Two pertinent limitations are noted on Figure 14. One is the
30-percent maximum thickness ratio discussed earlier in Section 3.1.7. The other
limit to be considered is the section lift coefficient for which an optimistic value
of 1.0 has been used for illustrative purposes. Realistically, a section lift coefficient
value in the 0.7 to 0.8 range is better suited to the early 1990 time period, based on
current technology levels and efforts.

Performance levels projected for the swept-wing, span-loaded aircraft con-
cept are partially attributable to the end plating from the vertical surfaces of the
wingtip-mounted empennages. Hoemer (Ref. 9) has provided an equation for cal-
culating the effective wing aspect ratio, AR_{eff}, resulting from the end plating.
This equation is

$$AR_{eff} = AR(1.0 + 1.9\ h/b)$$

where   AR is the actual geometric aspect ratio of the wing,

                      h is the height of the vertical end plate, and

                      b is the wing span.

Drag characteristics of the aircraft were estimated on a component buildup
basis. The skin friction drag was determined for the wetted area and characteristic
Reynolds number for each component and was referenced to the aircraft wing area.
Appropriate shape factors were applied to the skin friction drag to obtain the profile
drag for each component. The sum of these component profile drags formed the
basic profile drag. Roughness and interference drag corrections, equal to 2 and 4
percent of the basic profile drag, respectively, were included. The trim drag
penalty was assumed to be 12 counts. The induced drag was calculated using an

28

$\Lambda = 0$ rad (0 deg)

$\Lambda = 0.35$ rad (20 deg)

Thickness-to-Chord Ratio, T/C

0.28
0.24
0.20
0.16
0.12
0.08
0.04
0.00

M 0.65 0.4 0.2 C_L
0.6
0.8
0.75
0.85

M 0.65 0.4 0.2 C_L
0.6
0.8
0.75
0.85

$\Lambda = 0.52$ rad (30 deg)

0.28
0.24
0.20
0.16
0.12
0.08

C_L
0.2
M 0.65 0.4
0.6
0.8
0.75
0.85
$T C_n = 0.3$
$C_l = 1.0$

$\Lambda = 0.70$ rad (40 deg)

M 0.65
0.75
0.6
0.8 0.85
0.2
0.4
C_L

$\Lambda = 0.87$ rad (50 deg)

0.20
0.16
0.12

0.4 C_L
M 0.75 0.6
0.8 0.85

$\Lambda = 1.05$ rad (60 deg)

M 0.65
0.75 0.6
0.85
0.8
0.4
C_L

Note that this entire
range is excluded by $C_l > 1$
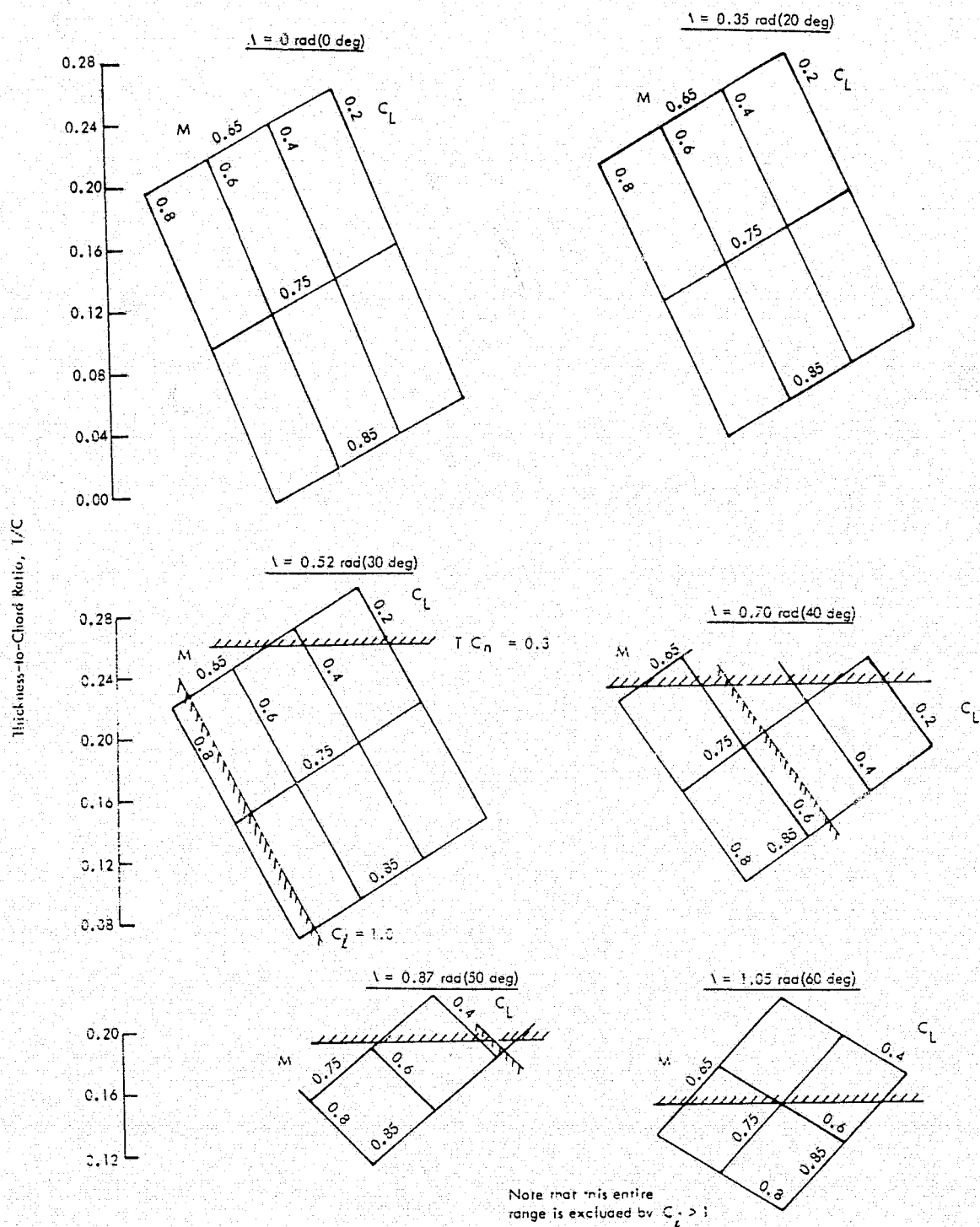
Figure 14. Allowable Lift, Mach Number, Sweep Angle Combinations

efficiency factor of 0.9 and the effective wing aspect ratio.

For a representative configuration with a 30-percent-chord flap, maximum lift coefficient values between 2.0 and 2.5 were judged to be achievable. Other characteristics assumed for the baseline designs are presented in Table IX. These estimates excluded the use of leading-edge devices which will be of small value because of the high wing thickness ratios typical of the span-loaded aircraft.

TABLE IX. EMPENNAGE GEOMETRIC CHARACTERISTICS SUMMARY

	Horizontal Tail	Vertical Tail
Aspect Ratio	3.0	1.5
Volume Coefficient	0.25	0.048
Sweep Angle, rad (deg)	0.7 (40)*	0.7 (40)*

*For wing sweep angles greater than 0.7 rad (40 deg), the empennage and wing sweep angles were equal.

3.2.1.3 Propulsion System

The propulsion characteristics used in this study were based on the parametric data for the Pratt & Whitney STF-429 engine concept which was devised to support the Advanced Technology Transport (ATT) Systems Study (Ref. 1). This engine was designed to achieve FAR 36 (Ref. 11) minus 10 EPNdB noise levels and minimum specific fuel consumption (SFC) at a cruise Mach number of 0.95.

Weights and data for the STF-429 engine were adjusted to account for anticipated improvements by 1995. Some of the improvements contained in the adjusted engine data of Table X reflect the benefits of a design cruise Mach number of 0.75 rather than 0.95.

TABLE X. STF-429 ENGINE ADJUSTED DATA

Bypass Ratio	Specific Fuel Consumption		Thrust-to-Weight Ratio	
	kg N-hr	lb lb-hr	N kg	lb lb
4.5	0.064	0.63	69.5	7.1
3.0	0.061	0.60	59.6	6.0

A cursory investigation of the effect of varying bypass ratio indicated that the extra weight associated with the large bypass-ratio engines exceeded the gains from improved specific fuel consumption and resulted in a poorer aircraft design. Performance improvements might result from using engines with a bypass ratio lower than 4.5; however, these performance gains would be accompanied by increased noise levels. Accordingly,

the engine with a bypass ratio of 4.5 was selected for use throughout the remainder of the study.

3.2.1.4 Flight Controls

Basic design criteria were selected for use in sizing the flight control surfaces. Military Specification MIL-F-8785B (Ref. 12) served as a guide in establishing criteria for the directional, lateral, and longitudinal flight controls.

The directional control system consisted of 25-percent-chord rudders on each wingtip-mounted vertical surface. The vertical surfaces were sized to provide adequate static directional stability and were located at the wingtips to increase the effective aspect ratio of the wing. The rudders were sized to provide adequate yaw control during cross-wind landings and critical engine-out cases.

The lateral control system consisted of fast-acting flaperons and spoilers on the outboard 30 percent of the wing span. These surfaces were designed to satisfy a roll performance requirement of 0.52 rad (30 deg) of bank in 4 seconds. This is a minimum requirement, but based on C-5 flight test experience, it results in adequate handling qualities.
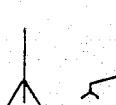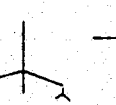
The longitudinal control system consisted of 25-percent-chord elevators on the horizontal surfaces of the wingtip-mounted T-tail empennages. The horizontal surfaces were designed to provide a stability margin of 5 percent at the most aft center-of-gravity position of 30 percent of the mean aerodynamic chord (MAC). Elevator size was selected to furnish adequate control for nose wheel lift-off and for free-air stall at the most forward center-of-gravity position of 20-percent MAC with high-lift devices deployed.

3.2.2 Baseline Configurations

Seven baseline configuration with widely differing wing geometries were developed using a constant weight of 48.8 kg/m^2 (10 psf) per unit of wing area. Characteristics of these baseline aircraft are listed in Table XI. Common features of all configuration are 272 155 kg (600 000 lb) payload, 5560 km (3000 n. mi.) range, 10 670 m (35 000 ft) cruise altitude, 8 engines, cargo doors at each wingtip, and a 24.4 m (80 ft) long fuselage cargo compartment that is 5.2 m (17 ft) wide and 4.1 m (13.5 ft) high.

The primary purpose for developing these baseline configuration was to provide typical wing planforms for structural analyses so that a relationship could be derived for estimating wing weights in subsequent parametric designs as a function of wing span, area, and sweep angle. The secondary purpose was to provide a variety of configurations to permit analysis of alternate fuselage locations relative to aircraft balance, of aircraft loadability and ground support equipment requirements, and

TABLE XI. BASELINE AIRCRAFT CHARACTERISTICS SUMMARY

Baseline Number	1	2	3	4	5	6	7
Wing Sweep, rad	0.70	0.70	0.70	0.70	1.05	0.35	0
deg	40	40	40	40	60	20	0
Cargo Rows	2	4	3	2	2	3	2
Cargo Density, kg/m^3	160	80	80	240	160	160	240
lb/ft^3	10	5	5	15	10	10	15
Thickness Ratio, %	19.5	20.4	20.9	16.4	17.2	19.4	19.9
Wing Span, m	101	110	143	32	70	80	77
ft	331	362	470	270	229	264	254
Aspect Ratio	5.6	4.8	7.3	3.1	3.0	4.1	4.5
Wing Loading, N/m^2	3610	2985	2705	5640	4610	4580	4759
lb/ft^2	75.5	62.5	56.6	118.0	96.5	95.8	107
Cruise Mach Number	0.75	0.75	0.75	0.75	0.85	0.70	0.70
Engine Thrust, 1000 N	224	288	274	351	32.6	295	281
1000 lb	50.5	64.7	61.6	79.0	73.3	66.4	63.2
Operating Weight, 1000 kg	228	293	304	230	265	246	215
1000 lb	502	646	671	506	584	542	474
Fuel Weight, 1000 kg	186	235	226	271	244	244	217
1000 lb	410	517	498	598	539	537	479
Gross Weight, 1000 kg	687	801	803	775	783	762	704
1000 lb	1512	1763	1769	1704	1723	1679	1553

Payload: 272 155 kg (600 000 lb)

Range: 5 560 km (3 000 n.mi.)

Cruise Altitude: 10 670 m (35 000 ft)

of the structural arrangement at the wing-fuselage intersection.

The first baseline aircraft, Figure 15, was configured with the entire fuselage cargo compartment positioned behind the carry-through structure of the wing cargo compartment. Access to the fuselage cargo compartment is provided by an aft door and an integral ramp.

Planforms for baseline configurations 2, 3, and 4 are presented in Figure 16. A common feature of these three configurations is the split-fuselage cargo compartment

32

Design Cargo Density - 160 kg/m^3 (10 lb/ft^3)
Number of Bays - 2 Per Side

0.7 rad
(40 deg)

20.4 m
(67 ft)

78 m (256 ft)

101 m (331 ft)
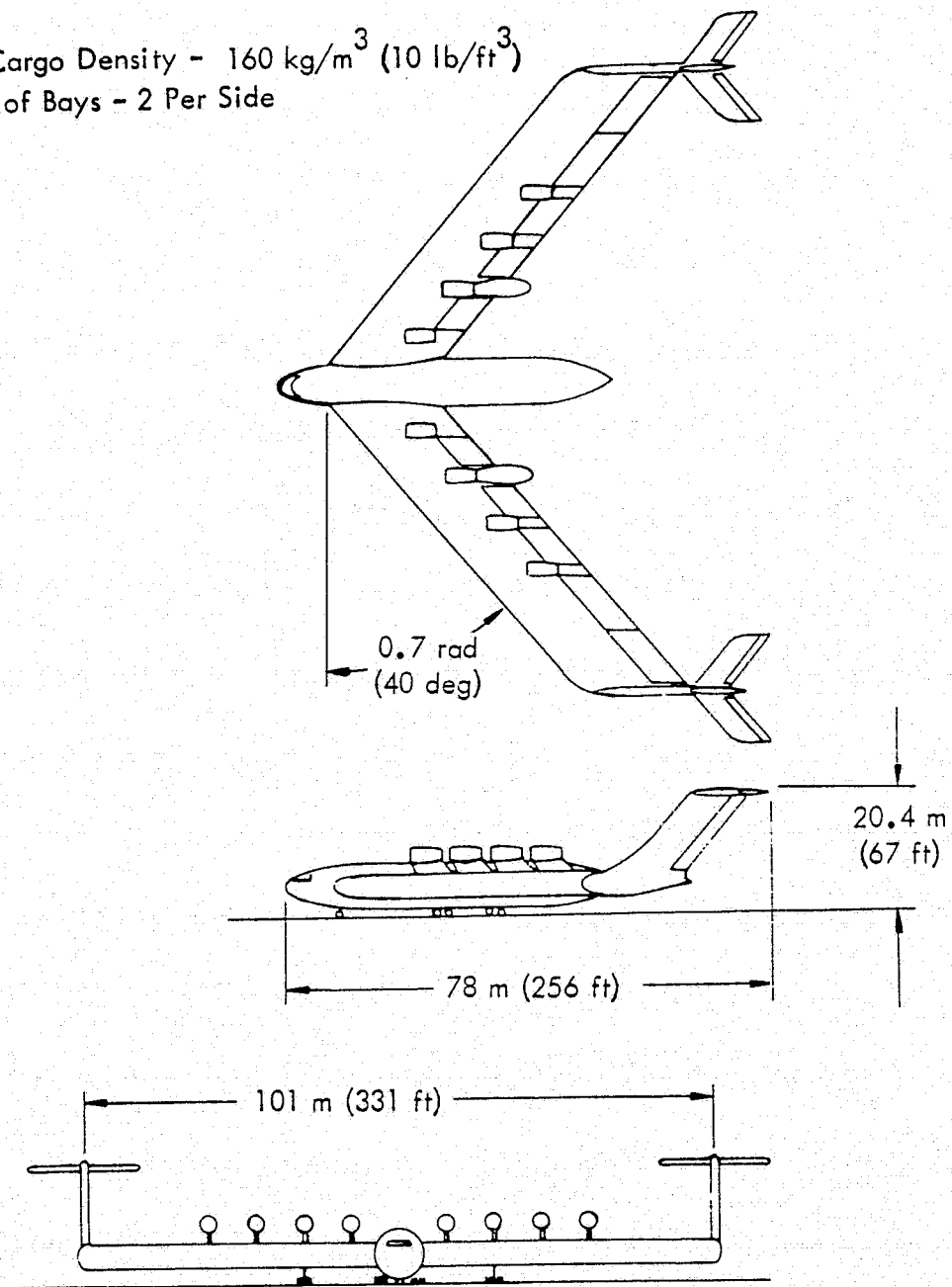
Figure 15. Baseline 1 Configuration

33

Baseline 2

Design Cargo Density – 80 kg/m³ (5 lb/ft³)
Number of Rows – 4 Per Side

101 m
(332 ft)

0.7 rad
(40 deg)

110 m
(362 ft)

22 m
(72 ft)

Baseline 3

Design Cargo Density –
80 kg/m³ (5 lb/ft³)
Number of Rows – 3 Per Side

0.7 rad
(40 deg)

143 m
(470 ft)

114 m
(374 ft)

20 m
(65 ft)

73 m
(240 ft)

Baseline 4

Design Cargo Density –
240 kg/m³ (15 lb/ft³)
Number of Rows – 2 Per Side

0.7 rad
(40 deg)

82 m
(270 ft)

18 m
(60 ft)
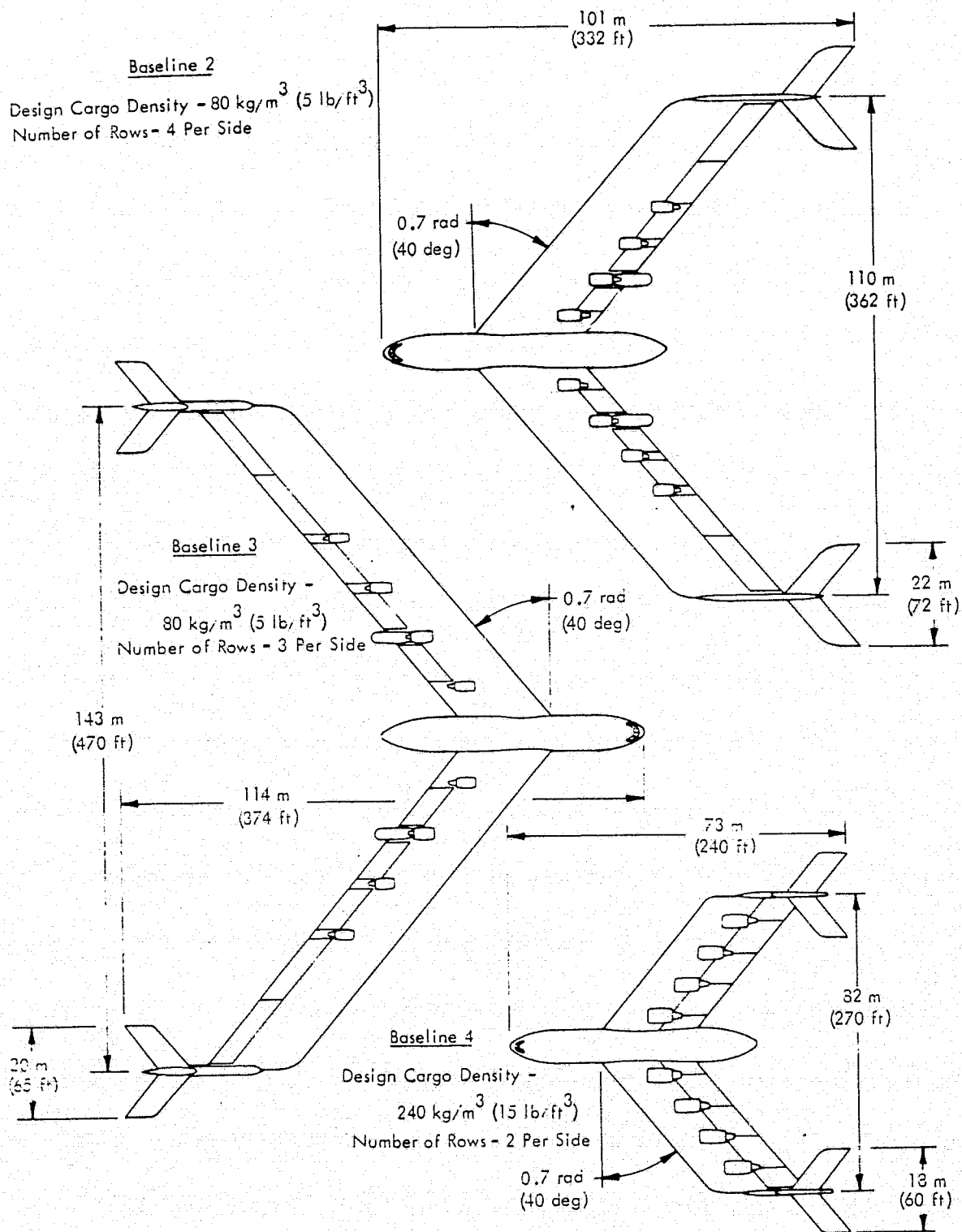
Figure 16. Planforms for Baseline 2, 3, and 4 Configurations

34

with equal portions on each side of the wing. Access to the fuselage cargo compartment is provided by a nose visor door and an aft door, each having an integral ramp. The split-fuselage concept embodied in these three configuration was rejected relative to the other configurations because of the additional structural weight penalty for the fourth cargo compartment door and additional ground facility requirements for cargo loading. Since the wing planforms for these three configurations were of interest for the wing weight analyses, the fuselages were shifted to positions behind the wing, similar to the Baseline 1 configuration, to achieve acceptable arrangements.

Planforms for baseline configurations 5 and 6 are shown in Figure 17. Both of these configurations have the fuselage cargo compartment in front of the wing. A nose visor door and an integral ramp provide access to the fuselage cargo compartment. Severe balance problems were encountered for these two configurations making them unacceptable. Since the wing planforms were of interest for the wing weight analyses, the fuselages were shifted to positions behind the wing, similar to the Baseline 1 configuration, to achieve acceptable arrangements.

For the 0 to 0.35 rad (0 to 20 deg) range of wing sweep angles, the short moment arm of the wingtip-mounted empennages precluded satisfactory longitudinal and directional control with control surfaces of reasonable size. This problem was overcome by positioning a single T-tail empennage on the aft fuselage for the Baseline 7 configuration shown in Figure 18. Baseline configurations 1 and 7 are similar in the wing and fuselage cargo compartment arrangements; the major configuration difference is the empennage location.

3.2.3 Analyses of Baseline Configurations

Structural and design analyses of the baseline configurations culminated in the definition of a new configuration for use in the parametric design study described in Section 3.3. As a result of the configuration changes, revisions were made in the approach for evaluating the aerodynamic performance. The types of studies that were conducted in each discipline area and the results which necessitated the configuration changes are described hereinafter.

3.2.3.1 Structural Analyses

Extensive structural analyses were performed to determine a parametric equation for estimating wing weight. The Baseline 1 configuration, shown previously in Figure 15, was selected for the initial analysis since this configuration exhibited the median values of the various wing geometry parameters under consideration. The first structural sizing was based on static, rigid airframe loads and an assumed wing weight of 48.8 kg/m^2 (10 psf). Eighty percent of the payload was distributed uniformly in

35

Design Cargo Density –
160 kg/m^3 (10 lb/ft^3)
Number of Rows – 2 Per Side

121 m
(398 ft)

70 m
(229 ft)

17 m
(57 ft)

1.05 rad
(60 deg)

Baseline 5

Design Cargo Density –
160 kg/m^3 (10 lo/ft^3)
Number of Rows – 3 Per Side

80 m
(263 ft)

30 m
(263 ft)

21 m
(68 ft)

0.35 rad
(20 deg)
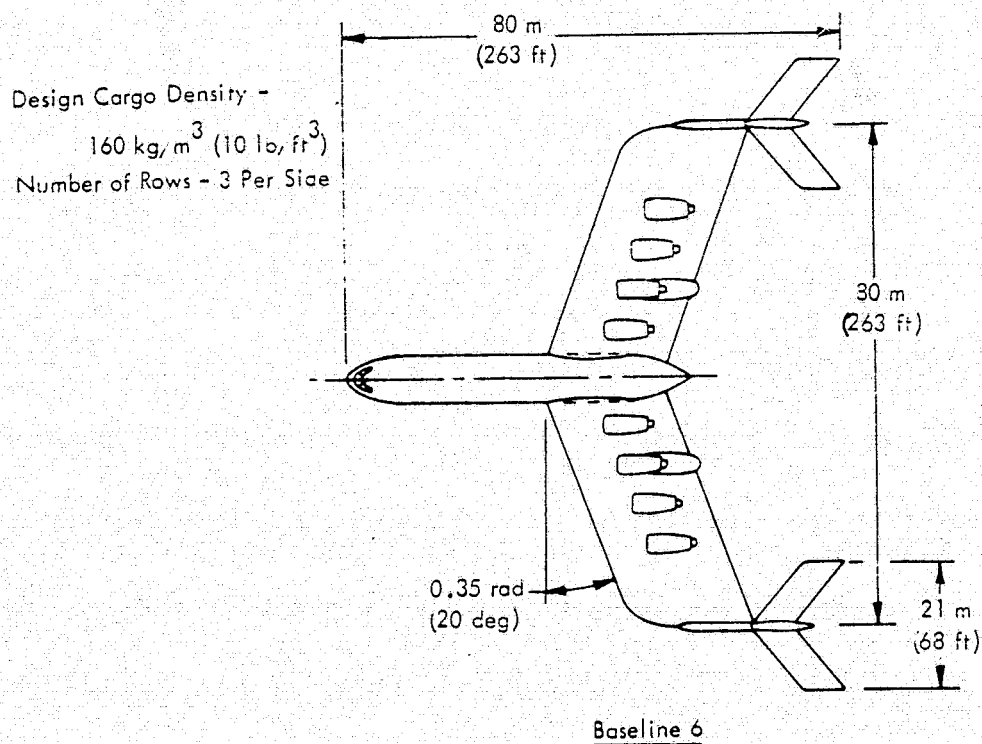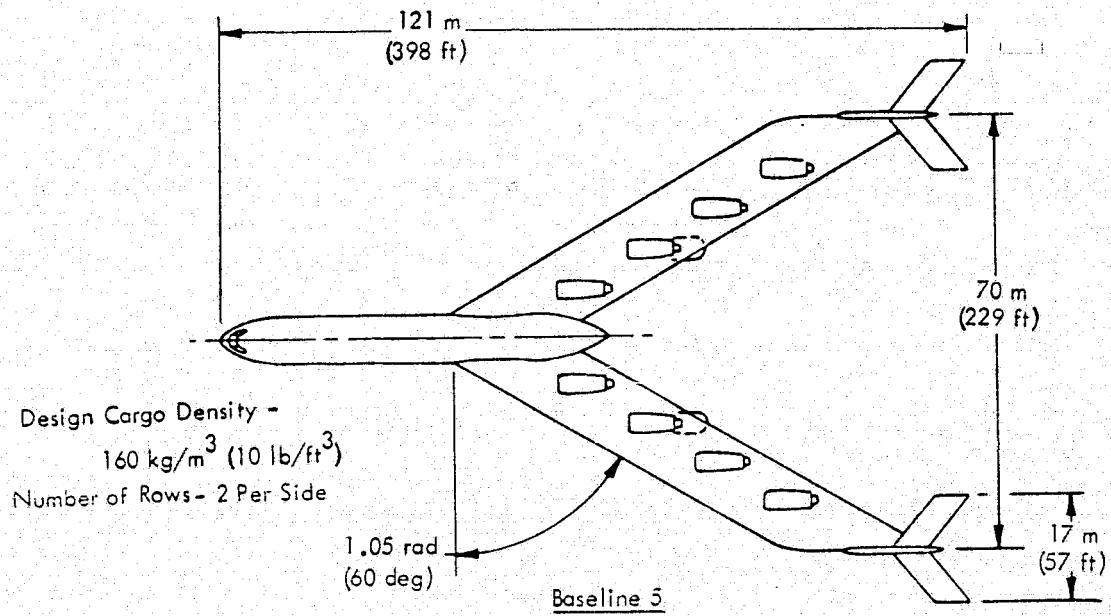
Baseline 6

Figure 17. Planforms for Baseline Configurations 5 and 6

DESIGN CARGO DENSITY 240 kg/m^3 (15 lb/ft^3)
NUMBER OF ROWS - 2 PER SIDE
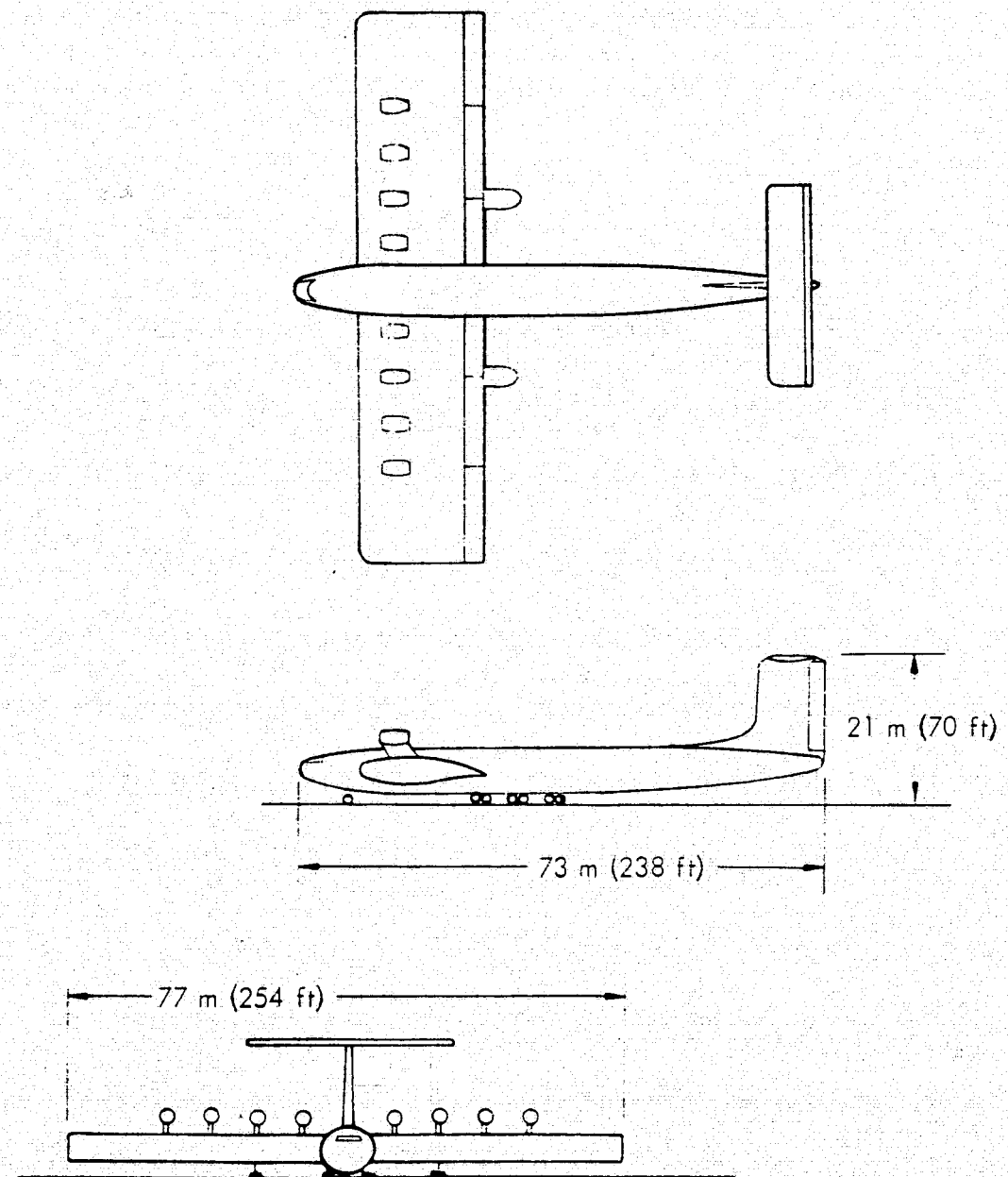
Figure 18. Baseline 7 Configuration

the wing, and the remaining 20 percent was carried in the fuselage. Both the wing and fuselage cargo compartments were pressurized. Fuel was uniformly distributed along the entire wing span.

For the structural loads analysis, aerodynamic loads data were synthesized by Lockheed's vortex-lattice lifting-surface program. Static aeroelastic effects were incorporated using discrete-element techniques. Lumped-weight distributions were devised from preliminary distribution data for the estimated aircraft component weights. Flexibility effects were included through conventional beam stiffness definitions.

From the initial load case investigated, it became apparent that the assumed wing weight of 48.8 kg/m^2 (10 psf) was low and should be increased. High bending loads were experienced as a result of the horizontal tail acting as both an extension of the wing and as a pitch control surface. Figure 19 illustrates the load distribution on the wing and shows the relatively high bending moment induced at the wing tips and carried over the entire wing span. The loads shown are for a 2.5-g steady pull-up maneuver using elevators at 10 670 m (35 000 ft). Figure 20 presents the loads and bending moments experienced by the empennage for the same case.

An explanation of the load distribution exhibited in this case is that the negative pressure field above the wing also acts on the inboard side of the vertical stabilizer and below the inboard half of the horizontal stabilizer, which is itself in the downwash field of the wing. The net effect is a marked asymmetry of loads on the horizontal tail coupled with an inward-acting side load on the vertical stabilizer, both producing a tip-up moment on the wing. Since the end-plate effect of the empennage reduces the normal tip loss at the wing tip, the overall result is an outward movement of the wing center of pressure when compared to a conventional aircraft design.

The effect of designing for such high wing bending would be to partially negate the advantage of span-distributed payloads. Ideally, the distributed payload should be supported by airloads, thereby practically eliminating wing bending moments associated with a typical cantilever wing.

Numerous schemes were explored for reducing the bending moments produced by the empennage. As shown in Figure 21, varying degrees of toe-out and rudder deflections were considered for the vertical fin. Other possible load alleviation schemes, such as active and passive controls and full-span pitch flaps, were considered but no significant improvements were noted.

Since the original loads were derived for a rigid structure, bending and torsional stiffnesses of the wing were estimated, and structural deflections were included in the loads analysis. However, only small reductions in wing bending moments were realized by including flexible structure in the analysis of the 2.5-g steady pull-up case, as shown on Figure 22.

38
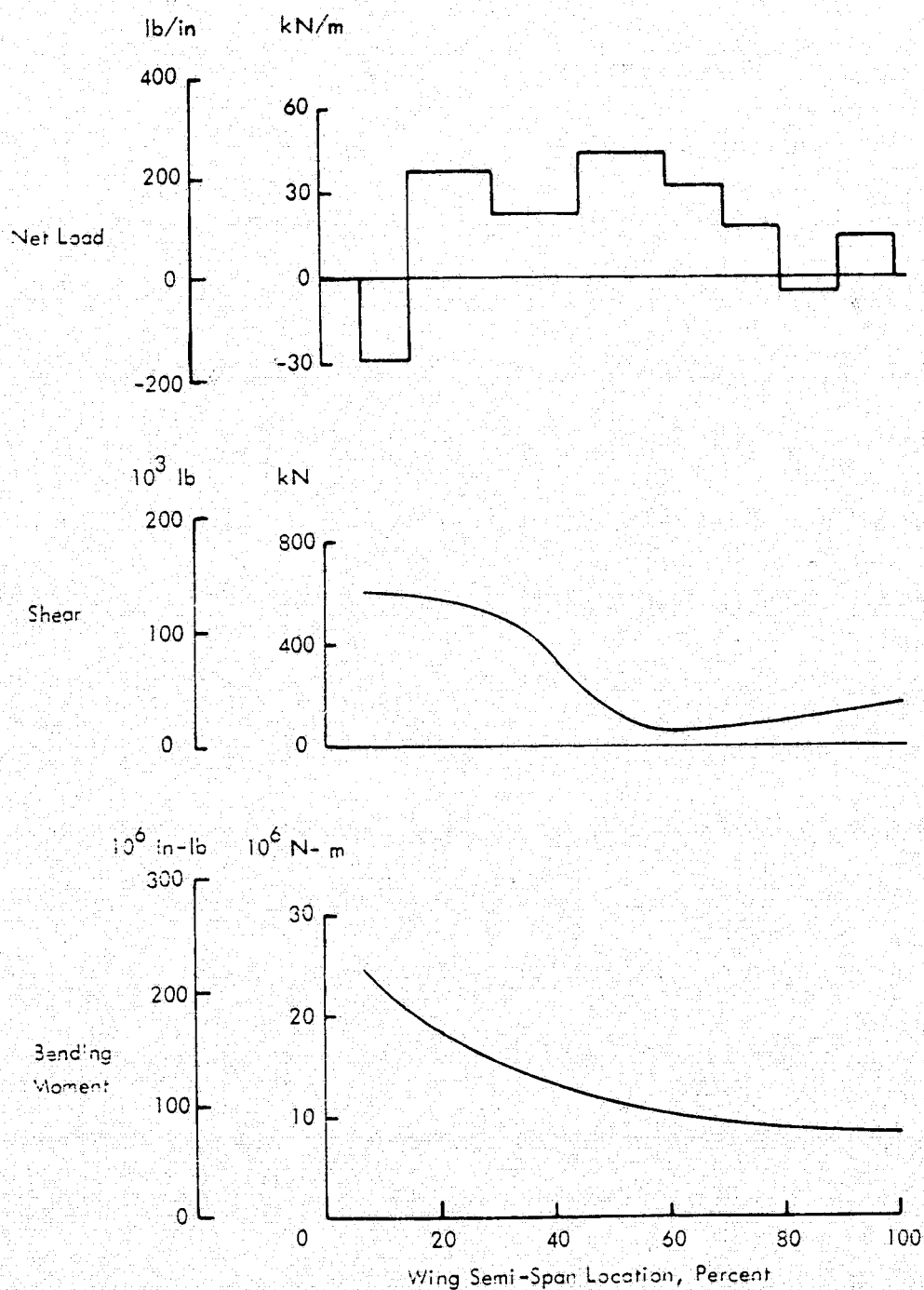
Figure 19. Applied Loads and Wing Bending for Baseline 1 Configuration
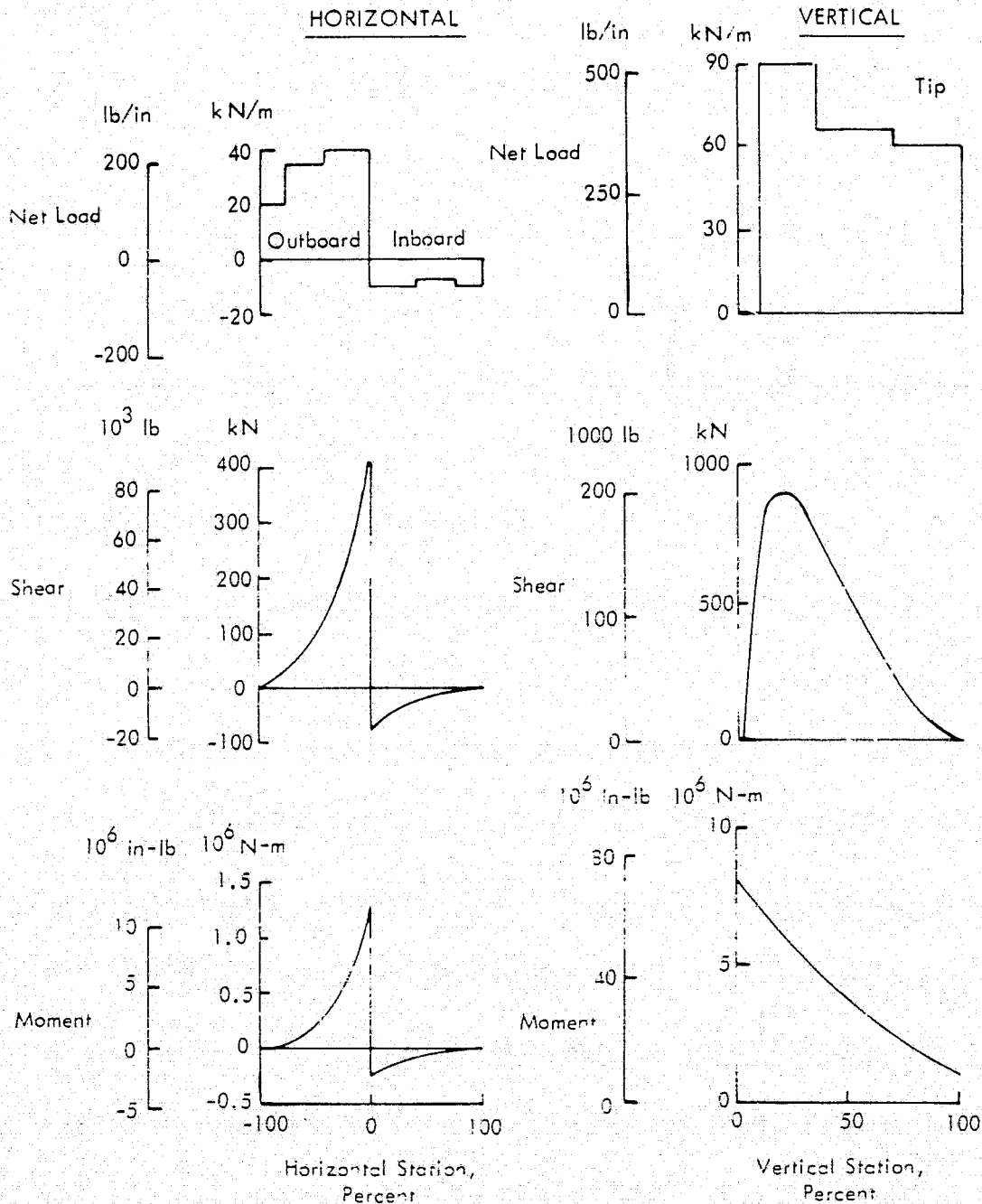
Figure 20. Applied Loads and Empennage Bending for Baseline 1 Configuration

40

2.5-g Steady Pull-Up Using Elevators
M = 0.75 at 10 670 m (35 000 ft)
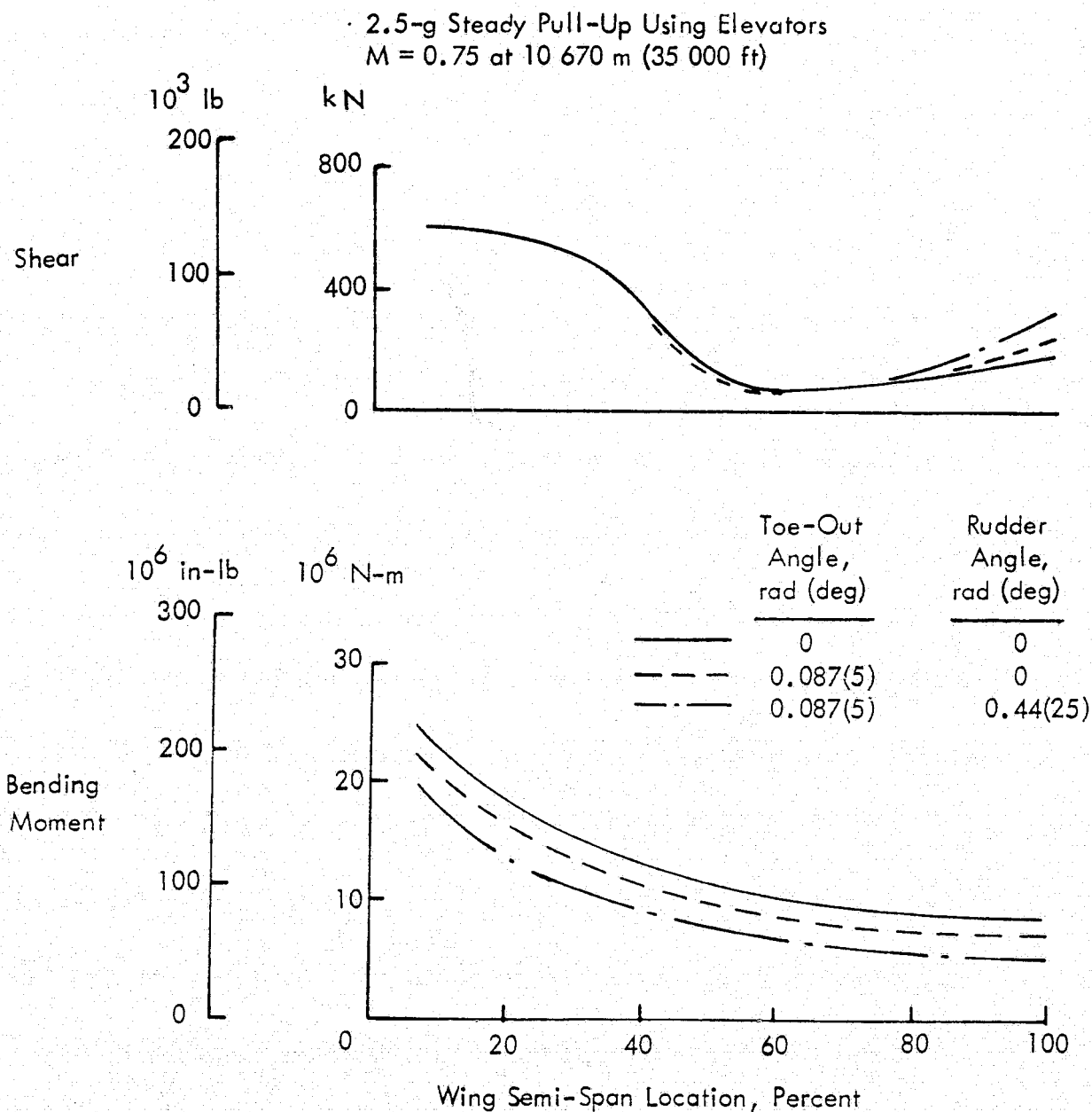
Figure 21. Effect of Vertical Fin Toe-Out on Wing Bending

2.5-g Steady Pull-Up Using Elevators
M = 0.75 at 10 670 m (35 000 ft)
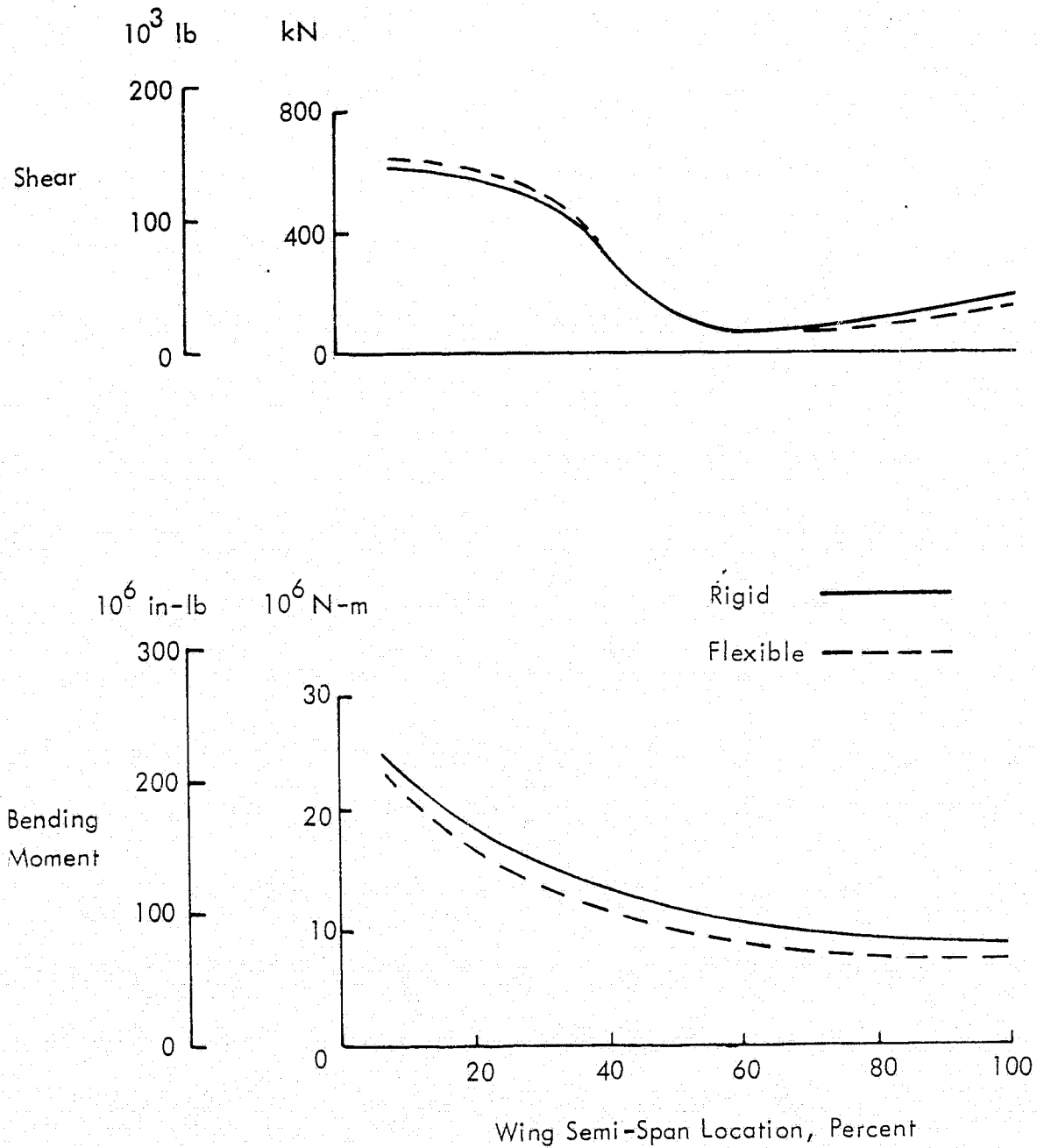
Figure 22. Effect of Flexible Structure on Wing Bending

All of the probable minor configuration modification had proved unsuccessful in achieving a significant reduction in the wing bending moment resulting from the wingtip-mounted empennage. Thus, a major configuration change appeared to be in order to eliminate the wingtip-mounted horizontals. An alternate configuration, similar to the Baseline 7 configuration with its aft-fuselage-mounted epennage, was considered but was unsatisfactory at sweep angles greater than 0.35 rad (20 deg) because of short moment arms for the empennage. Another alternate configuration, Baseline 1A shown in Figure 23, was configured with a fuselage-mounted canard control surface to eliminate the horizontal tails from the wingtip empennage. Analysis of this alternate revealed significant reductions in the bending moment. For the particular loading case checked, the airload distribution resulted in a negative bending moment near the wing root as shown in Figure 24. This figure illustrates an extreme variation in the wing loads. With normal load distribution, the inertia of the fuselage would produce a positive bending moment.

The wing cross-section in Figure 25 shows a structural arrangement for handling the various wing-loading conditions. Thicknesses and materials for the structural elements are tabulated at the bottom of the figure. Cylindrical shells are used to provide the two pressurized cargo bays. The primary wing structure uses the leading edge, three spars, and upper and lower covers for supporting shear, bending, and torsion loads and for providing torsional and bending rigidity. Fuel is carried in the copious volume of the leading edge, an advantageous location that places the weight of the fuel forward of the elastic axis for aeroelastic and flutter consideration. For illustrative purposes, the fuel tank has an inverse "D" shape. It is formed as an integral part of the wing leading edge, element 1, and the forward section of the front spar, element 10.

The load in the covers was approximated by dividing the bending moment by the area of the wing box. In this case, the ultimate bending moment was 1.5 times 41.8 MN-m (370×10^6 in-lb) and the area inclosed by the wing box was approximately 7.37 m (24.2 ft) by 3.51 m (11.5 ft). The resulting surface load of 2.43 MN/m (13 870 lb/in) required an average equivalent thickness, $\bar{t}$, in graphite epoxy of 5.87 mm (0.231 in) when subjected to a stress level of 413.7 MN/m^2 (60 000 psi). Studies have shown that this stress level is attainable in a structure with ribs spaced at 0.51-m (20-in) intervals by using a hat-stiffened graphite-epoxy cover for this surface load level. The average thickness shown includes all the material used in the wing covers, spar caps, and pressure diaphragms to react the wing bending loads.

Wing bending and torsional stiffness were also approximated by using the average wing-box equivalent thickness and the area of the wing box. The following values were estimated for use in flexible loads and flutter analyses:

$$EI = 1.7 \times 10^{10} \text{ N-m}^2 \ (5.8 \times 10^{12} \text{ lb-in}^2)$$
$$GJ = 1.0 \times 10^{10} \text{ N-m}^2 \ (3.5 \times 10^{12} \text{ lb-in}^2)$$

43

Design Cargo Density – 160 kg/m^3 (10 lb/ft^3)
Number of Rows – 2 Per Side
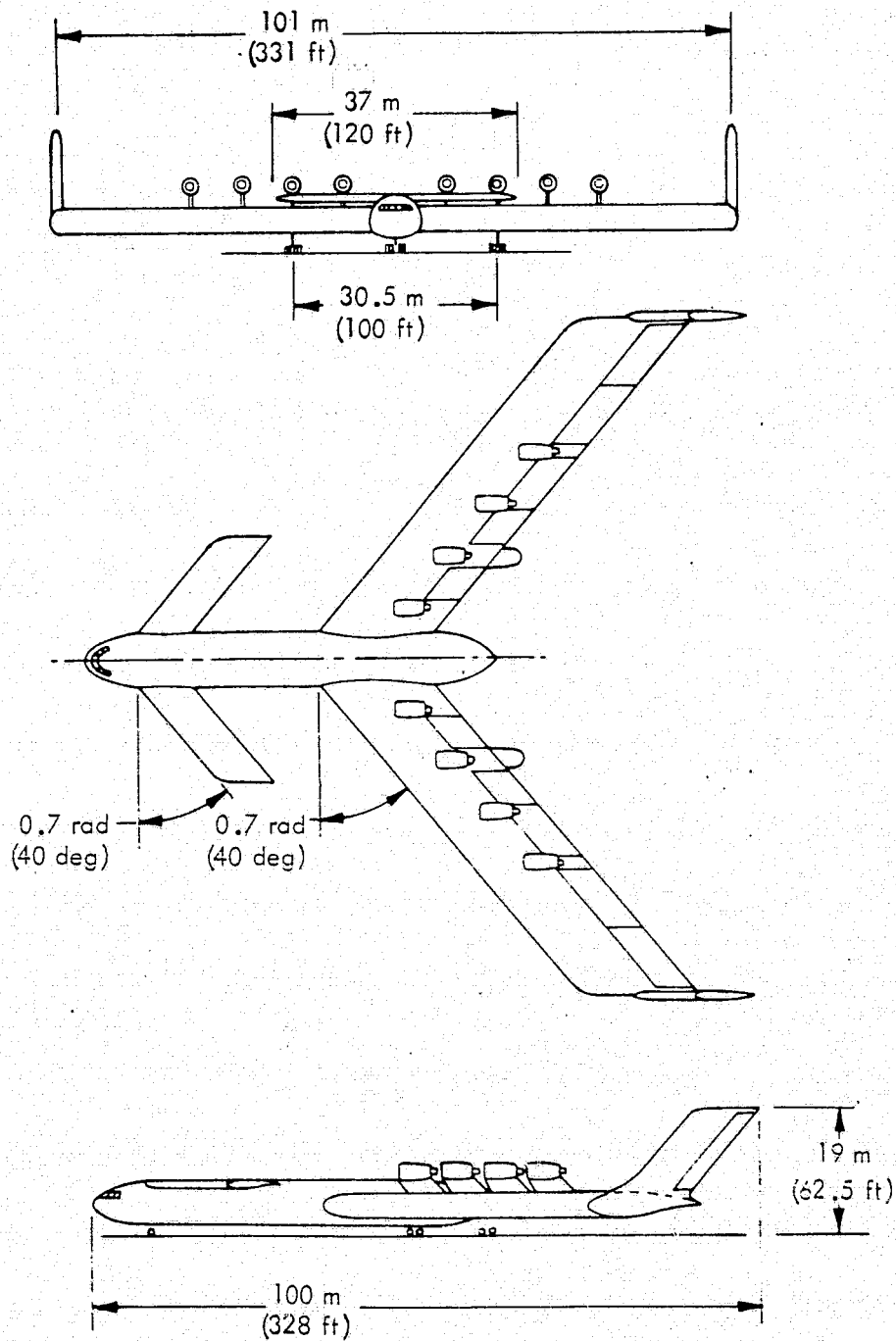
Figure 23. Baseline 1A Configuration

2.5-g Steady Pull-Up Using Elevators
M = 0.75 at 10 670 m (35 000 ft)
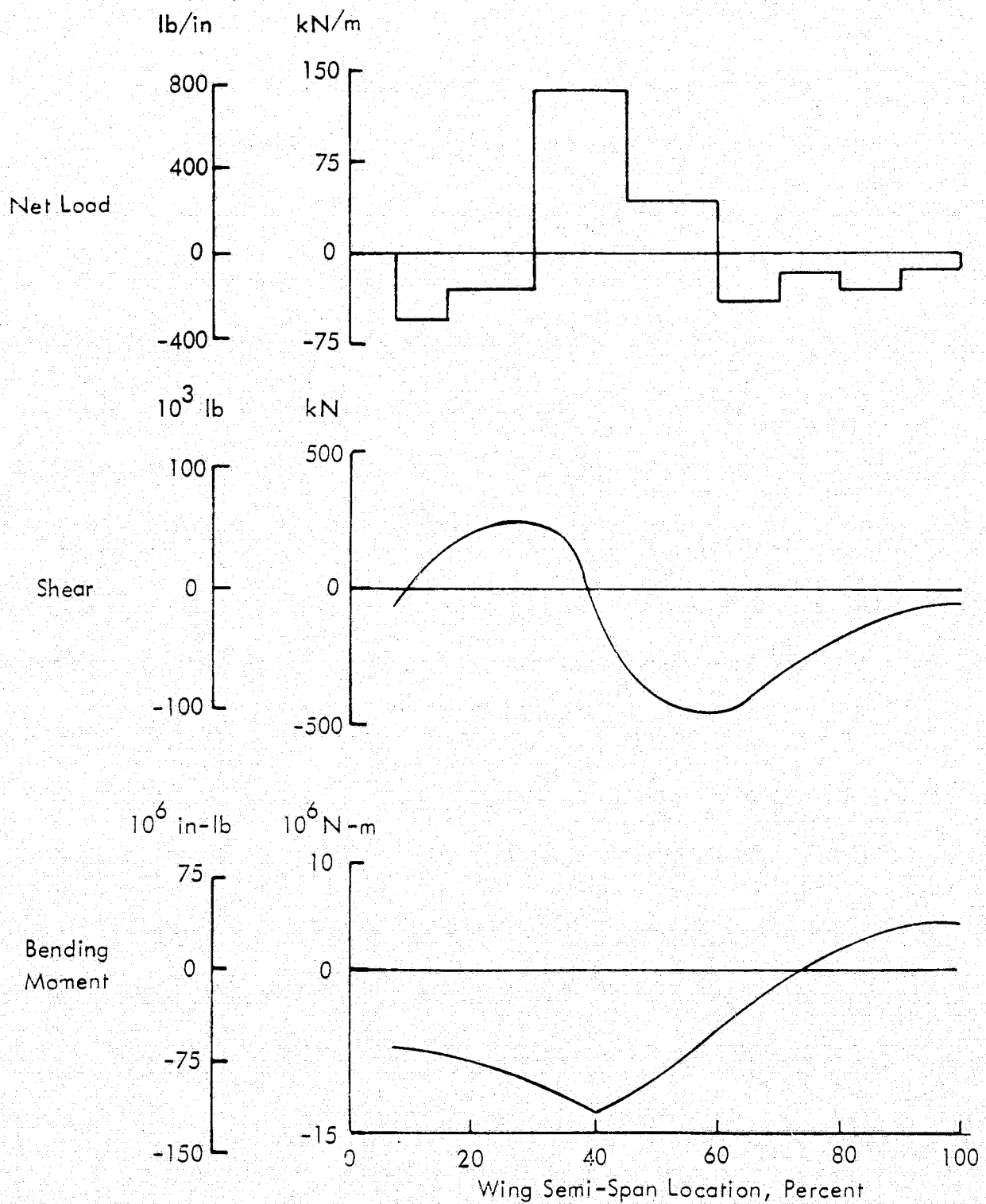
Figure 24. Applied Loads and Wing Bending for Baseline 1A Configuration
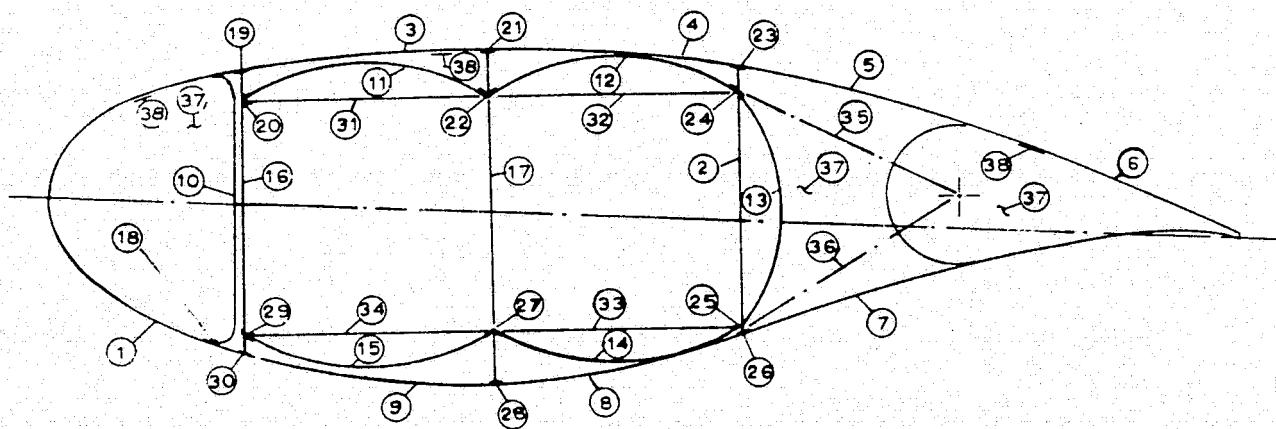
Element	Mat'l	$\bar{t}$		Length		Element	Mat'l	Area	
		cm	in	m	in			cm^2	in^2
1	G/E	0.51	0.20	5.85	230	18	Al	12.90	2.000
2	G/E	0.25	0.10	3.00	118	19	Al	4.36	0.675
3	G/E	0.43	0.17	2.74	108	20	Al	4.36	0.675
4	G/E	0.43	0.17	2.74	108	21	Al	4.36	0.675
5	G/E	0.15	0.06	2.79	110	22	Al	5.16	0.800
6	G/E	0.13	0.05	8.59	338	23	Al	4.36	0.675
7	G/E	0.13	0.05	2.67	105	24	Al	5.16	0.800
8	G/E	0.43	0.17	2.79	110	25	Al	5.16	0.800
9	G/E	0.43	0.17	2.79	110	26	Al	4.36	0.675
10	G/E	0.15	0.06	2.54	100	27	Al	5.16	0.800
11	G/E	0.15	0.06	2.92	115	28	Al	4.36	0.675
12	G/E	0.15	0.06	2.92	115	29	Al	4.52	0.700
13	G/E	0.15	0.06	2.54	100	30	Al	4.36	0.675
14	G/E	0.20	0.08	2.90	114	31	G/E	17.41	2.700
15	G/E	0.15	0.06	2.92	115	32	G/E	17.41	2.700
16	G/E	0.25	0.10	3.18	125	33	G/E	17.41	2.700
17	G/E	0.25	0.10	3.71	146	34	G/E	17.41	2.700
						35	G/E	35.50	5.500
						36	G/E	35.50	5.500
						37	G/E	375.00	58.100
						38	Al	304.00	47.100

Total Weight = 401.9 kg/m (22.5 lb/in)

Figure 25. Cross-Section of Wing Structural Arrangement

These values are subject to variations by tailoring the lay-up of the graphite epoxy. For example, by orienting all the plies in the $\pm$ 0.79 rad (45 deg) direction on the leading edge and rear spar, a GJ approaching 1.7×10^{10} N-m^2 (6.0×10^{12} lb-in^2) is obtainable. Values of this magnitude are beneficial for preventing flutter - a problem investigated as part of the configuration refinement studies in Section 4.1.

By summing the weights of all the elements shown in Figure 25, a resultant weight of 401.9 kg/m (22.5 lb/in) per unit of span length, or 30.8 kg/m^2 (6.3 psf) per unit of surface area is obtained. This weight does not include allowances for overlaps, joints, pressurization systems, cargo loading systems, control systems, insulation and the other items necessary for a complete aircraft. Adding these additional items to the structural weight, gives a total unit wing weight of 63.6 kg/m^2 (13.0 psf) for the Baseline 1A configuration.

Similar studies were performed on the wing structure of the other baseline configurations. Based on the results of all of these cases, an empirical equation for estimating the wing weight was derived of the form:

$$W_u = 5.5 \qquad\qquad\qquad\qquad\qquad \text{if } b \leq 68.7 \text{ m}$$
$$\quad = 5.5 + 0.0694 \, (b - 68.7) / \cos \Lambda \qquad \text{if } b \geq 68.7 \text{ m}$$

or in English units:

$$W_u = 11.05 \qquad\qquad\qquad\qquad\qquad \text{if } b \leq 225 \text{ ft}$$
$$\quad = 11.05 + 0.0142 \, (b - 225) / \cos \Lambda \qquad \text{if } b \geq 225 \text{ ft}$$

where

W_u is the wing weight in kg/m^2 (psf)

b is the wing span in m (ft) and

Λ is the wing sweep angle

This equation was used in developing all of the aircraft designs for the parametric study.

3.2.3.2 Design Analysis

As just described, the horizontal tails were removed from the wingtip-mounted empennages to alleviate the high bending loads imposed on the wing structure. In relocating the horizontal controls as a canard surface on the forward fuselage, consideration was given to both high and low positions. The high position selected for the canard, as shown in Figure 26, fared better in a qualitative evaluation of the two locations. The low position experienced two disadvantages of marginal canard flap-ground clearance and of difficult structural carry-through arrangement due to the presence of the nose landing gear. In the high position, there is ample room for the carry-through structure behind the crew compartment which has been located above the

47

fuselage cargo compartment to permit straight-in loading of outsize military equipment. The front beam of the canard coincides with the front of the fuselage cargo compartment, providing the maximum moment arm for the canard without adding unnecessary fuselage length.
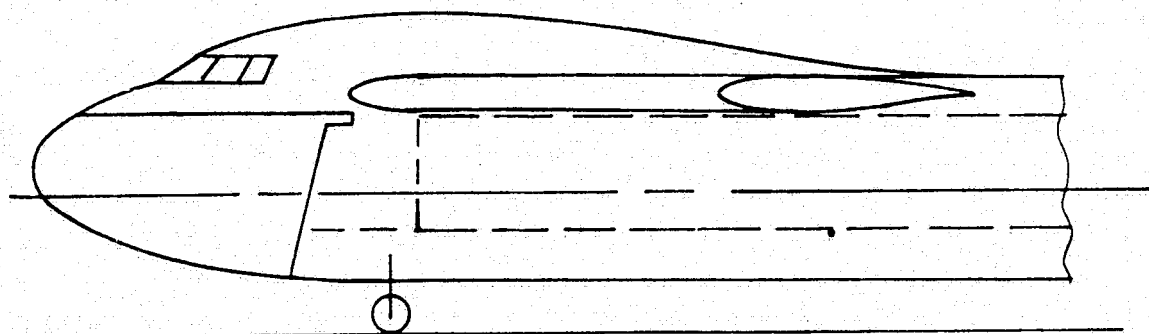
Figure 26. Canard Location

Studies were made of the four wing-fuselage structural arrangements shown in Figure 27. The first option has the three wing spars continued straight through without interruption by the fuselage cargo compartment which precedes the wing. The four longerons of the wing-fuselage intersection corners serve as the main structure for attaching the fuselage to the wing. With this arrangement, the entire aircraft can be loaded with containers not exceeding 6.1 m (20 ft) in length from just one of the three openings, that is, nose or either wingtip. All three openings must be used to load the aircraft with 12.2 m (40 ft) long containers. Outsized military equipment can be loaded only through the nose visor door into the fuselage compartment. This arrangement was selected for all of the parametric design cases since it offers the simplest structural design. With the entire fuselage preceding the wing, there are two additional advantages of the greatest moment arm for the canard without excess fuselage structure, and the minimum wing span for airport compatibility.

The second option considered for the structural arrangement has the outsized fuselage cargo compartment extending through the wing. This arrangement suffers the disadvantages, relative to the first option, of requiring considerably more structure for the wing-fuselage joint, of having a shorter moment arm for the canard, and of experiencing more airport compatibility problems due to the greater wing span.

The third option experiences the same disadvantages as the second, but one is more severe. With the large unpressurized area for rotating 12.2 m (40 ft) long containers at the wing-fuselage intersection, this structural arrangement does offer the advantage of single point loading. However, this advantage does not offset the penalty of considerably more structure at the wing-fuselage joint than for option two.

48

OPTION 1
Continuous Wing Structure
Through Fuselage

Section W - W
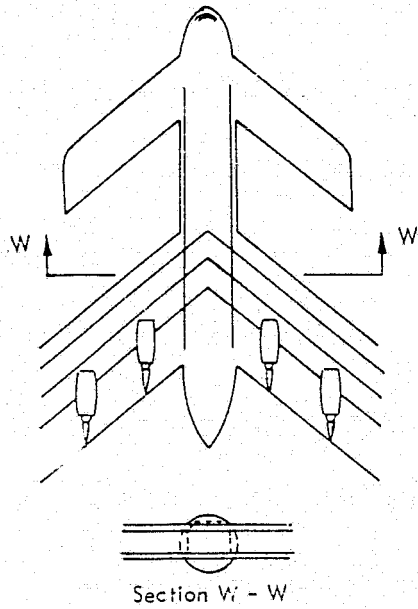
OPTION 2
Continuous Wing Structure
Opening Through Wing

Section X - X
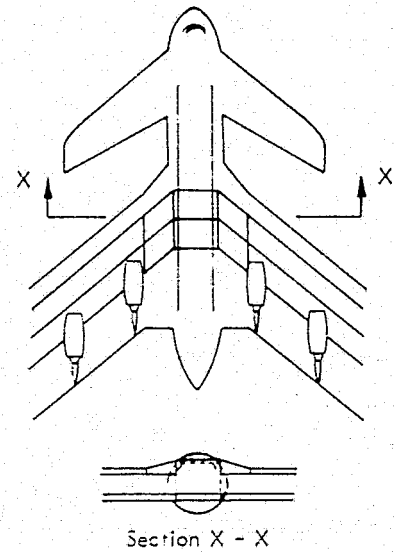
OPTION 3

Single Point Nose Loading
Unpressurized Area for
Rotating 12.2 m (40 ft) Containers

Section Y - Y
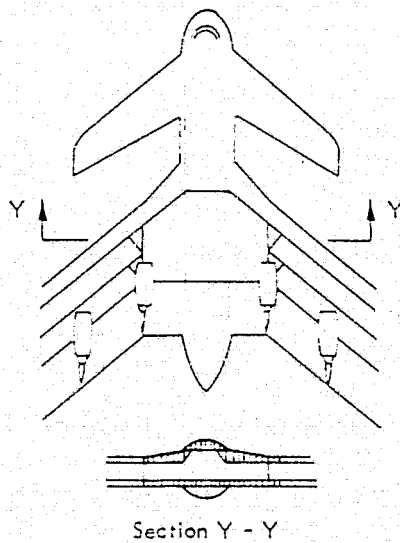
OPTION 4

Side Doors for
Loading Containers

Section Z - Z
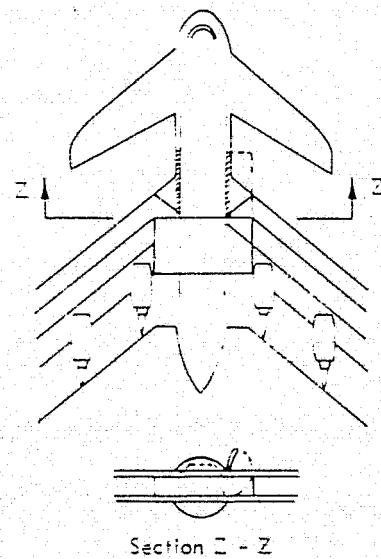
Figure 27. Wing-Fuselage Structure Alternatives

49

In the fourth option considered, the wingtip openings were replaced with fuselage side doors. This approach was abandoned since it offered no advantages over the other options. As a disadvantage, the side doors encroached well into the wing leading edge, further complicating the structural design and the door operation.

3.2.3.3 Aerodynamic Analysis

For purposes of identification, the Baseline 7 configuration used for all of the low sweep angle design cases is designated the "T-tail" configuration, while the "Canard" is the nomenclature applied to the configurations with wing sweep angles between 0.35 and 1.05 rad (20 and 60 deg). Geometric and aerodynamic characteristics selected for the empennages of both the T-tail and canard configurations used in the parametric designs are summarized in Table XII. All other aerodynamic features of the Baseline 1 configuration, as reviewed in Section 3.2.1.2, are equally applicable to these two alternate configuration geometries.

TABLE XII. SUMMARY OF EMPENNAGE CHARACTERISTICS FOR ALTERNATE CONFIGURATIONS

	Canard	T-Tail
Horizontal Tail or Canard		
Aspect Ratio	4.5	4.5
Volume Coefficient	0.43	0.43
Sweep Angle, rad (deg)	0.7 (40)*	0
Vertical Tail		
Aspect Ratio	1.5	1.5
Volume Coefficient	0.049	0.075
Sweep Angle, rad (deg)	0.7 (40)*	0
Trim Drag Penalty	One percent of wing induced drag	12 counts
Wing Efficiency Factor	0.9	0.9

*The empennage and wing sweep angles were equal for angles greater than 0.7 rad (40 deg).

The design criteria and guidelines noted in Section 3.2.1.4 for the flight controls were generally adherred to for the two alternate configurations. Only the longitudinal control system required modification for the canard version. The forward-fuselage mounted canard had no effect on basic airplane stability but did provide inputs for trim, maneuver, and stability augmentation. This was accomplished by having a control system that could be set at any required moment value or allowed to weathercock at constant hinge moment with sudden changes in angle of attack. A damping system was also included to activate in the event of flutter difficulties. With this system which could be set based on aircraft center of gravity to yield an acceptable level of aerodynamic

stability with tail removed, there was minimum need for longitudinal stability augmentation.

3.3 PARAMETRIC STUDY AND OPTIMUM CONFIGURATION SELECTION

Parametric design points were defined in Section 3.1 and baseline configuration data were established in Section 3.2 to permit the development of aircraft designs from which an optimum point design configuration was selected. The purpose of this section is to describe the parametric design study assumptions, selection criteria and practical considerations, which led to the selection of the optimum configuration.

3.3.1 Parametric Study Assumptions

As per NASA instructions, the magnitude and location of the landing and taxi loads on the aircraft were assumed to be non-critical considerations for all of the parametric design cases. The effects of the landing gear on the aircraft structural and configurational design and on aircraft-airport compatibility were assessed as part of the selected aircraft refinement studies, described in Section 4.0.

Adequate volume was assumed to be available in the wing to carry the mission fuel. In an earlier illustration, Figure 5, of the wing profile, there appeared to be plenty of space for fuel in the leading edge and beneath the cargo compartment. This assumption was subsequently confirmed, as noted in Section 4.2.3.

All of the aircraft designs were assumed to have eight engines with a bypass ratio of 4.5. With the maximum engine thrust levels expected to be about 310 000 N (70 000 lb) in 1990, this number of engines was judged to be consistent with the anticipated thrust requirements for the median aircraft in the parametric study. For the selected optimum configuration, it was found that six engines would suffice; while for the worst configuration, ten engines were required. This substantiated the assumption that eight engines would, on the average, be most suited to all aircraft in the study.

All of the aircraft were designed to cruise at one of two fixed altitudes – the canard configuration at 10 670 m (35 000 ft) and the T-tail configuration at 7620 m (25 000 ft). These two altitudes were selected as being close, on the average, to the optimum cruise altitude projected for each configuration design on the basis of the ranges of wing sweep angles, thickness ratios, and cruise Mach numbers.

3.3.2 Basis for Configuration Selection

Minimum 15-year life-cycle cost for the fleet of aircraft required to provide the specified annual productivity of 113 billion revenue-ton km (67 billion revenue-ton n.mi.) was the criterion used to select the best aircraft from the parametric matrix of candidate designs. The life-cycle costs were calculated in January 1975 dollars and included the direct operating costs, the production program cost, and the total RDT&E program costs. Detailed descriptions of the methodology for computing these cost

elements are presented in Section 5.0.

Values used in determining the life-cycle cost for each design were:

- Fuel price - 9.8 ¢/l (37 ¢/gal)
- Crew size- 3 persons
- Utilization rate - 3000 hours per year
- Load factor - 65 percent
- Revenue tonnage - 91.8 percent of total payload

The first four of these parameters are the baseline values for the economic sensitivity studies performed on the refined aircraft configuration. The remaining 8.2 percent of the payload not included in the revenue tonnage was assumed to be container tare weight.

In a parametric study, the relative magnitudes of the points, rather than the absolute values, are of importance in determining the optimum point. For this reason and because the individual aircraft designs were not sufficiently-well refined by Lockheed's standards for absolute cost evaluation, all of the cost data were normalized for the parametric design. The arbitrarily-selected base case was the configuration with 3 rows of cargo at a density of 160 kg/m^3 (10 lb/ft^3), zero wing sweep, and a 20-percent thickness ratio. No significance is attached to the base case which was chosen merely to adjust the data scale for simplicity of use.

3.3.3 Selection Procedure Considerations

Lockheed's Generalized Aircraft Sizing and Performance (GASP) computer program was used in developing aircraft designs for the points in the reduced parametric matrix shown in Figure 12. For some points, excessively high wing loadings and cruise lift coefficients were encountered in attempting to design aircraft with the required geometric characteristics. Whenever it became apparent that a wing loading greater than 6700 N/m^2 (140 psf) would result for a particular point, the design effort was discontinued. This wing loading limitation was imposed based on previous design experience. The cases eliminated by this constraint were:

Rows	Sweep Angle, rad (deg)	Density, kg/m^3 (lb/ft^3)	Thickness Ratio, percent
3	0.35 (20)	240 (15)	25
3	0	240 (15)	25
4	0.35 (20)	160 (10	25
4	0	160 (10)	25
4	0	160 (10)	20

The fixed relationships illustrated in Figure 14 for wing sweep angle and thickness ratio and for cruise Mach number and lift coefficient were responsible for some design-point aircraft having Mach numbers approaching a value of one to achieve the required thickness ratio. At cruise Mach numbers greater than 0.9, area ruling of aircraft configurations is necessary to avoid wave drag penalties. No attempt was made to area rule any of the high cruise Mach number configurations. Thus, the drag levels computed for these configurations represent the minimum achievable values. Since the transonic aircraft designs were proving to be economically undesirable even with these minimum drag values, design cases requiring cruise Mach numbers greater than 0.9 were omitted from further consideration. The effect of this limitation is illustrated on Figure 28. Several points, which were eliminated by previous constraints, have been included on this figure and Figure 29 to define the curve shapes. Cutoff lines labelled A (aspect ratio) and T (thickness ratio) have been drawn to show the limits of valid results based on the study constraints.

A rule of thumb limitation on the maximum cruise lift coefficient achievable with the projected state of the art for the near term future is

$$C_{L_{max_{cruise}}} = 0.7 \cos^2 \Lambda$$

where Λ is the wing sweep angle. The effect of this limit in reducing the number of eligible points for consideration is shown by Figure 29. Cruise Mach number cutoff lines shown on this figure have been labelled M.

Normalized 15-year life cycle costs are presented in Figure 30 for the reduced remaining parametric matrix. It is apparent from these results that the lower costs were achieved with a two-row configuration than with the one, three, and four-row designs.

The minimum cost occurred for the point with the 0.7 rad (40 deg) sweep, 160 kg/m³ (10 lb/ft³) density and 20-percent thickness ratio. While the costs for the 2-row cases with 240 kg/m³ (15 lb/ft³) density, 25-percent thickness and 0 to 0.35 rad (0 to 20 deg) sweep angles were close to the minimum point, the higher density was significant in eliminating these points. Historically, transport aircraft have exhibited the tendency to be cargo volume limited rather than weight limited. Thus, if all other factors are essentially equal, the aircraft designed for the lighter cargo density should be selected since it has the greater cargo compartment volume.

Analysis of the results for two rows of cargo with a density of 160 kg/m³ (10 lb/ft³) revealed that the 15 and 20-percent thickness-ratio curves were somewhat parallel. The tendency of the 25-percent thickness curve to cross the 20-percent curve suggested that some intermediate thickness-ratio value might be optimum. This was confirmed by cross plotting the results, as in Figure 31, whereupon an optimum thickness ratio of 21.8 percent was defined.
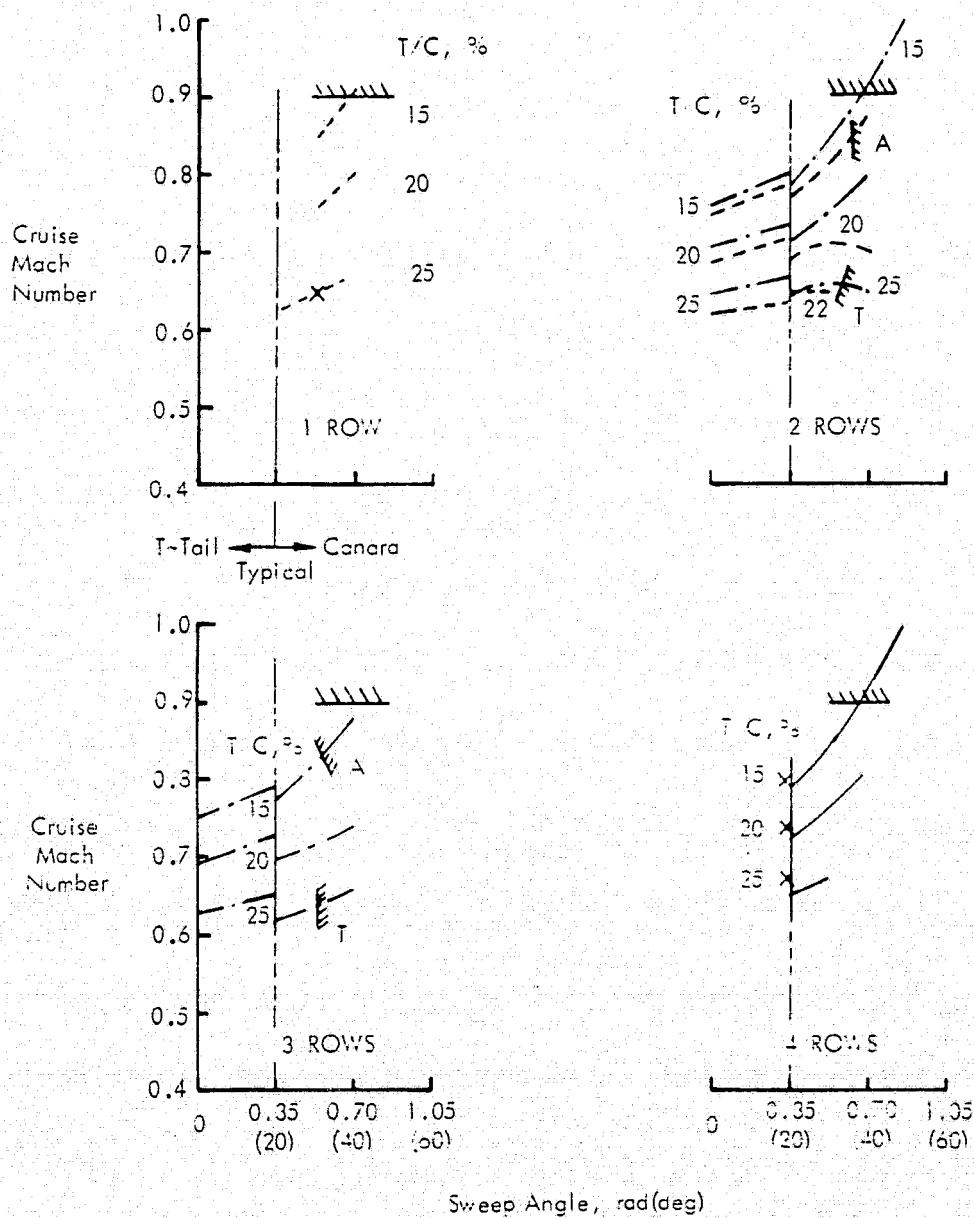
Figure 28. Effect of Cruise Mach Number Limitation
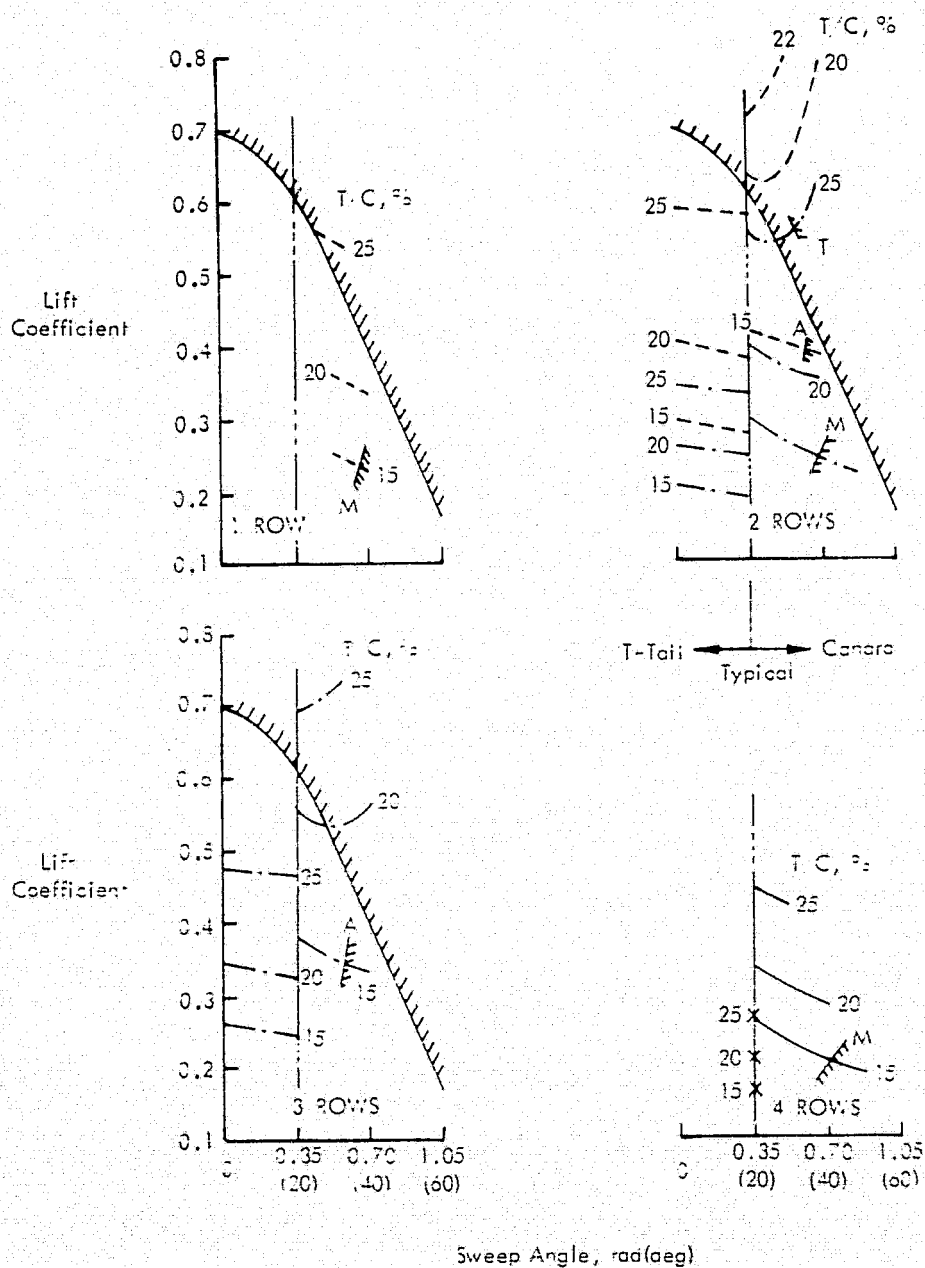
Figure 29. Effect of Cruise Lift Coefficient Limitation

55
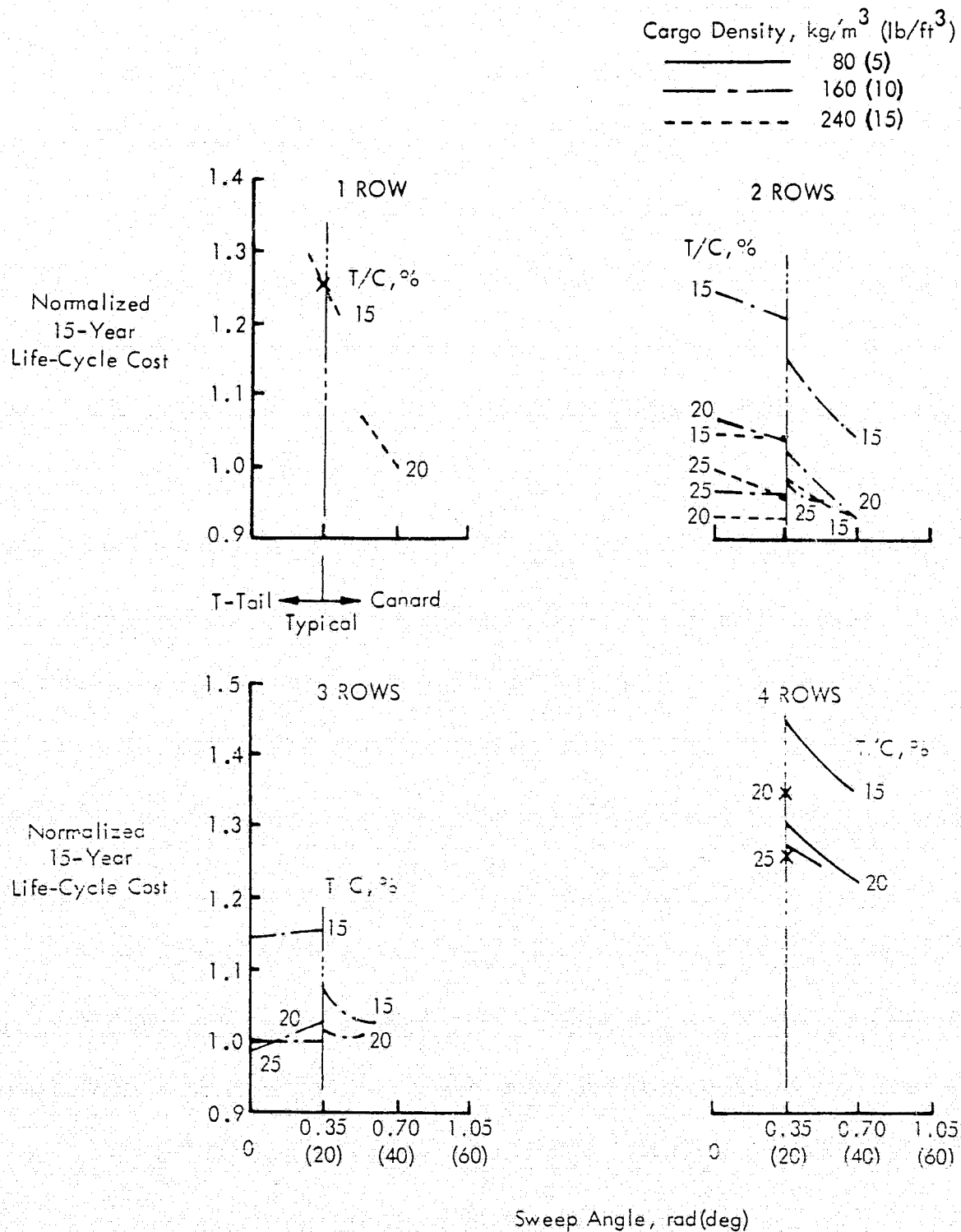
Figure 30. Parametric Study Cost Results

2 Rows

160 kg/m^3 (10 lb/ft^3) Cargo Density

0.70 rad (40 deg) Sweep Angle
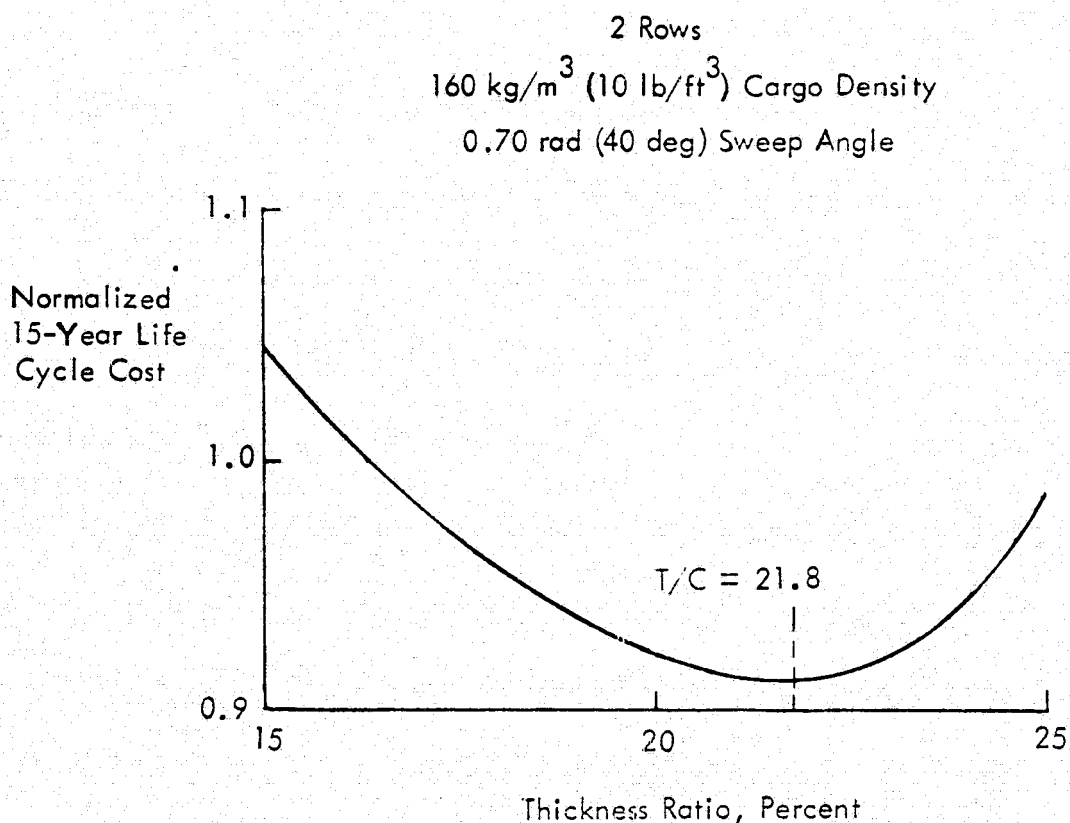
Figure 31. Optimum Thickness Ratio Determination

3.3.4 Selected Configuration Characteristics

The selected configuration is shown in Figure 32. Pertinent design and performance characteristics are summarized in Table XIII, while a weight statement is presented in Table XIV. The geometric aspect-ratio value of 5.9 is shown in Table XIII; an effective aspect-ratio value of 7.6 was achieved through the end-plating effect of the wingtip-mounted vertical surfaces.

The engine thrust value for each of the eight engines was considerably lower than the maximum level of 310 000 N (70 000 lb) projected for the 1990 time period. The use of fewer engines with higher thrust levels is addressed in the next section on refinement studies.

Minimum 15-year life-cycle cost was the criterion for selecting the optimum configuration in this study. Some alternate selection criteria, which have been used in the past, include minimum operating weight, block fuel weight, ramp or gross weight, and direct operating costs (DOC). For each of these parameters, Table XV shows a comparison of the values for the selected configuration with the minimum values achieved

57

Design Cargo Density - 160 kg/m^3 (10 lb/ft^3)
Number of Rows - 2 Per Side
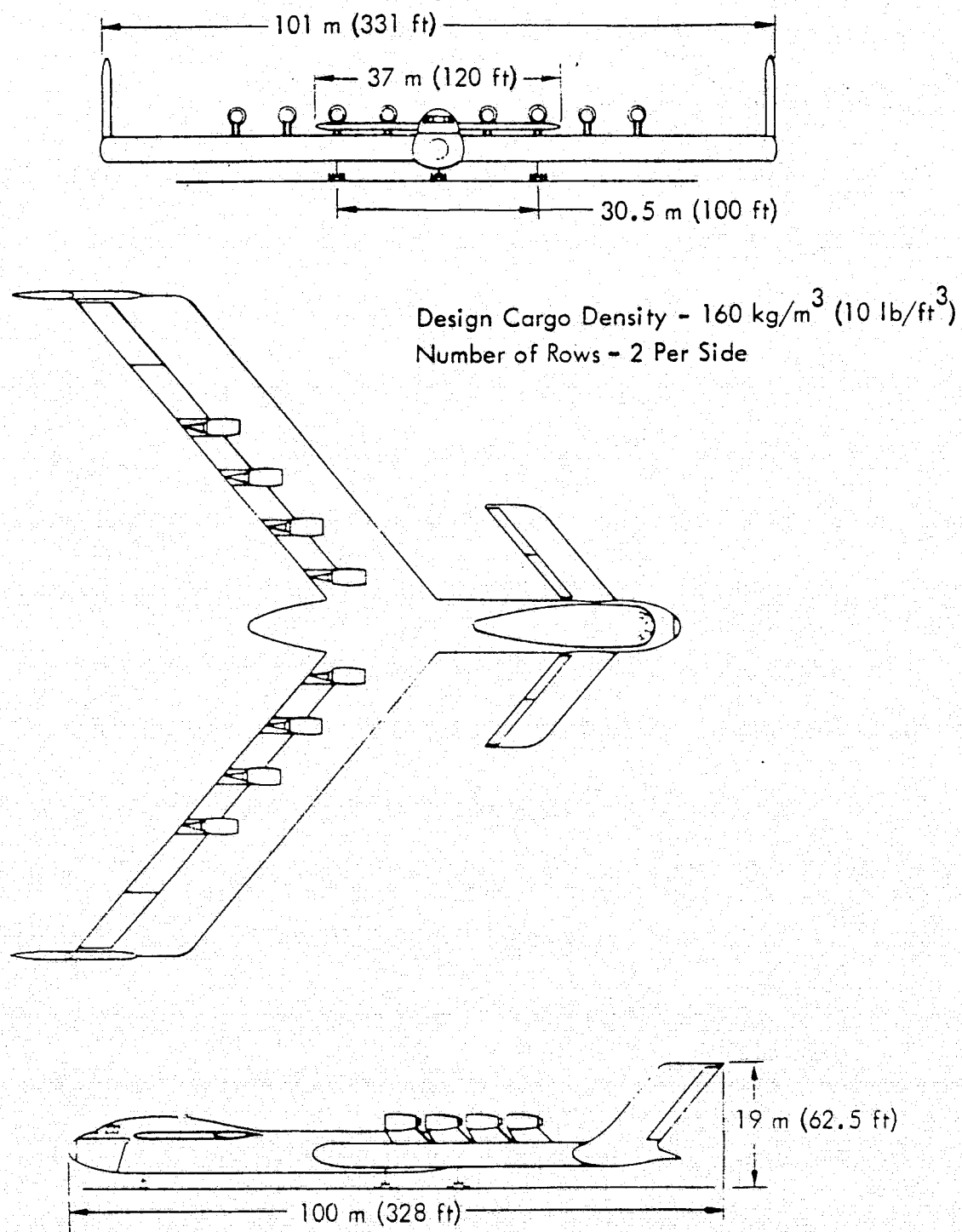
Figure 32. Selected Configuration

TABLE XIII. SELECTED CONFIGURATION CHARACTERISTICS SUMMARY

<u>DESIGN</u>

Rows of Cargo	2	
Cargo Density	160 kg/m^3	(10 lb/ft^3)
Sweep Angle	0.7 rad	(40 deg)
Thickness Ratio	21.8 %	
Wing Span	101 m	(331 ft)
Aspect Ratio	5.9	
Wing Loading	38.4 N/m^2	(80.3 lb/ft^2)
Wing Area	1 725 m^2	(18 559 ft^2)

<u>PERFORMANCE</u>

Cruise Mach Number	0.75	
Cruise Altitude	10 670 m	(35 000 ft)
Range	5 560 km	(3 000 n. mi.)
Lift/Drag	19.88	
FAA Field Length	1 830 m	(6 000 ft)
Fleet Size	302	
Engine Thrust	209 000 N	(47 111 lb)

TABLE XIV. SELECTED CONFIGURATION WEIGHT SUMMARY

	kg	lb
OWE	248 000	545 851
Fuel	176 000	338 318
Payload	272 155	600 000
Ramp	696 150	1 534 169

TABLE XV. ALTERNATE SELECTION CRITERIA EFFECTS

Parameter	Selected Configuration Value		Minimum Value Experienced In Study	
Operating Weight, kg (lb)	248 000	(545,851)	188 000	(413 879)
Block Fuel Weight, kg (lb)	146 000	(322 076)	146 000	(322 076)
Ramp Weight, kg (lb)	696 000	(1 534 169)	695 500	(1 533 357)
Normalized DOC		0.878		0.878
Normalized 15-Year Life Cycle Cost		0.912		0.912

by any configuration considered in the study. Based on the comparison, the same configuration would have been chosen for the alternate selection criteria of minimum DOC or block fuel weight. In terms of ramp weight, the selected configuration was very close to the minimum. Only the operating weight of the selected configuration varied substantially from the minimum value of any airplane in the study. The minimum operating weight aircraft was a T-tail, 0.35 rad (20 deg) sweep configuration which carried cargo with a density of 240 kg/m^3 (15 lb/ft^3).

4.0 CONFIGURATION REFINEMENT

Structural, aerodynamic and design studies were undertaken for the selected configuration. The purpose of these studies was to refine the design concept, to evaluate performance levels or confirm previous estimates, and to address potential problem areas through establishment of solution feasibility.

4.1 STRUCTURES REFINEMENT ANALYSES

Structural loads studies, supplementing the previous efforts of Section 3.2.3.1, were concentrated on the landing gear system and on the effect of payload weight distributions. Upon completion of the loads analyses, a flutter analysis resulted in several configuration modifications. A weight statement and a balance summary were prepared for the resulting final configuration. As a possible design requirement alternative, the weight penalty for a pressurized cargo compartment was checked.

4.1.1 Loads Analyses

Inertia loads are balanced by air loads for an ideal span-distributed loading aircraft during flight. To take advantage of the balanced-load principle during ground operations, a distributed landing gear system arrangement is needed to replace air loads. Unfortunately, the requirement for the landing gear system to be airport compatible mitigates against a distributed arrangement.

Figure 33 illustrates some of the problems in determining landing gear location. The picture at the top of the figure shows the selected 101 m (331 ft) span aircraft sitting on a standard 45.8 m (150 ft) wide commercial runway. With a minimum clearance of 3.05 m (10 ft) from the runway edge to the gear, the maximum gear tread width is limited to 39.6 m (130 ft). The graph at the bottom of Figure 33 gives the variation of equivalent wing cover thickness, $\bar{t}$, as a function of wing semi-span. In moving inboard from the wing tip (100-percent position), the $\bar{t}$ required for ground operations increases until it equals the thickness required for flight loads, $\bar{t}_{REF}$, at a 62-percent wing semi-span location. If the gear tread width is only 39.6 m (130 ft), the $\bar{t}$ continues to increase until at the wing root position, it is 3.5 times that required for flight conditions. With a tread width of 64 m (210 ft), the $\bar{t}$ for ground operations does not exceed that for flight, but the gear is off the runway.

Structural deflections of the wing were a prime consideration in locating the landing gears. As the main landing gears were moved inboard, wing tip deflections became higher and required excessively longer landing gear struts to provide tip ground-clearance. The model, weight distribution, and constants shown in Figure 34 were used to evaluate the effect of varying the locations and numbers of gears. Six cases were considered. The resulting deflections, forces, and wing bending moments are summarized in Figure 35. The inboard and outboard main gear locations are 15.25 and 30.5 m (50 and 100 ft) from the fuselage centerline, respectively.
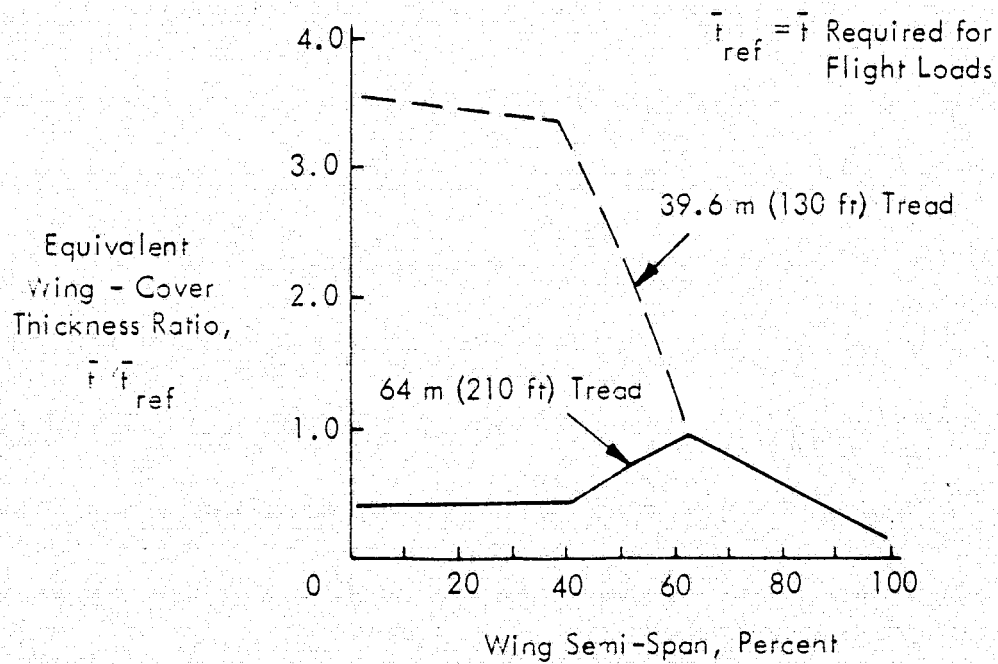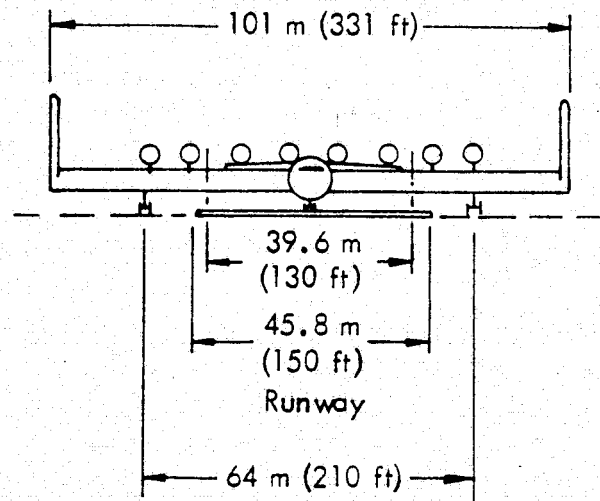
Figure 33. Landing Gear Location Considerations

Grid Points	X m	X in	Y m	Y in	Weight 1000 kg	Weight 1000 lb
1	-53.4	-2100	0	0	10.9	24
2	-47.0	-1850	0	0	29.0	64
3	-35.6	-1400	0	0	29.0	64
4	-25.4	-1000	0	0	29.0	64
5	-18.5	-730	0	0	10.9	24
6	- 7.6	-300	0	0	10.9	24
7	0	0	0	0	10.9	24
8,9	-12.7	-500	±7.6	±300	45.4	100
10,11	- 5.8	-230	±15.2	±600	45.4	100
12,13	0	0	±22.9	±900	45.4	100
14,15	7.1	280	±30.5	±1200	45.4	100
16,17	15.2	600	±40.6	±1600	45.4	100
18,19	23.4	920	±50.4	±1980	50.0	110
20,21	2.5	100	±30.5	±1200	5.9	13
23	-47.0	-1850	0	0		
24	-7.6	-300	0	0		
25, 26	2.5	100	∓30.5	∓1200		
27, 28	2.5	100	∓15.2	∓600	5.9	13
31, 32	2.5	100	∓15.2	∓600		

	Weight		Center of Gravity	
	1000 kg	1000 lb	m	in
Fuselage	131	288	-30.6	-1205
Wing	283	623	4.8	190
Aircraft	697	1534	-1.9	-73

$$EI_f = 8.6 \times 10^{10} \, N - m^2 \, (3 \times 10^{13} \, lb - in^2)$$

$$EI_w = 14.3 \times 10^{10} \, N - m^2 \, (5 \times 10^9 \, lb - in^2)$$

$$k_{gear} = 360\,000 \, N \cdot m \, (20\,600 \, lb/in)$$
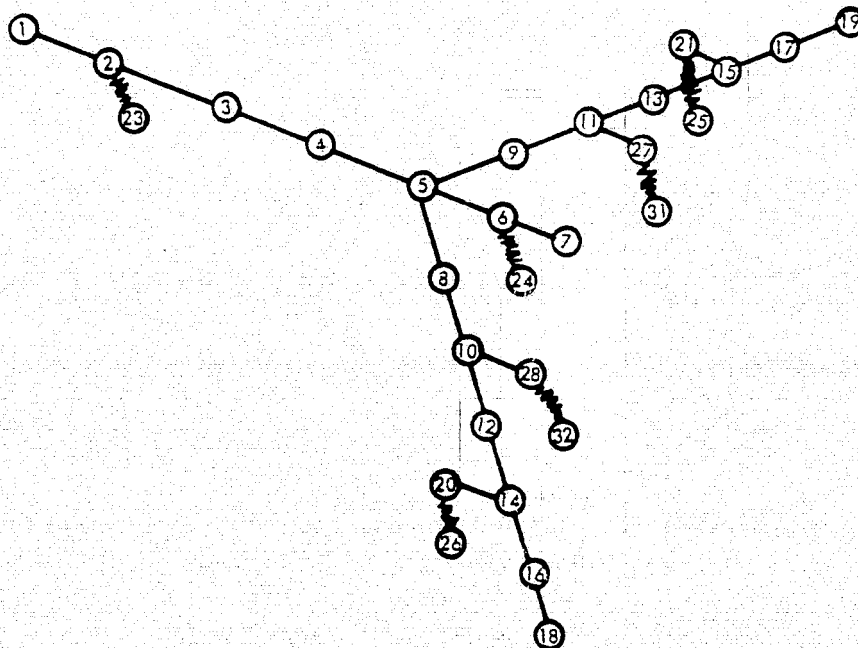
Figure 34. Model for Gear Deflection Study
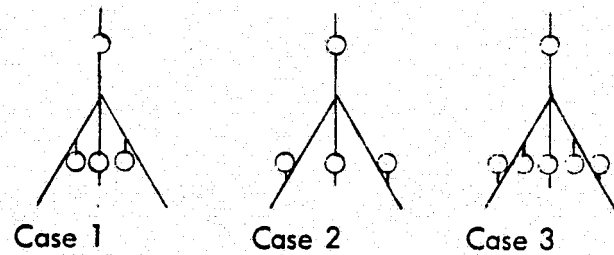
	Case 1	Case 2	Case 3
Tip Deflection, cm (in)	483 (190.2)	206 (81.0)	191 (75.4)
Max Moment, 10^6 N-m (10^6 in-lb)	50.9 (451)	27.8 (247)	23.8 (211)
Root Moment, 10^6 N-m (10^6 in-lb)	29.4 (261)	6.3 (56)	5.6 (50)
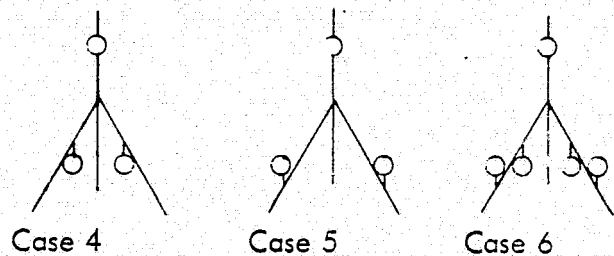
	Case 4	Case 5	Case 6
Tip Deflection, cm (in)	480 (188.9)	178 (70.3)	182 (71.9)
Max Moment, 10^6 N-m (10^6 in-lb)	50.9 (451)	27.2 (241)	23.8 (211)
Root Moment, 10^6 N-m (10^6 in-lb)	24.0 (213)	-12.9 (-119)	-0.055 (-0.49)

Figure 35. Summary of Gear Deflection Study

The first three cases considered include a main gear on the aft fuselage. A comparison of these cases with similar arrangements in later cases, for example, compare case 1 with case 4, showed that the aft fuselage mounted main gear resulted in greater tip deflection. The arrangement depicted for case 6 was selected as the best compromise for minimizing tip deflection and bending moments simultaneously. With the selected arrangement, four 8-wheel bogies permit a better weight distribution for the wing and on the runway pavement.

Wing bending loads were sensitive to the airload distribution, payload distribution, and landing gear tread width. Sensitivity studies were performed for various payload distributions to help assess the penalty for carrying cargo in the fuselage. Portions of the maximum payload of 272 155 kg (600 000 lb) were distributed with either 0 or 80 percent in the wing and 0 or 20 percent in the fuselage. Uniformly-distributed full and zero fuel loads were considered in combination with the payload

64

distributions to give a total of eight cases.

Wing bending loads for these cases are shown on Figure 36 for a 2.5-g steady pull-up maneuver at a cruise Mach number of 0.75 and an altitude of 10 670 m (35 000 ft). The results represent a rigid balance solution in which 1-g trim was achieved by canard incidence and elevator angle was used to balance the 1.5-g incremental moment. The highest wing root moments resulted for cases 3 and 7 which have the fuselage fully loaded but the wing cargo compartment empty. Rather than design the airplane for these peak loads, restrictions would be imposed requiring that wing cargo or ballast be carried whenever the fuselage is loaded.

The next most severe loads were encountered for cases 1 and 5 which have the maximum cargo uniformly distributed in both the wing and fuselage. Some reduction of the root bending moment could be obtained by either fuel management or by changing the airload distribution, but such alternatives open up an infinite number of possible load cases for configuration refinement. For this study, the peak loads of case 5 were used as the maximum wing upbending design requirements. Proper fuel management was assumed to alleviate the case 1 loads to the case 5 level.

During ground operations, the relatively high down loads on the wing are balanced by ground loads transmitted through the landing gear. As a result of the loading, that portion of the wing outboard of the landing gear reacts as a uniformly-loaded cantilever beam. The down-bending moment experienced along the wing is also shown on Figure 36 for a static 1-g ground condition. Allowing an incremental load factor of 0.5 for dynamic magnification to reach the 1.5-g design load-factor criteria for ground loads, the peak down-bending moment shown of 20.0 MN-m (185 × 10⁶ in-lb) was increased to 31.4 MN-m (278 × 10⁶ in-lb). This value is greater than the bending moment for case 5 at the gear location. Further outboard movement of the gear would be required to balance the bending moments at the gear location for flight and ground conditions.

4.1.2 Flutter Analyses

Analyses were performed to determine if any major flutter problems existed for the selected configuration design. As criteria for this determination, commercial guidelines (Ref. 10) were used which specify a minimum flutter speed of 1.2 times the aircraft dive speed. For the selected configuration, the guidelines prescribed a minimum flutter speed of 252 m/s (492 kts) EAS.

Configuration flutter speeds of 190 and 180 m/s (370 and 350 kts) were encountered in the anti-symmetric and symmetric modes, respectively. These speeds were well below the commercial design criteria and necessitated several configuration modifications to achieve acceptable values. The anti-symmetric flutter problem was eliminated by moving the engines forward, unsweeping the vertical tails, and shifting the vertical tails closer to the wing leading edge. As a result of these three changes, the anti-symmetric flutter speed was increased well above 257 m/s (500 kts) and the symmetric flutter speed improved

| | Fuel | | Cargo | | | |
| | | | Wing | | Fuselage | |
Case	1000 kg	1000 lb	1000 kg	1000 lb	1000 kg	1000 lb
1	176	388	218	480	55	120
2	176	388	218	480	0	0
3	176	388	0	0	55	120
4	176	388	0	0	0	0
5	0	0	218	480	55	120
6	0	0	218	480	0	0
7	0	0	0	0	55	120
8	0	0	0	0	0	0
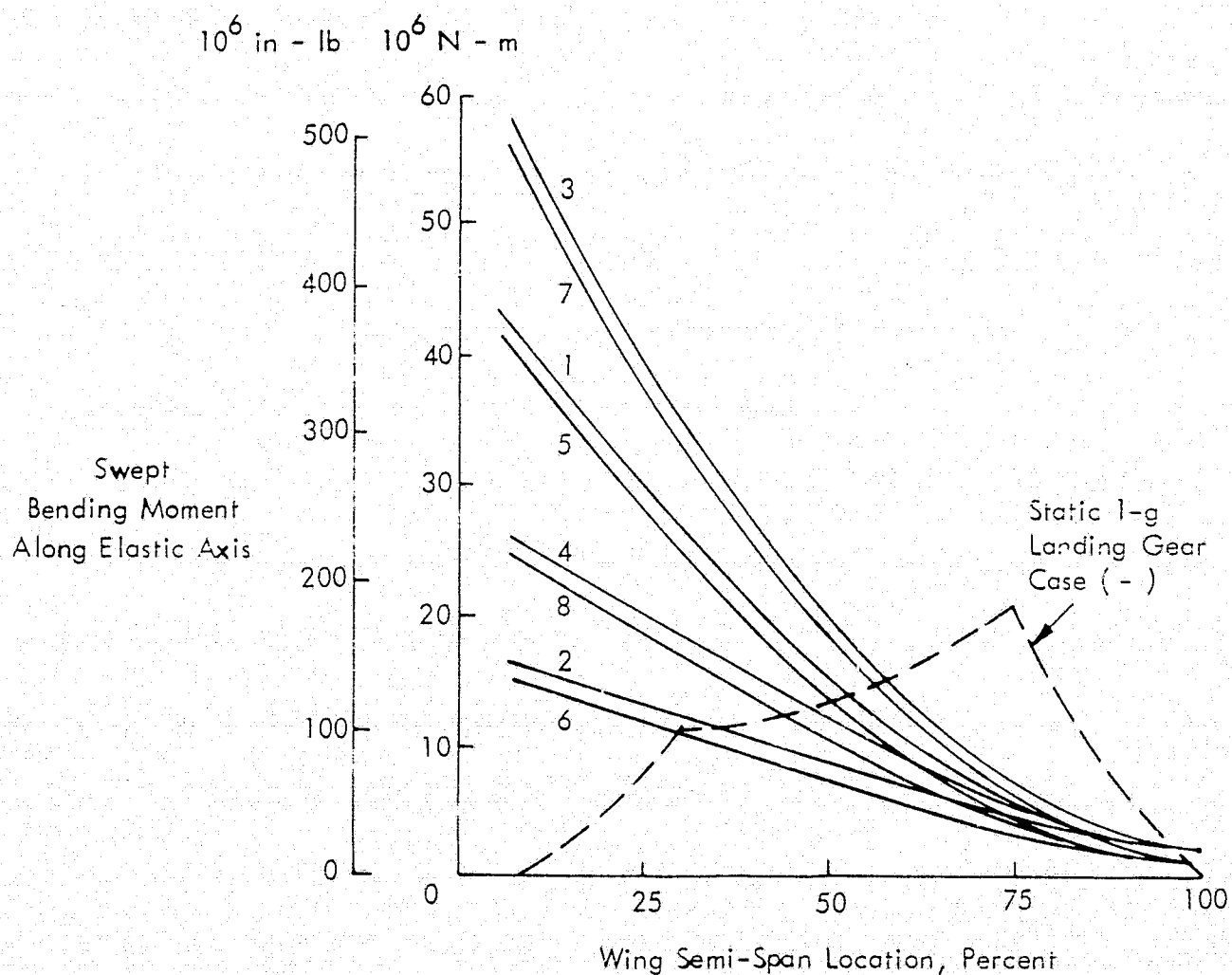
Figure 36. Effect of Variable Payload Distributions

66

to 208 m/s (404 kts). Further details on these changes are presented in Section 4.2.1.

Both active controls for flutter suppression and material tailoring to improve torsional stiffness offered the potential to overcome the symmetric flutter-speed problem The increase in torsional stiffness required was found from Figure 37. This curve was generated with representative aerodynamic data for a Mach number of 0.8 and an average altitude of 6700 m (22 000 ft). A nominal torsional stiffness of 10×10^9 N-m^2 (24.3 x 10^9 lb-ft^2) corresponds to the flutter speed of 208 m/s (404 kts). To achieve the desired minimum flutter speed of 252 m/s (492 kts), a torsional stiffness of approximately 16×10^9 N-m^2 (38.8 x 10^9 lb-ft^2) would be required. Such a value could be obtained without penalty through proper orientation of the plies in the composite material used for the wing structure.
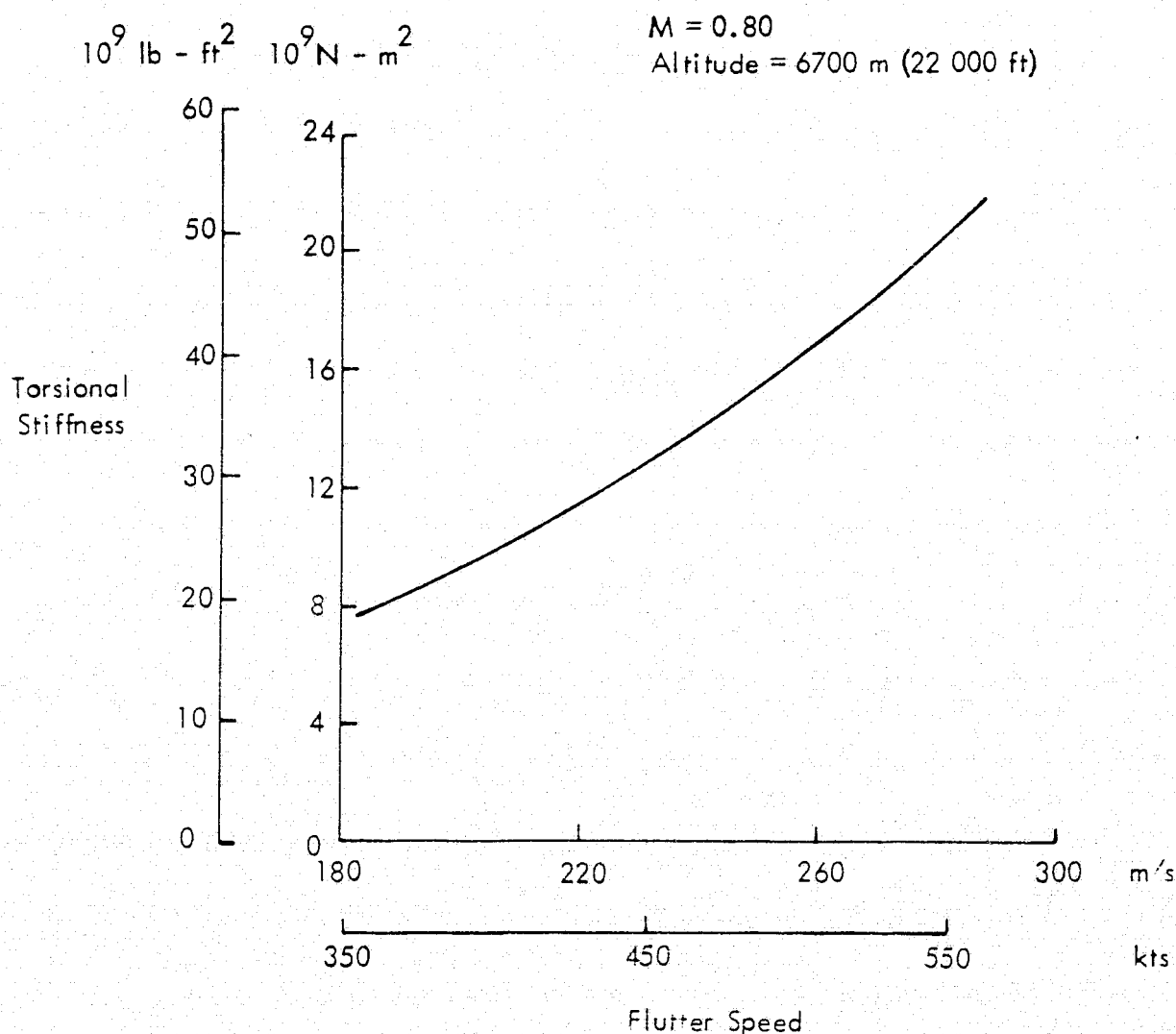
Figure 37. Torsional Stiffness for Flutter Suppression

67

If active controls are assumed to provide flutter suppression above the aircraft dive speed, the torsional stiffness required would drop to 9.4×10^9 N-m^2 (22.8×10^9 lb-ft^2). Since both alternatives offered equally feasible solutions, no further effort was expended on this problem.

4.1.3 Weight and Balance

Previously-existing Lockheed preliminary design parametric methods were used to estimate the weights of all aircraft components except the wing. As discussed in Section 3.2.3.1, preliminary structural analyses were performed on several baseline aircraft wing designs to determine the wing weights and an empirical relationship for predicting wing weights in parametric design studies.

Upon completion of modifications to the selected configuration to overcome flutter problems, the resulting final configuration was subject to further preliminary structural analysis to substantiate the weight estimates. A weight summary for the final configuration is presented in Table XVI. Due to the flutter modifications, the gross weight of the selected configuration was increased by approximately 4080 kg (9000 lb) in becoming the final configuration. Enlargement of the vertical tails to compensate for the reduced control moment arm as a result of the tail relocation was responsible for most of this increase.

The range of travel for the center of gravity for the final configuration is shown in Figure 38. These data were estimated based on the weight summary of Table XVI and the assumption that the payload and fuel were distributed symmetrically about the fuselage centerline.

The solid line envelope is for the design "X-point" mission, while the dashed line envelope is for the "Y-point" mission. Two different loading sequences are shown for both missions to establish the limits of travel for the center of gravity. In reality, the aircraft would not be loaded according to the sequences shown because during the process the aircraft center of gravity would be shifted outside the acceptable 3 to 15-percent MAC range with damaging consequences. Obviously, the wing and fuselage need to be loaded somewhat simultaneously and in some instances must be accompanied or preceded by partial or full fuel loading.

For the design mission gross weight, the center of gravity is at 8 percent MAC. The center of gravity for the alternate mission gross weight can be shifted throughout the entire allowable range by various loading arrangements. For off-design missions, the loading distribution must be checked to assure that the cargo distribution is compatible with center-of-gravity shifts that occur during flight due to fuel burn-off.

4.1.4 Effect of Unpressurized Cargo Compartment

Most of the wing structure, including that in the cargo compartment, was designed

TABLE XVI. FINAL CONFIGURATION WEIGHT SUMMARY

	kg	lb
Wing	109 594	241 614
Canard	7 358	16 221
Vertical Tail	6 093	13 433
Fuselage	21 309	46 978
Landing Gear	32 013	70 576
Nacelle	11 107	24 487
Propulsion	32 331	71 277
Systems and Equipment	21 521	47 445
Weight Empty	241 32	532 031
Operating Equipment	7 429	16 378
Operating Weight	248 753	548 409
Payload	272 155	600 000
Zero Fuel Weight	520 910	1 148 409
Fuel	179 104	394 857
Gross Weight	700 014	1 543 266

for bending, torsional rigidity, or other critical loads. Through judicious design layout, part of the structure was arranged to fulfill a double function by providing a pressurized cargo compartment in the wing at a small structural weight penalty.

The pressurization system weight was estimated to be 1996 kg (4400 lb), all of which could be removed for a non-pressurized compartment. By designing the aircraft without pressurization, an additional 1043 kg (2300 lb) savings in fuel and structural weight would be realized due to the reduced loads and gross weight. Thus, the total weight penalty for the pressurized cargo compartment was 3039 kg (6700 lb).

4.2 DESIGN REFINEMENT ANALYSES

Several features of the selected configuration were analyzed in a series of refinement studies. As a result of the flutter studies discussed in Section 4.1.2, the engines were relocated and the vertical tails were redesigned and relocated. Studies pertaining

69
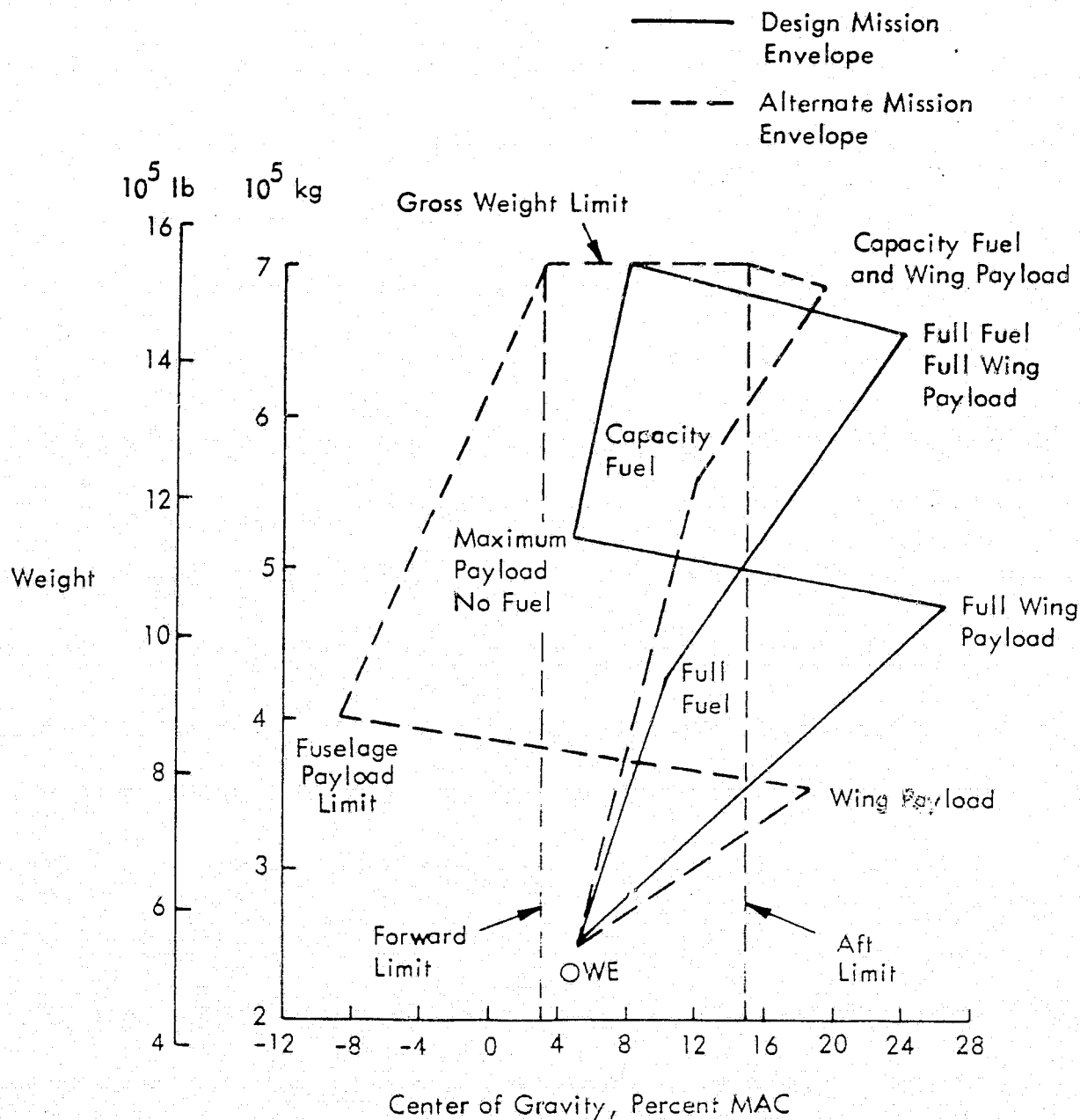
Figure 38. Center of Gravity Envelope

to the landing gear were made to select positions for gear mounting and stowage. In designing a fuel system to fit in the aircraft wing, several different tank concepts and locations were considered. Cargo loading and potential problems were analyzed to ascertain that no insurmountable obstacles would be encountered. The design refinements inaugurated by these studies and the problem areas considered are discussed hereafter.

4.2.1 Effects of Flutter on Design

Flutter analysis revealed both symmetric and anti-symmetric flutter modes at speeds well below the critical flutter speed of 252 m/s (492 kts) for the selected configuration. To solve this flutter problem, it was necessary to move certain aircraft masses to a more forward position relative to the wing elastic axis. Consequently, the vertical tails were redesigned and relocated, and the engines were repositioned.

The before and after sketches shown on the left and right, respectively, of Figure 39 illustrate the changes in the design and wing attachment point of the vertical tails. The 0.7 rad (40 deg) sweep and the aft wing position characteristics of the selected configuration vertical tails were beneficial in providing a yaw control moment arm of 30.5 m (100 ft). Changes to the sweep angle and the relocation of the vertical tails to overcome the flutter problem reduced the moment arm to 22.5 m (73.9 ft). To compensate for this reduction, the area of each vertical tail increased from 136 m^2 (1472 ft^2) to 166 m^2 (1780 ft^2) to maintain the same control capability. The weight of each vertical tail increased by 770 kg (1694 lb) as a result of this additional area.
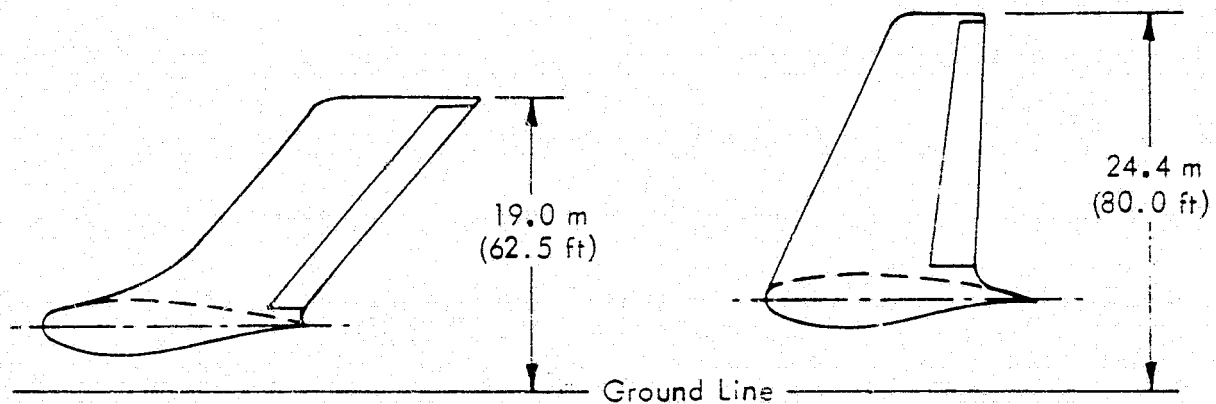
	SELECTED CONFIGURATION	FINAL CONFIGURATION
Sweep, rad (deg)	0.70 (40)	0.35 (20)
Area, m^2 (ft^2)	137 (1472)	166 (1780)
Aspect Ratio	1.5	1.96
Taper Ratio	1.0	0.4

Figure 39. Vertical Tail Modifications for Flutter Solution

71

The larger overall aircraft height resulted from a combination of greater vertical tail span due to changes in sweep, area, and taper and of increased landing gear length to provide outboard engine clearance. Moving the engines forward and beneath the wing as part of the flutter problem solution, resulted in a landing gear length increase of 1.37 m (4.5 ft) to maintain a minimum ground clearance of 0.92 m (3.0 ft). This subject is discussed further in Section 4.2.2.

In relocating the engines, it was recognized that the 210 000 N (47 100 lb) thrust level of the 8 engines on the selected configuration was considerably lower than projected state-of-the art thrust levels for 1990. By changing to 283 000 N (63 800 lb) thrust engines consistent with future technology, the total number of engines was reduced to 6 for the final configuration. A net decrease in gross weight of 613 kg (1350 lb) was realized by reducing the number of engines and moving them forward. This decrease resulted partially from shorter engine pylons and less drag.

Figure 40 shows a relocated-engine and wing arrangement. As noted on the figure, the engines are housed in nacelles having a maximum diameter of 2.9 m (9.6 ft) and a length of 7.3 m (23.8 ft). The engine inlet is approximately one-half the nacelle length forward of the wing leading edge; and the wing-nacelle separation distance is over one-half of the nacelle diameter.
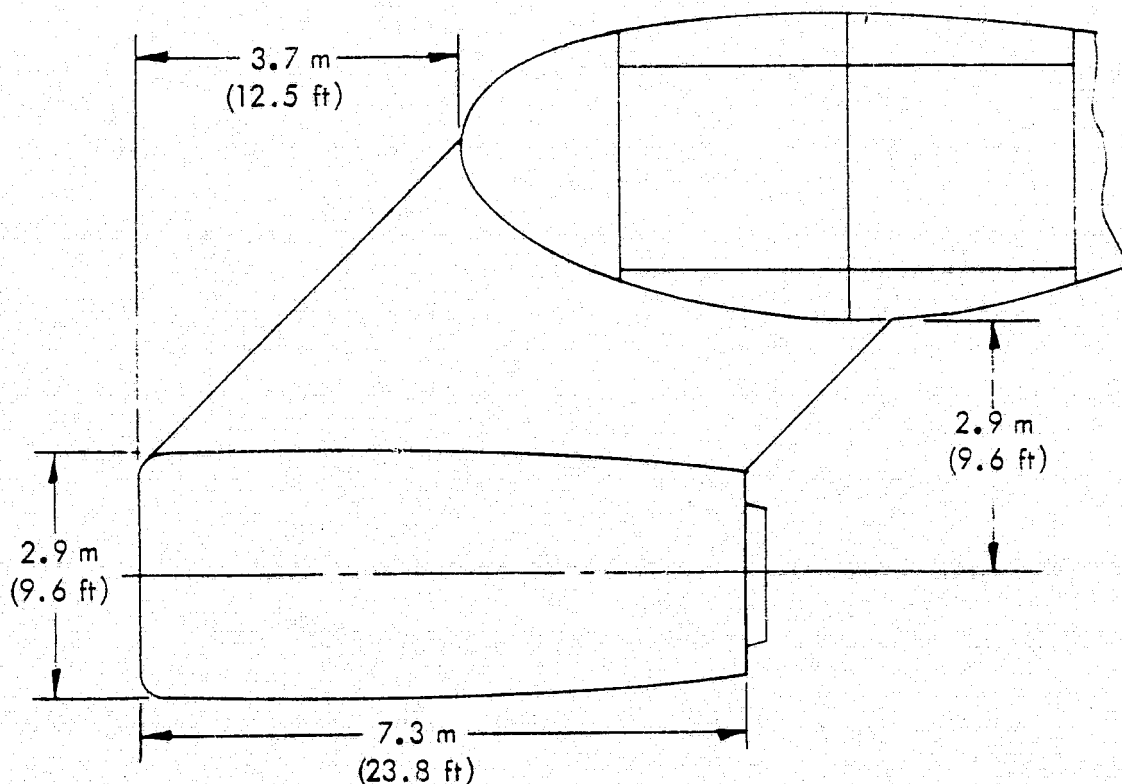
Figure 40. Engine Mounting Arrangement

4.2.2 Landing Gear Placement

Structural studies indicated that the gear arrangement for case 6 in Figure 35 offered the best compromise for minimizing both wingtip deflections and bending moments. The actual gear arrangement used varied slightly from that of case 6 to assure compatibility with the flutter problem solution. This arrangement, along with the various flutter modifications, on the final configuration are shown in Figure 41.

The main gear consists of four 8-wheel bogies attached at the 57-percent wing chord line. The inboard and outboard bogies are located 21.4 m (70 ft) and 33.2 m (109 ft), respectively, from the aircraft center line. The main gears retract inboard and forward for stowage between the rear cargo compartment beam and the flap beam, as shown on Figure 42. Negligible drag is produced by the landing gear fairing since it has a relatively small frontal area and is located well aft on the wing lower surface. Retraction is accomplished by pivoting the bogie 1.57 rad (90 deg) about the strut followed by a 0.7 rad (40 deg) rotation of the strut about its vertical axis for alignment with the wheel well.

The total landing gear arrangement is completed by a forward retracting 4-wheel nose gear which carries approximately 10 percent of the aircraft gross weight. Tire size at all positions is 1.27 m x 0.46 m (50 in x 18 in).

There is a relative longitudinal displacement of 10.5 m (34.5 ft) between the inboard and outboard main gears. Because of the displacement, a hydraulic system is required to extend the forward gears and retract the aft gears during takeoff rotation. A maximum takeoff rotation angle of 0.09 rad (5 deg) is achievable.

Figure 43 shows the effect of 1-g and 1.5-g wing deflections on landing gear strut length and outboard engine ground clearance. The outboard engine clears the ground by 1.46 m (4.8 ft) under 1-g conditions and by 0.91 m (3.0 ft) under 1.5-g conditions. To satisfy these clearances, the outboard main gear length is 7.5 m (24.5 ft) and the inboard gear length is 7.9 m (25.8 ft), both measured relative to the wing neutral axis. With these gear lengths, the distance from the ground to the lower surface of the wing is 4.2 m (13.8 ft). The distance from the ground to the cargo floor is 5.1 m (16.7 ft) at the wing tip and 6.7 m (22.0 ft) at the fuselage.

When the engines were relocated forward and beneath the wing as part of the flutter problem solution, it was necessary to respace the main landing gear to assure sufficient tire clearance from engine exhaust in the gear extended position and throughout the gear retraction cycle. Figure 44 reflects the main landing gear and engine relative locations for the final configuration. The distances used were intended to limit the maximum engine exhaust temperature experienced by the tires to 366 K (200°F).

101 m (331 ft)

37 m (120 ft)

41.1 m (135 ft)

66.5 m (218 ft)

Design Cargo Density - 160 kg/m^3 (10 lb/ft^3)
Number of Rows - 2 Per Side

24.4 m (80 ft)

90.5 m (297 ft)
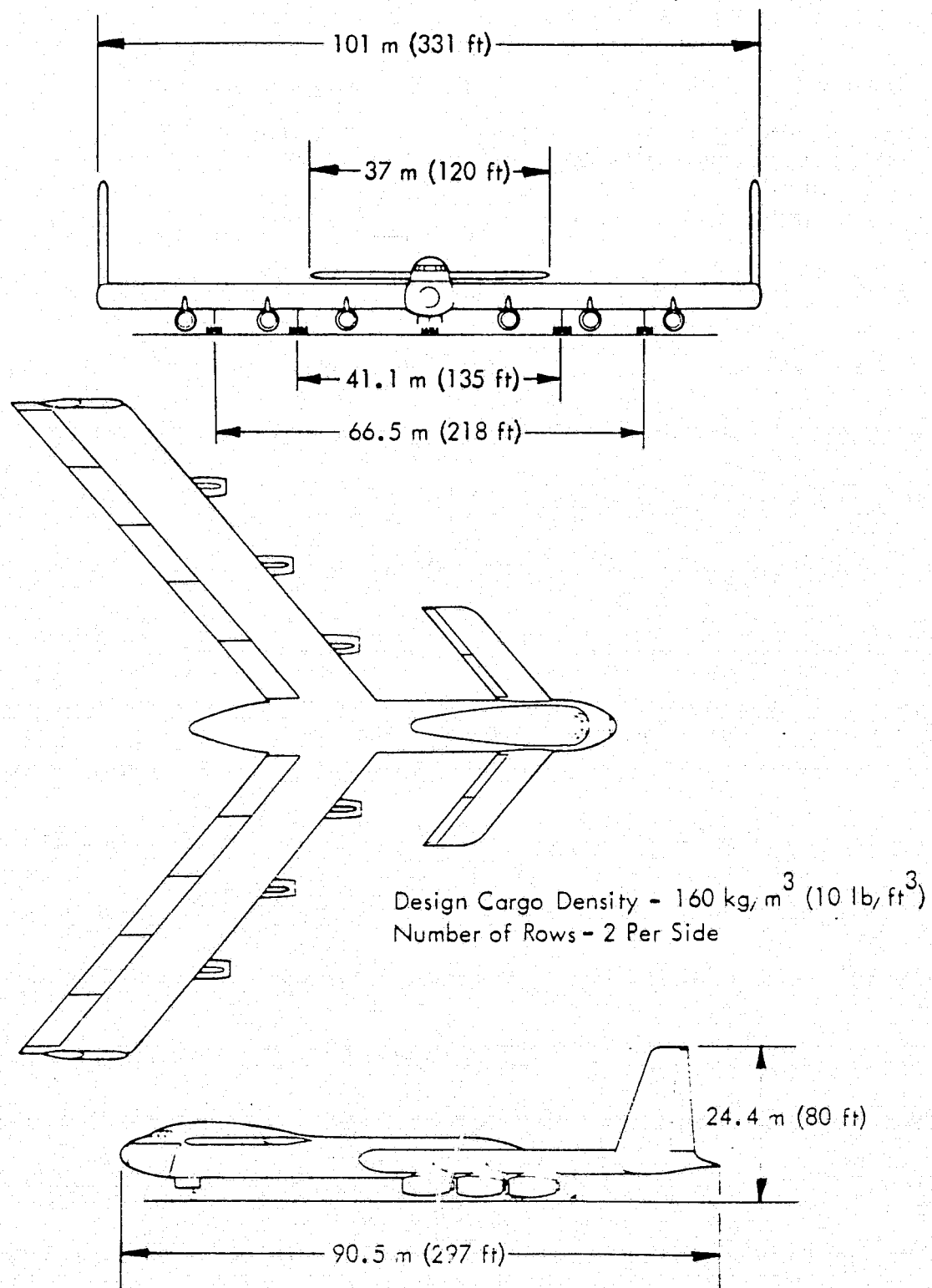
Figure 41. Final Configuration

74
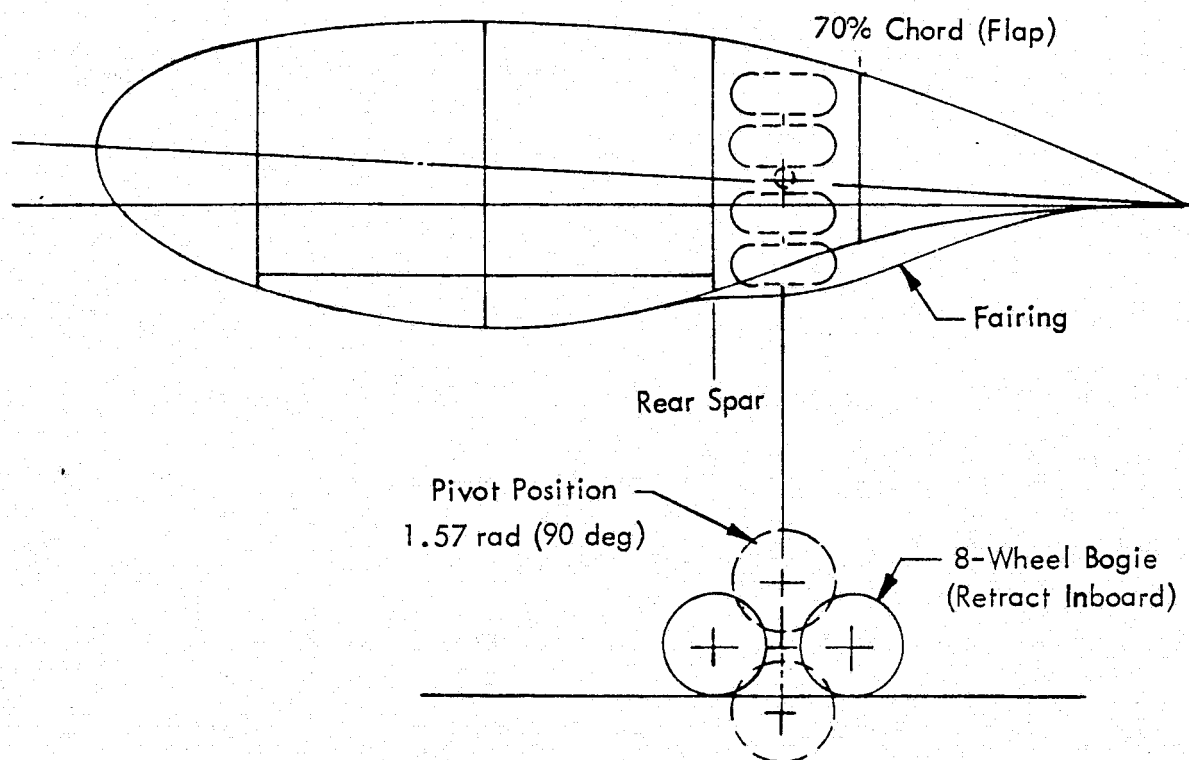
Figure 42. Main Landing Gear Stowage
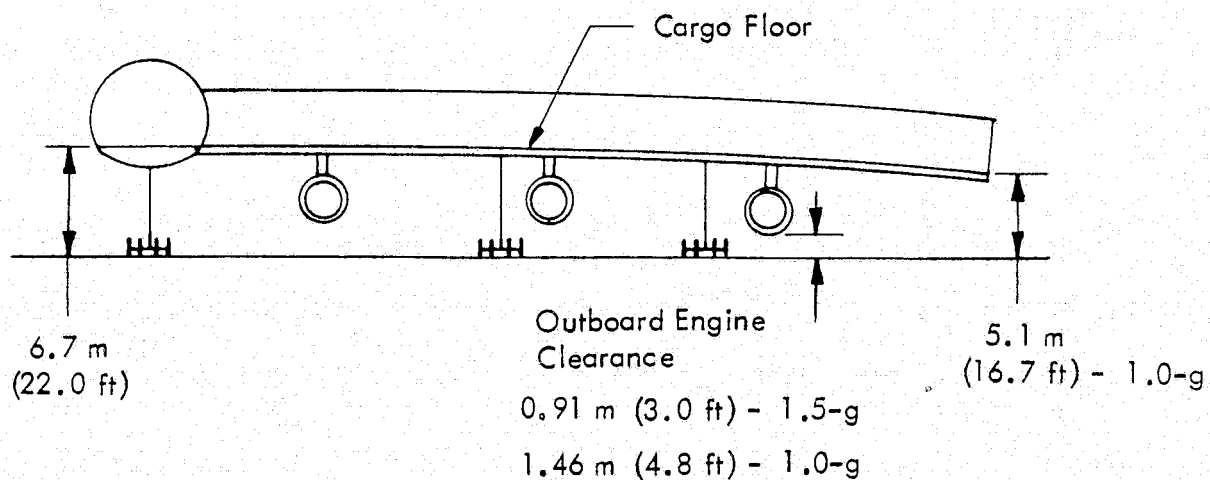
Figure 43. Wing Deflection

3.05 m (10 ft) Exhaust Core Clearance (Typical)

3.68 m (12 ft) Exhaust Core
Clearance (Typical)
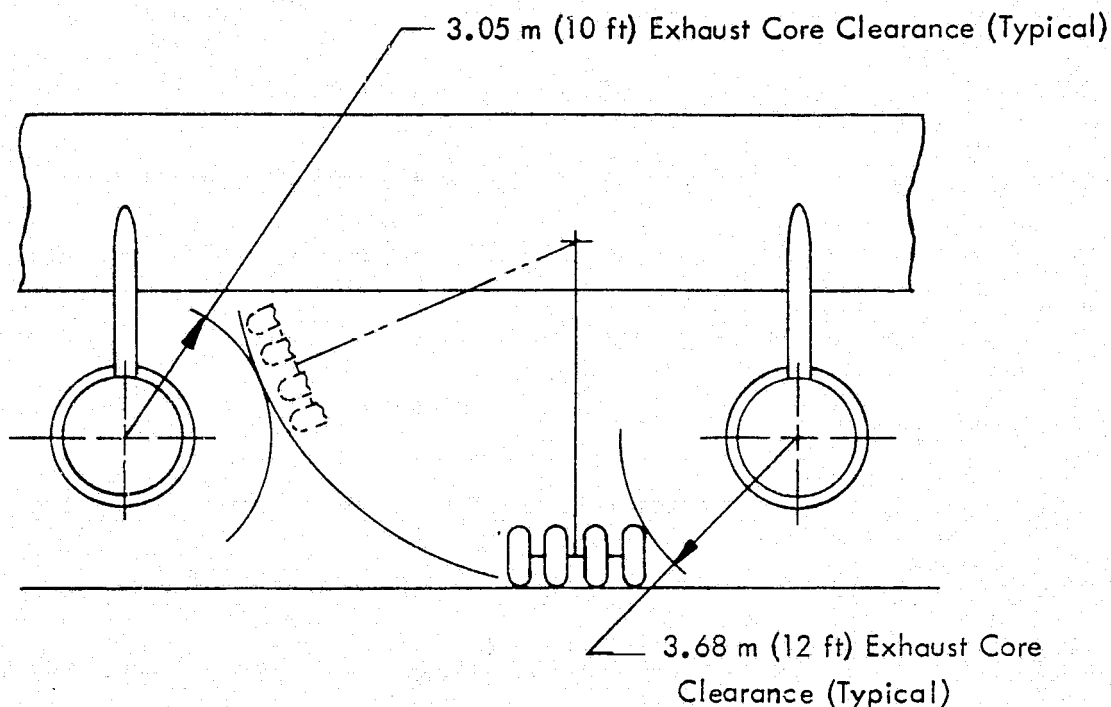
Figure 44. Landing Gear - Engine Exhaust Core Clearance

4.2.3 Fuel Volume Analysis

Based on the engine cruise specific fuel consumption characteristics, the taxi-takeoff fuel requirements and fuel reserves, it was established that a fuel volume of 368 m^3 (13 000 ft^3) would be required to fly a 11 100 km (6000 n.mi.) mission. Figure 45 shows the spaces in the wing leading edge and beneath the cargo floor that were considered for fuel storage. It also shows both integral tanks and a separate cylindrical tank in the wing leading-edge space, which were investigated.

The maximum diameter cylindrical tank that can be installed in the wing leading edge is 1.68 m (5.5 ft). This yields a tank cross-sectional area of 2.2 m^2 (23.8 ft^2) and a volume of 234 m^3 (8280 ft^3) over the 107 m (350 ft) of usable wing span. Allowing 10 percent for structure, baffles, tank sectioning, etc., produced a net volume of 211 m^3 (7450 ft^3). Since 368 m^3 (13 000 ft^3) of fuel volume were required, the wing leading-edge cylindrical tank by itself proved unsatisfactory. Even if the tank were continued from wing tip to wing tip for the full 122 m (400 ft) of structural span, the fuel volume would be insufficient.

Quite coincidently, the cross-sectional area and volume underneath the wing cargo floor turned out to be the same as for the cylindrical tank. By itself this fuel system would also be inadequate. A dual tankage system involving both of the foregoing approaches would be more than sufficient and would offer one distinct advantage of a limited center-

76

212 m^3 (7500 ft^3) Usable Volume

1.68 m (5.5 ft) Tank Diameter
212 m^3 (7500 ft^3) Usable Volume

396 m^3 (14 000 ft^3) Usable Volume

Tank Length 107 m (350 ft)
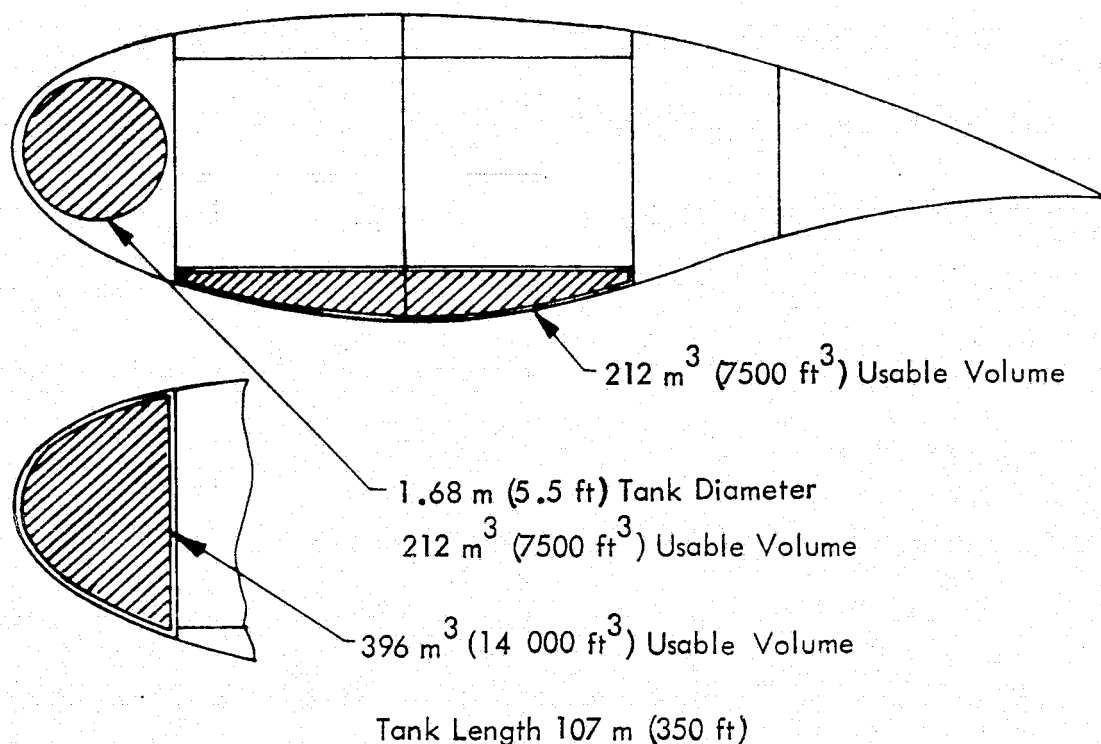
Usable volume based on 10 percent allowance for structure, equipment, baffles, etc.

Figure 45. Fuel Tank System

of-gravity travel control system. The dual system had an overriding disadvantage in that excess weight and cost would be incurred in the fabrication and installation of tanks and equipment for two separately-located fuel supply systems. Hence, this concept was discarded.

The concept selected for the fuel system uses an integral tank and occupies the entire volume in the wing leading edge. With a tank cross-sectional area of 4.12 m^2 (44.4 ft^2), a usable volume of 396 m^3 (14 000 ft^3) was obtained for the 107 m (350 ft) of length available. This value includes the 10 percent allowance for unusable space. More than sufficient volume was provided by this concept, and it contributed favorably toward a more forward center of gravity, which is desirable for aircraft balance. This system also offered the advantage of reducing the flutter problem.

4.2.4 Cargo Loading Analysis

To minimize aircraft turnaround time and to maintain aircraft static balance, it was assumed that cargo loading would normally occur in a symmetrical pattern – that is, both wing tip openings and/or nose visor door opening. There could be circumstances, however, under which aircraft loading from a single point would be either desired or required. To this extent, studies were performed to determine aircraft configuration requirements for

single point loading of 2.44 m x 2.44 m (8 ft x 8 ft) containers up to 12.2 m (40 ft) in length.

Shown previously in Figures 4 and 5 are the minimum widths of 5.2 and 5.5 m (17 and 18 ft) for the fuselage and wing cargo compartments, respectively, to accommodate two rows of containers. Using these widths, it was determined that the aircraft could be fully loaded with 6.1 m (20 ft) long containers from a single point, but that 12.2 m (40 ft) containers could not be moved from one section to another. Figure 46 shows the technique for single point loading of 6.1 m (20 ft) containers. In moving a container from one wing side to the other, the container transitions between the wing and fuselage identical to the movement experienced from nose loading. Similar single point loading of 12.2 m (40 ft) containers would require a much wider fuselage cargo floor, removal of a large inboard section of the center spar, or a combination of both.
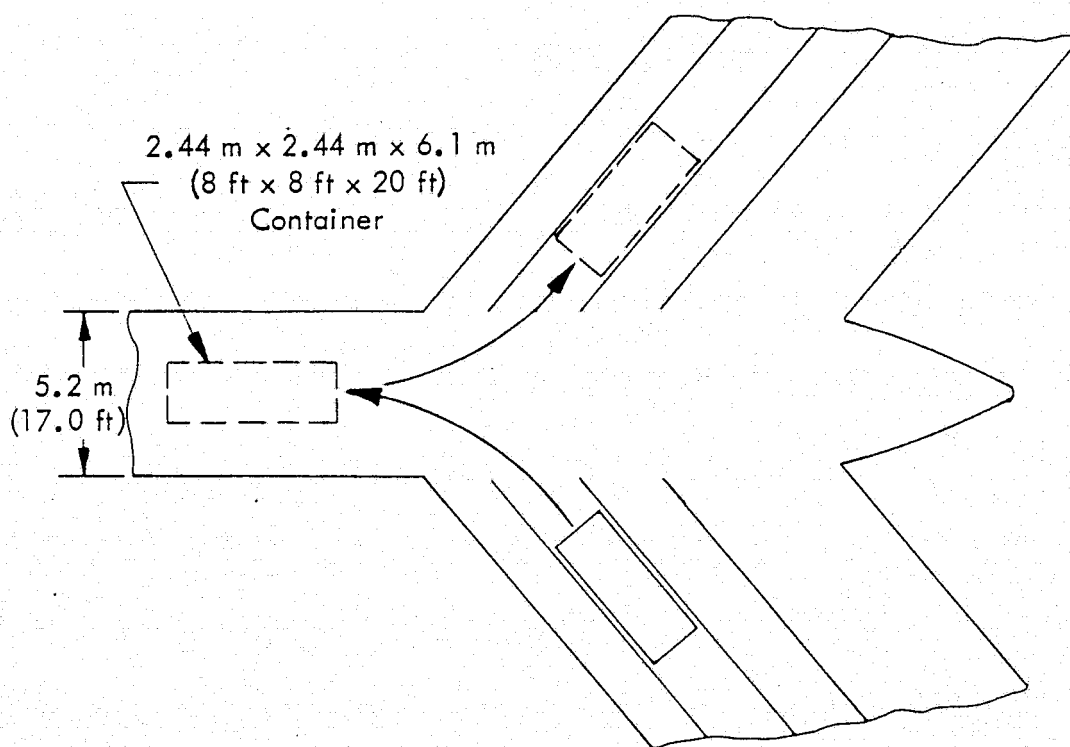
Figure 46. Single Point Loading Technique for 6.1 m (20 ft) Containers

The preponderance of commercial containers today are 6.1 m (20 ft) in length. Containers of 12.2 m (40 ft) lengths have been predicted as the way of the future. Any attempt to confirm this prediction would be beyond the scope of this study and would probably prove futile. Thus, 6.1 m (20 ft) was accepted as design criterion for single-point loading.

78

Container locking restraints and roller assemblies are similar to those used on the C-5 aircraft. The fuselage cargo compartment rollers are flush type or "flip-flop" rollers since this compartment also serves wheeled and tracked vehicles. Wing cargo compartment rollers are permanently installed since containers are the only type of cargo transported therein.

Access to wing cargo compartment containers is not available once the containers are loaded. Electro-mechanical indicators are required to assure proper engagement of the container restraints. Access to the fuselage cargo compartment containers is limited, but available, since this compartment has a height of 4.1 m (13.5 ft) for outsized equipment.

External support for the wing and special loading systems are required to compensate for the high cargo floor heights above the ground and for static wing deflections, such as those shown earlier in Figure 43. Figure 47 illustrates an adaptable technique for loading whereby an adjustable-powered wing-cradle jack is used to stabilize the wing, and an adjustable rail-mounted conveyor flat bed positions the cargo at the wingtip openings.
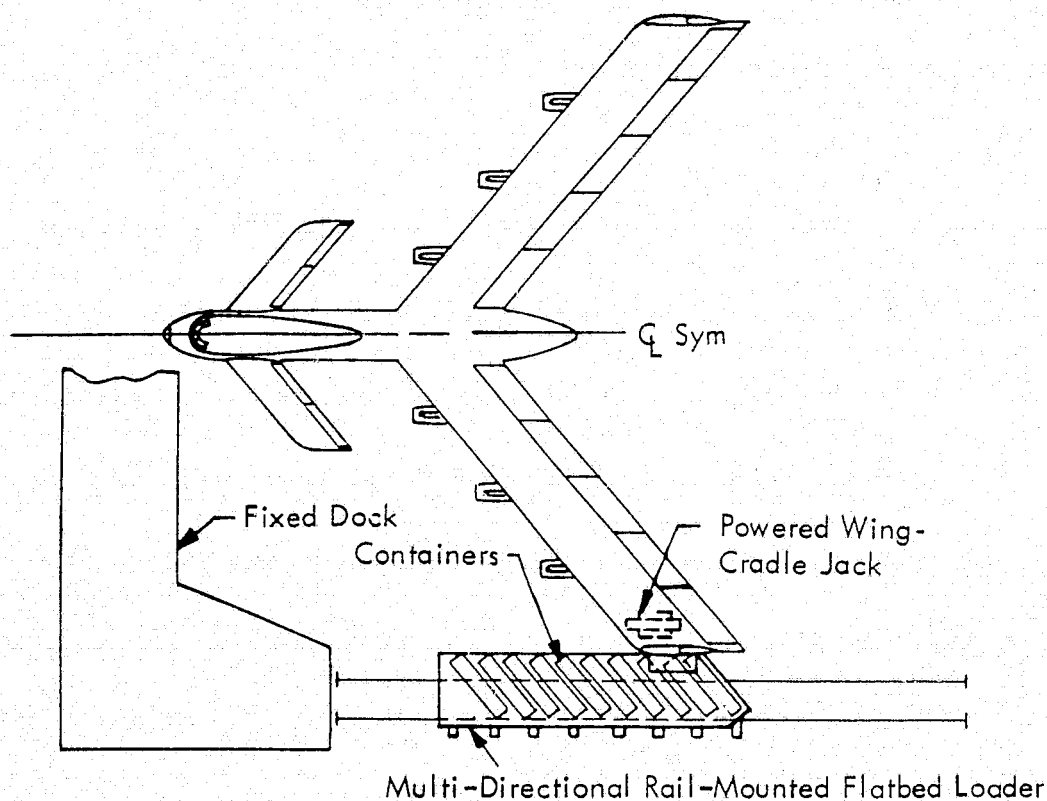
Figure 47. Wing Loading Concept

An aircraft integral ramp is used for nose loading. Loose equipment support jacks are used for straight-in loading and to prevent excessive nose gear loads during the loading of outsized equipment.

4.3 FLIGHT SCIENCES ANALYSES

Analyses of the final configuration were performed to check earlier assumptions pertaining to the propulsion system and the stability and control system and to refine the estimated levels of performance.

4.3.1 Propulsion System Analysis

Preliminary studies (Section 3.2.1.3) had indicated that the optimum bypass ratio was 4.5 for a modified Pratt & Whitney STF-429 engine applied to a span-loaded aircraft. A sensitivity study confirmed that higher bypass-ratio engines on the final configuration were non-optimum. The results of this study in Table XVII show that

TABLE XVII. ENGINE BYPASS RATIO SENSITIVITY STUDY RESULTS

Bypass Ratio	4.5	6.0	8.0
Cruise SFC, kg N-hr	0.064	0.062	0.061
lb lb-hr	0.63	0.61	0.60
Aircraft Weight, kg	694 470	700 187	719 819
lb	1 543 266	1 555 970	1 599 598
Engine			
Weight, kg	4 039	4 797	5 041
lb	8 976	10 560	13 425
Thrust, N	283 525	313 127	359 493
lb	63 857	70 524	80 767
Thrust, N kg	69.5	64.7	58.9
lb lb	7.11	6.62	6.03
DOC, c T-km	3.61	3.66	3.79
c T-nm	6.78	6.88	7.13
15-Year Total Cost, Billion $	114.67	116.38	120.63

as the bypass ratio was increased from 4.5 to 6.0 and 8.0, undesirable increases were experienced in aircraft weight, direct operating costs, and 15-year life-cycle costs.

80

Extra weight associated with the higher bypass-ratio engines exceeded the gain from improved specific fuel consumption and resulted in poor aircraft designs. Use of lower bypass-ratio engines was precluded by noise problems and additional insulation weight to meet FAR 36 regulations (Ref. 11) minus 10 EPNdB projected for the 1990 time period.

4.3.2 Stability and Control Analysis

Basic and dynamic stability characteristics provided by the flight controls of the final configurations were compared to the design criteria and guidelines outlined in Section 3.2.1.4. Handling qualities, an area normally included in a discussion of stability and control, was not addressed in this study but is the subject of several recommendations in Section 8.0.

Flight control systems on the final configurations were found to be adequate for the established design criteria. A check of the basic static longitudinal stability confirmed that the aircraft design was consistent with conventional aerodynamic practice of having the aircraft center of gravity forward of the neutral stability point for the tail-off configuration. The final span-loaded configuration has a center-of-gravity range of 3 to 15-percent MAC, while the neutral point is at 22-percent MAC. This provides a low-speed minimum stability margin of 7 percent; 2 percent greater than required by the design criteria. With this margin, artificial augmentation is not needed.

The wingtip-mounted vertical surfaces, which provide directional stability, gave an estimated change in moment coefficient of 0.0011. The canard longitudinal-control system was not a factor in basic aircraft stability but did provide inputs during dynamic conditions and high Mach number instabilities. The canard surface size was verified as adequate for both standard critical cases of stall out of ground effect and of nose wheel lift-off at 80 percent of stall speed for the most forward center-of-gravity condition.

Three areas of dynamic stability that often pose problems for large aircraft are:

o   Short-period longitudinal oscillations

o   Long-period (phugoid) longitudinal oscillations

o   Lateral-directional oscillations

During development of the C-5 aircraft, it was found that the short period longitudinal oscillations were approximately three times longer than expected. Also, these oscillations were heavily damped. Based on this background and with an artificially-damped longitudinal control system, short-period longitudinal oscillations are not expected to be a problem area for large span-loaded aircraft.

Damping of the long-period phugoid longitudinal oscillation is predominately a function of aircraft lift-to-drag ratio. Since the lift-to-drag ratio of the span-

loaded aircraft corresponds to those of conventional large aircraft, similar phugoid oscillation damping is expected.

Lateral-directional oscillations, resulting from the coupling of forces about these two axes, are the classical dynamic stability and control problem for large swept-wing aircraft. This problem is magnified at low speeds by the influence of the effective dihedral on the swept wings.

The minimum value of 0.15 and the maximum of 0.35 recommended by Ref. 12 for the product of frequency and damping ratio for aircraft of the C-5, B-747, and larger-size category are shown in Figure 48. Points on the figure designate the characteristics of the final span-loaded configuration both with and without augmentation in the form of inputs to the rudders and ailerons.
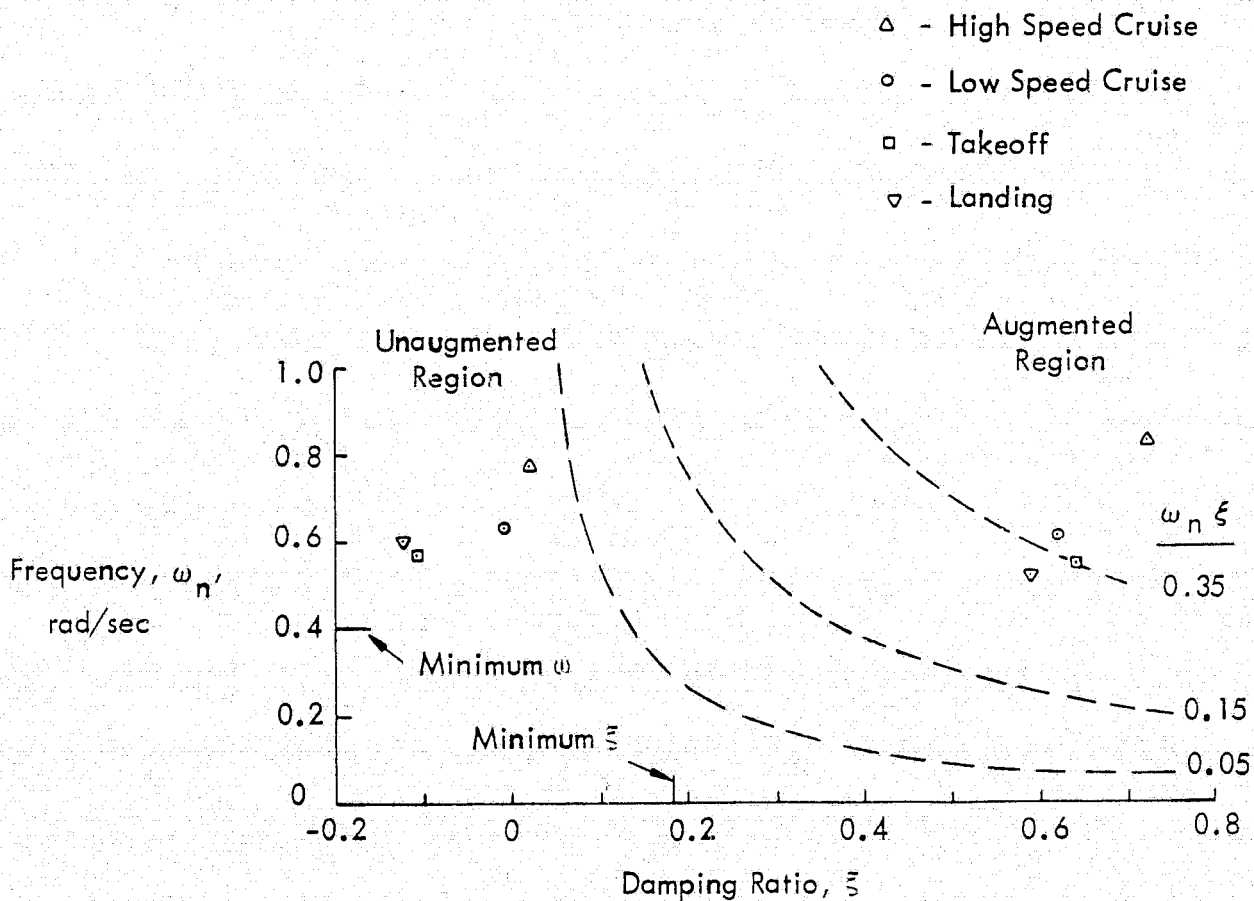
Figure 48. Dutch Roll Oscillation Characteristics

During C-5 flight tests, favorable pilot ratings were obtained, even with very low damping, due to the relatively long period of the oscillations. These oscillations were very controllable and did not increase the pilot work load as much as a shorter period oscillation would. In the C-5 tests, a value of 0.05, also shown on Figure 48, for the product of frequency and damping ratio was found to be pilot acceptable even though it was only one-third of the minimum value recommended by Ref. 12. Thus, it appears that considerably-less damping authority is required than is available with the proposed augmentation system.

4.3.3 Aerodynamic Performance

An assessment was made of the drag buildup for the final configuration, using a methodology similar to that described in Section 3.2.1.2. The drag for each of the major aircraft components and the total drag buildup are listed in Table XVIII. A lift-to-drag ratio of 19.71 was obtained for the final configuration based on this drag estimate and the cruise lift coefficient value of 0.412 given by the drag polar in Figure 49.

TABLE XVIII. DRAG BUILDUP

PROFILE DRAG		INDUCED DRAG	
Aircraft Components	Drag		
Wing	0.0070	Cruise Lift Coefficient	0.412
Fuselage	0.0012	Efficiency Factor	0.90
Pylon	0.0002	End-Plating Correction	1.3433
Nacelles	0.0006	Induced Drag	0.0077
Horizontal Tail	0.0010		
Vertical Tail	0.0011	TOTAL DRAG	
Total for Components	0.0111	Profile Drag	0.0121
Interference	0.0004	Induced Drag	0.0077
Roughness	0.0002	Trim Drag	0.0001
Miscellaneous	0.0004	Compressibility Drag	0.0010
Total Profile Drag	0.0121	TOTAL	0.0209

LIFT DRAG RATIO = 0.412/0.0209 = 19.71

M = 0.75
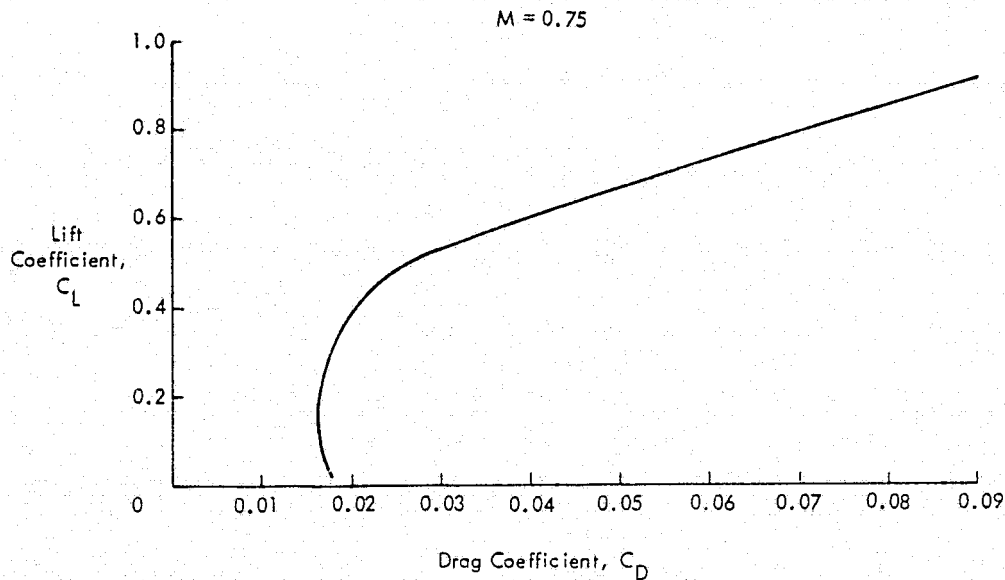
Figure 49. Drag Polar for Final Span-Loaded Configuration

Figure 50 shows the 30-percent-chord, double-flap, high-lift device used along the entire wing trailing edge to provide excellent airport performance characteristics for the aircraft. A maximum streamwise deflection of 0.7 rad (40 deg) is permitted for the aft flap. During the flap deflection process, the fore-flap deflection lags that of the aft flap by 0.175 rad (10 deg).
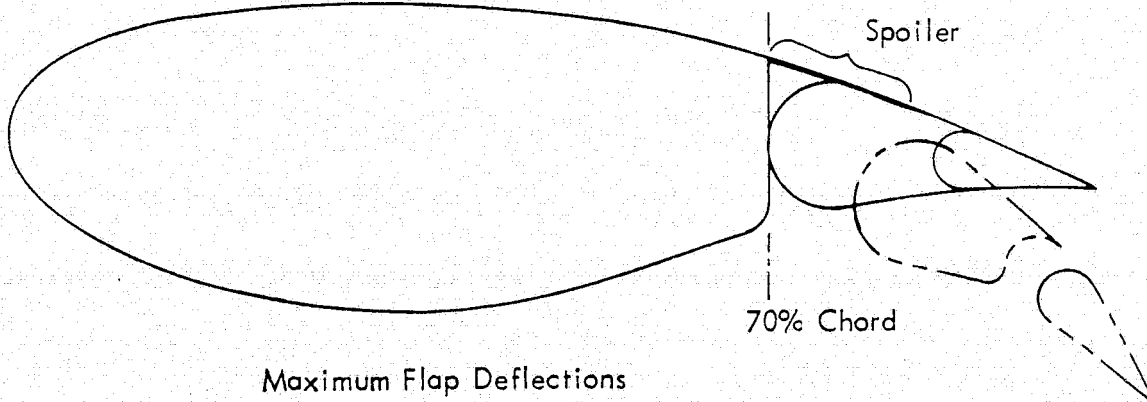
Maximum Flap Deflections

Aft Flap - 0.700 rad (40 deg)

Fore Flap - 0.525 rad (30 deg)

Figure 50. Double-Flap High-Lift System

84

The lift, drag, and pitching moment characteristics for this high lift system are presented in Table XIX. During the deflection process, the flap system extends aft by 7 percent of the chord length to compensate for the reduction in total flap effectiveness caused by the wing sweep.

TABLE XIX. HIGH-LIFT SYSTEM PERFORMANCE DATA

Streamwise Deflection Angle, rad (deg)		Lift Coefficient*		Drag Coefficient**		Moment Coefficient Increments
Fore Flap	Aft Flap	Flaps	Total	Flaps	Total	
0.175 (10)	0.350 (20)	0.56	2.16	0.040	0.0607	0.23
0.350 (20)	0.525 (30)	0.78	2.38	0.055	0.0757	0.31
0.525 (30)	0.700 (40)	0.90	2.50	0.084	0.1047	0.36

* Maximum Clean Lift Coefficient Equaled 1.6

** Clean Profile Drag Coefficient Equaled 0.0207

Takeoff performance estimates were made of the critical field length and of the normal takeoff distance over a 15.2 m (50 ft) obstacle. In the critical field length analysis, the aircraft was accelerated to critical-engine failure speed, and then, either stopped or further accelerated on five engines for takeoff over a 10.7 m (35 ft) obstacle. The critical-engine failure speed was selected so that the total distance to stop equalled the total distance to clear the obstacle. The critical field length of 1830 m (6000 ft), as determined in Figure 51, included a two-second decision time at critical-engine failure. Also, a friction coefficient of 0.3 was assumed for braking, and reverse thrust was not applied.

The normal takeoff distance over a 15.2 m (50 ft) obstacle was determined for a standard day and all six engines operative. The aircraft was rotated 0.058 rad (3.3 deg) before the takeoff speed of 1.2 times the stall speed was reached. With this rotation angle, there remained a comfortable margin relative to the maximum allowable rotation angle of 0.087 rad (5 deg). Table XX shows the derivation of the required rotation angle for both the takeoff and landing operations. Parameters used in calculating the normal takeoff distance of 1740 m (5572 ft) are listed in Table XXI.

Derivation of the FAA landing distance of 1712 m (5620 ft) is presented in Table XXII. The landing weight of 608 000 kg (1 339 000 lb) corresponds to the aircraft gross weight less one-half of the fuel weight. The landing sequence assumed was a normal instrument final approach on a 0.052 rad (3 deg) glide slope with flaps fully deployed, as per Table XIX. A two-second free roll was assumed after touchdown

85

followed by full braking (friction coefficient of 0.3) with spoilers deployed but no reverse thrust.

The payload and range characteristics of the final configuration are depicted on Figure 52. The "X-point" design mission is 272 155 kg (600 000 lb) payload and a 5560 km (3000 n.mi.) range, while the alternate "Y-point" mission is a 146 000 kg (322 000 lb) payload and a 12 400 km (6700 n.mi.) range. The ferry range of the aircraft is 17 050 km (9200 n.mi.).
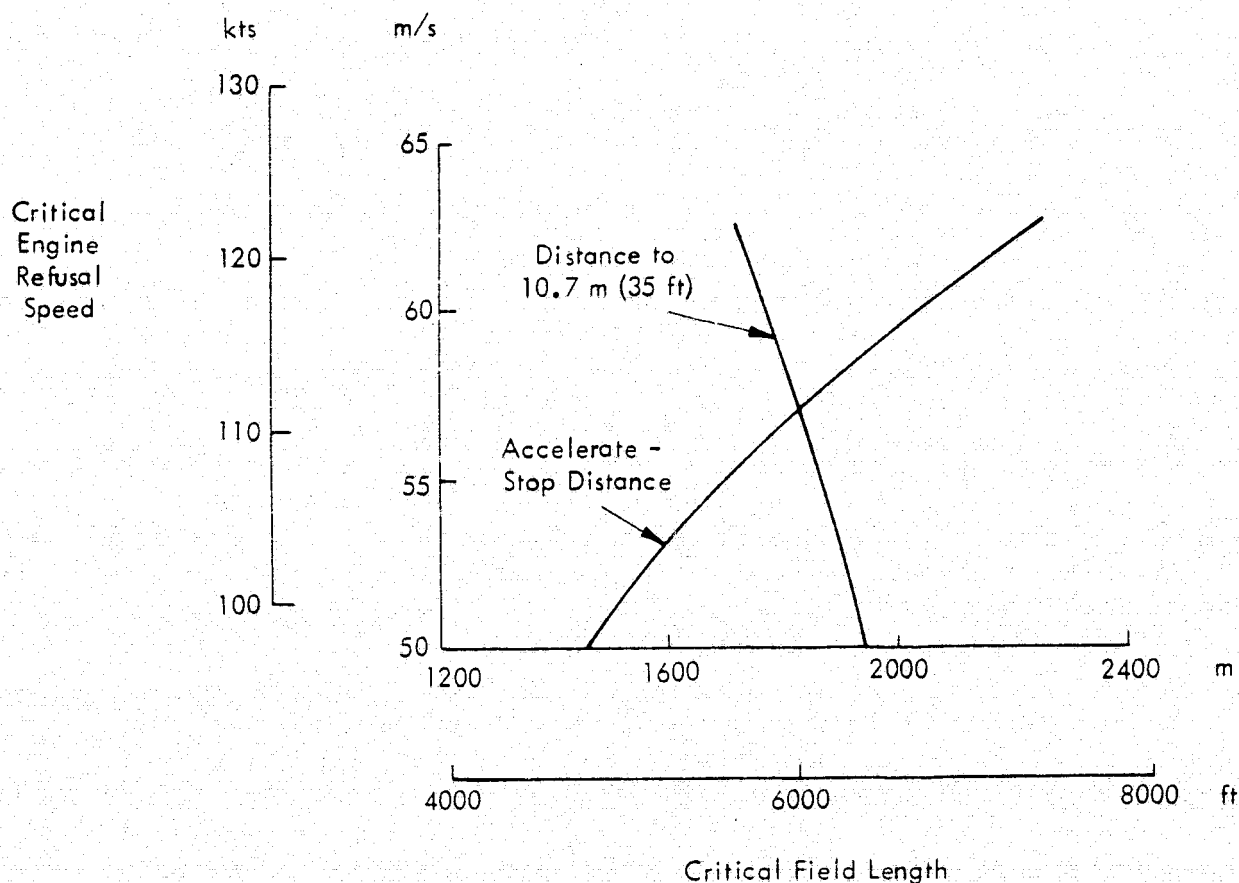
Figure 51. Critical Field Length Determination

TABLE XX. DERIVATION OF ROTATION ANGLES

	Takeoff	Landing
Lift Coefficient with No Rotation	0.4	0.4
Lift-Curve Slope at Effective Aspect Ratio (Free Air)	0.06	0.06
Lift-Curve Slope Corrected for Ground Effect (25% Increase)	0.075	0.075
Lift Increment Due to 0.052 rad (3 deg) Incidence	0.225	0.225
Lift Coefficient in Ground Effect	0.625	0.625
Fore and Aft Flap Deflections, rad (deg)	0.350; 0. _ _ (20; 30)	0.525; 0.700 (30; 40)
Lift Increment Due to Flaps	0.78	0.90
Total Lift Coefficient	1.405	1.545
Lift Required	1.650	1.740
Required Lift Coefficient Increment	0.245	0.195
Required Rotation Angle, rad (deg)	0.058 (3.3)	0.051 (2.9)

TABLE XXI. TAKEOFF DISTANCE DETERMINATION

Maximum Takeoff Lift Coefficient	2.38	
Takeoff Lift Coefficient at 120% Stall Speed	1.65	
Takeoff Weight	700 643 kg	(1 543 266 lb)
Wing Area	1 725 m^2	(18 559 ft^2)
Takeoff Speed	62.5 m s	(122 kts)
Ground Roll Distance	1 410 m	(4 635 ft)
Distance to Climb to 15.2 m (50 ft)	286 m	(937 ft)
Normal Takeoff Distance	1 740 m	(5 572 ft)
Critical Field Length	1 830 m	(6 000 ft)

TABLE XXII. LANDING DISTANCE DETERMINATION

Maximum Landing Lift Coefficient	2.5	
Landing Lift Coefficient at 120% Stall Speed	1.74	
Landing Weight	608 000 kg	(1 339 000 lb)
Landing Speed	57 m/s	(111 kts)
Distance from 15.2 m (50 ft) Obstacle Height to Touchdown	334 m	(1 095 ft)
Distance During 2 Sec. Roll	114 m	(375 ft)
Stopping Distance	581m	(1 902 ft)
Total Distance	1 029 m	(3 372 ft)
FAA Landing Distance (1 0.6 Factor)	1 712 m	(5 620 ft)

Cruise Mach Number: 0.75
Cruise Altitude: 10 670 m (35 000 ft)
Gross Weight: 700 643 kg (1 543 266 lb)
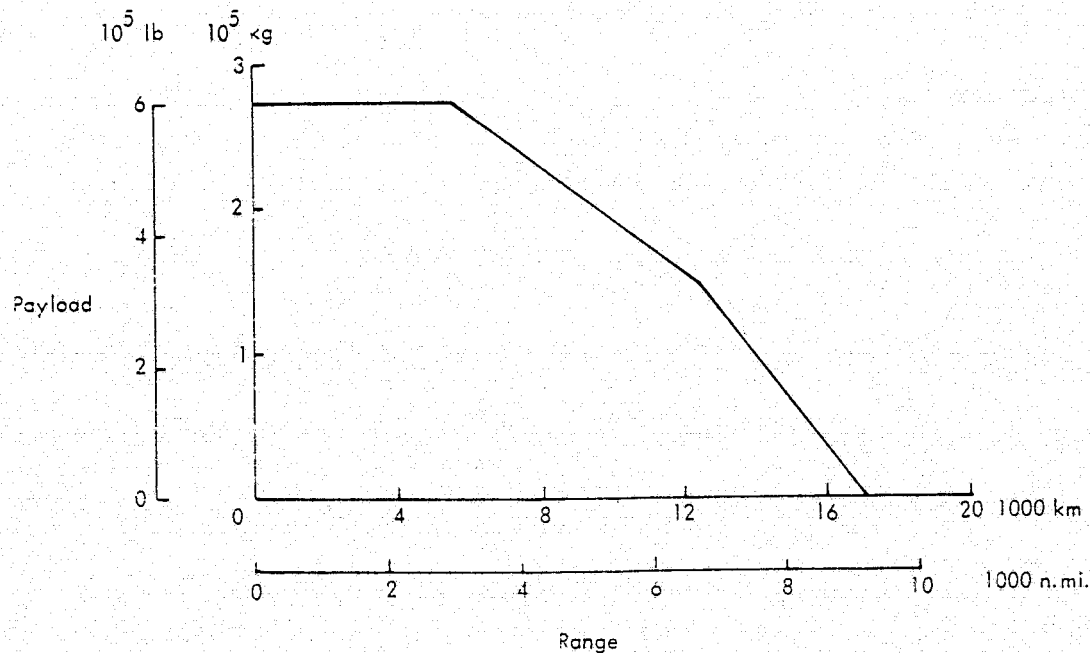
Figure 52. Payload-Range Characteristics of Final Configuration

5.0 ECONOMIC ANALYSES

For the final span-loaded aircraft configuration, studies were performed to evaluate the aircraft costs in January 1975 dollars and to assess cost sensitivities for variations of several cost elements and mission range.

5.1 COST EVALUATIONS

Total acquisition costs for the span-loaded aircraft were determined and depreciated over a 15-year lifetime for inclusion in the estimate of the direct operating cost. Life-cycle costs for the 15-year period were evaluated for the fleet needed to satisfy the annual productivity guideline. Throughout all of the cost studies, the economic guidelines adhered to were those outlined in Section 2.2.

The costing methodology used in previous studies for NASA (Refs. 14 and 15) was modified slightly for application to a span-loaded aircraft concept. The only major change in computer program logic was the addition of a routine for determining the aircraft fleet size to provide the specified annual productivity of 113 billion revenue-ton km (67 billion revenue-ton n.mi.) for the aircraft design speeds and payloads.

Table XXIII contains a listing of the various cost elements and the values that were computed for each in determining the aircraft acquisition cost. All of the manufacturing cost elements and the production cost items are for a single aircraft. The engine cost is for all six engines on the aircraft. In the total program R&D costs listed at the bottom of the table, avionics and engine development costs were not included since they were incorporated with the production costs for these systems. The total program R&D costs were prorated over the total fleet of 216 aircraft, dictated by the productivity requirement, in arriving at the unit aircraft flyaway cost of approximately $134 million.

Preparatory to determining aircraft acquisition prices, labor and material base rates were established for the major structural subsystems. Due to the limited scope of this study, the rates do not include the potential cost savings that may accrue from part commonality for the spanloader concept. The rates do reflect a 60-percent level of composite material in the wing, fuselage, empennage and pylon structural subsystems. Labor and material learning curve slopes were assumed to be 75 and 89 percent, respectively. Profit levels for the engine and airframe manufacturers were assumed to be 12 and 15 percent.

The contribution of the unit aircraft acquisition and spares costs, depreciated over a 15-year time period, is included in the direct operating cost shown in Table XXIV. Values for the various operating cost elements in this table are the total costs experienced while flying the design point 5560 km (3000 n. mi.) mission. Crew cost was based on a crew of 3 persons, and the fuel cost was based on a price of 9.8 ¢/1 (37 ¢/gal). A quick scan of the table data reveals that depreciation and fuel accounted for approximately two-thirds of the direct operating cost of 4.04 ¢/T-km (6.78 ¢/T-n. mi.).

TABLE XXIII. SPAN-LOADED AIRCRAFT ACQUISITION COSTS

MANUFACTURING

Wing	$ 44 093 884
Tail	3 927 779
Body	4 507 423
Landing Gear	1 628 021
Flight Controls	1 363 044
Nacelles	6 071 413
Propulsion	133 193
Instruments	162 356
Hydraulics	312 822
Electrical	310 303
Electronics	169 920
Furnishings	468 101
Air Conditioning	426 131
APU	46 136
Final Assembly	1 658 564
Production Flight	817 203
System Integration	1 014 172
Total Empty Manufacturing Cost	$ 67 110 465

PRODUCTION

Sustaining Engineering	$ 5 144 694
Tooling Maintenance	7 216 863
Quality Assurance	7 393 849
Airframe Warranty	4 334 658
Airframe Fee	13 654 172
Airframe Cost	$104 854 701
Engine Warranty	469 861
Engine Fee	1 184 051
Engine Cost	11 051 141
Avionics Cost	500 000
Research and Development	17 849 298
Total Flyaway Cost	$134 255 140

TOTAL PROGRAM RESEARCH AND DEVELOPMENT

Develop Technical Data	$ 68 670 401
Design Engineering	1 528 442 465
Develop Tooling	1 318 499 755
Develop Test Article	543 196 848
Flight Test	98 449 326
Special Support Equipment	18 312 107
Development Spares	280 046 312
Engine Development	0
Avionics Development	0
Total	$3 855 448 335

TABLE XXIV. SPAN-LOADED AIRCRAFT DIRECT OPERATING COSTS

Item	Cost on 5560 km (3000 n.mi.) Mission
Crew	S 2 681
Fuel & Oil	18 472
Insurance	4 625
Aircraft Labor	962
Aircraft Material	5 448
Engine Labor	720
Engine Material	3 432
Maintenance Burden	3 027
Depreciation (Including Spares)	21 676
Total	S 61 043
Direct Operating Cost	4.04 ¢ T-km (6.78 ¢ T-nm)

5.2 SENSITIVITY STUDIES

Studies were performed to assess the sensitivity of the operating costs to variances in crew size, maintenance costs, aircraft purchase price, fuel cost and mission range. Results of the sensitivity studies for the first four of these variables are presented in Figure 53. The relative effects of each are indicated by the slope of the curves. Clearly, the direct operating cost is most sensitive to purchase price. Maintenance and fuel have similar effects on the operating costs, while the flat slope of the crew-size curve indicates an insignificant influence.

As a variation from the baseline crew size of three, a crew of two was considered. For this reduction in crew size, a 24-percent savings in crew costs was realized. However, the effect on direct operating cost was very minor, providing only a one-percent reduction.

Variations of the baseline maintenance costs by 25 percent were evaluated. A one-percent change in direct operating cost occurred for each 4.4-percent change in maintenance cost. Thus, the direct operating cost would change by 5.68 percent for a 25-percent variation in the baseline maintenance value.

The effect was investigated of 25-percent variations of the baseline purchase price on direct operating cost. This variation affected the four operating cost elements of insurance, depreciation, and maintenance material for both the aircraft and engines.
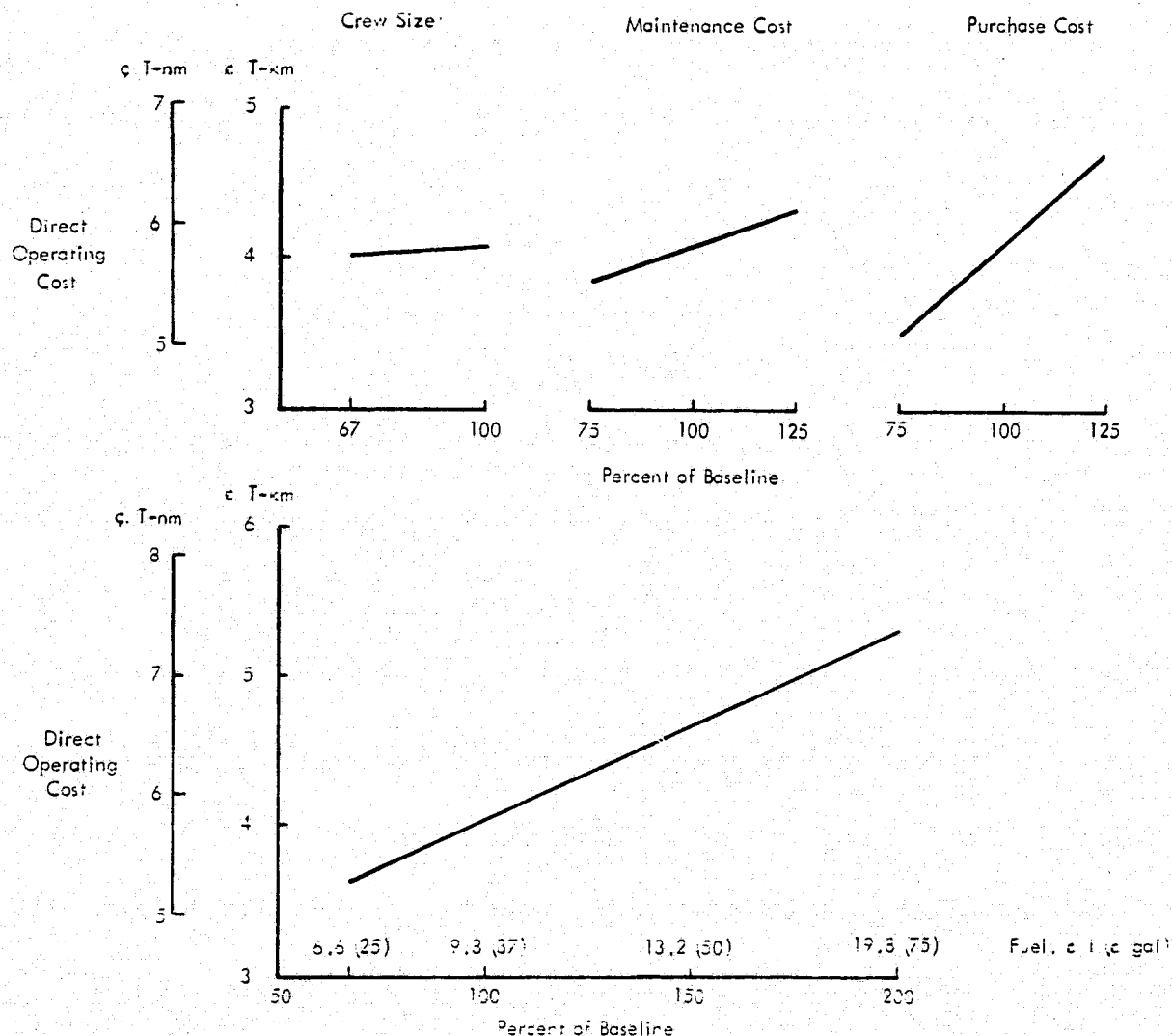
Figure 53. Economic Sensitivity Study Results

For each 1.72-percent change in aircraft purchase price, a one-percent change in operating cost occurred. Correspondingly, a 25-percent change in purchase price produced a 14.55-percent change in direct operating cost.

Fuel prices of 6.6 ¢/1 (25 ¢/gal) and 19.8 ¢/1 (75 ¢/gal) were considered as alternatives to the baseline value of 9.8 ¢/1 (37 ¢/gal). A one-percent variation in direct operating cost resulted for each 3.33-percent change in fuel price.

Figure 54 shows the effect on direct operating cost and productivity from flying the fleet of aircraft at off-design mission ranges. For an 11 120 km (6000 n.mi.) mission, the productivity has declined to less than two-thirds of that for the design mission range since less than the maximum payload can be carried on each trip. As a result of the

decrease in productivity for the off-design ranges, the operating costs increased sub-stantially. Approximately 50-percent greater costs occurred for the 11 120 km (6000 n.mi.) mission than for the design mission.
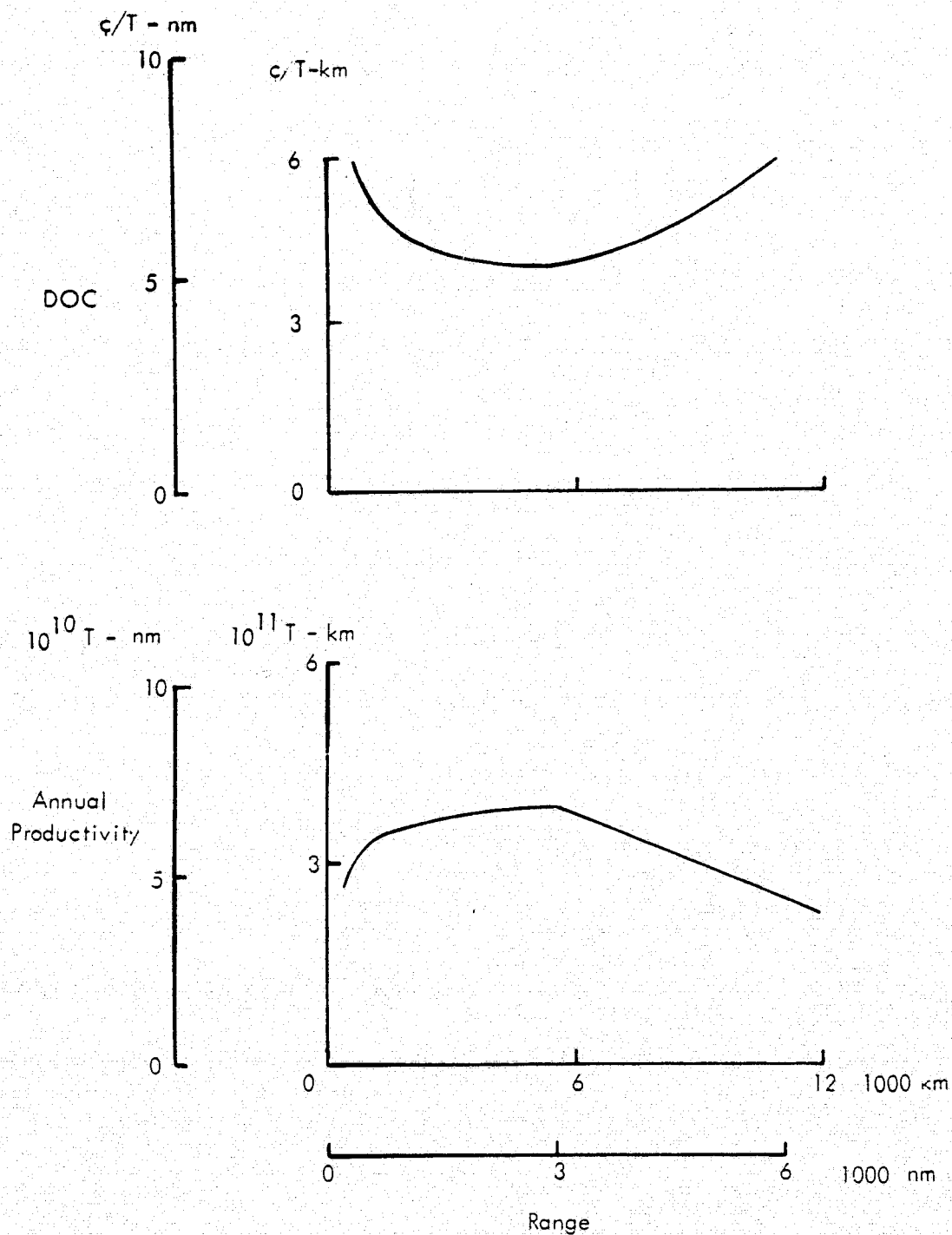
Figure 54. Range Sensitivity Study Results

6.0 COMPARISON OF SPAN-LOADED AND CONVENTIONAL AIRCRAFT

A conventional aircraft design, that is one with the payload carried only in the fuselage, was developed and costed to serve as a basis for assessing the technical and economic feasibility of the span-loaded aircraft. The mission and economic guidelines of Section 2.2 for the span-loaded aircraft were also applied to the conventional aircraft design. Both aircraft have equivalent technology levels, identical cruise speeds and altitudes, and common values for many other characteristics to give as fair a comparison as possible. Details are presented about the conventional aircraft design and the results of the comparison.

6.1 CONVENTIONAL AIRCRAFT CHARACTERISTICS

The fuselage of the conventional aircraft was configured, as shown in Figure 55, to carry the 272 155 kg (600 000 lb) payload in four parallel rows of 2.44 m X 2.44 m (8 ft X 8 ft) containers. At a cargo density of 160 kg/m^3 (10 lb/ft^3), a cargo compartment length of 73.2 m (240 ft) was required. The forward 24.4 m (80 ft) of length of the compartment was sized with a height of 4.1 m (13.5 ft) to accommodate outsized military equipment – consistent with the span-loaded aircraft design. The remainder of the compartment was designed with a height of 2.6 m (8.5 ft) for containers only.
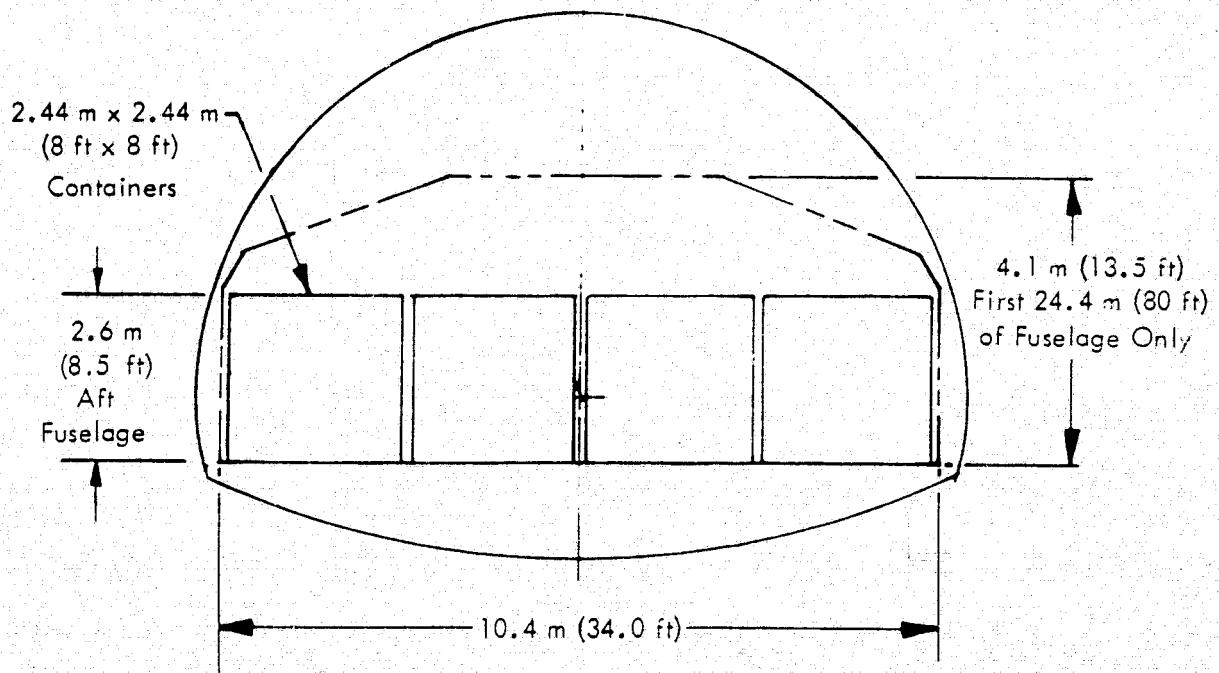
Figure 55. Conventional Aircraft Fuselage Cross-Section

A cruise Mach number of 0.75 and a cruise altitude of 10 670 m (35 000 ft) were chosen for the conventional aircraft to be consistent with the span-loaded aircraft and to provide the same productivity capability with equal fleet sizes. Based on previous experience, a wing sweep angle of 0.35 rad (20 deg) was selected as close to optimum for the cruise conditions. Parametric variations of wing aspect ratio and wing loading were investigated to optimize the conventional aircraft design. The results of the investigation are presented in Figure 56.
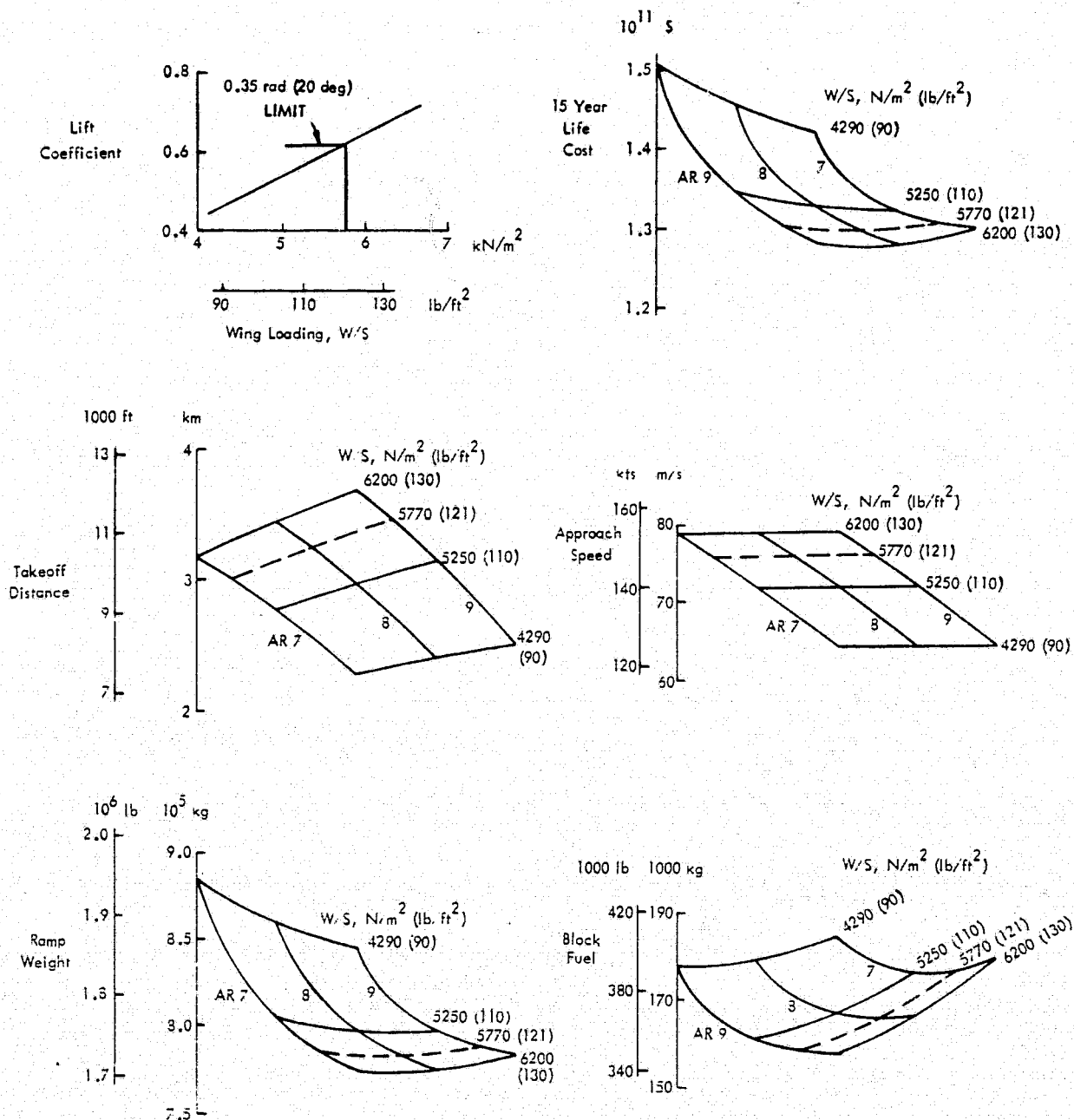
Figure 56. Conventional Aircraft Design Selection

In Section 3.3.3, a relationship was given for estimating the maximum lift coefficient available as a function of wing sweep angle. For the conventional aircraft with a 0.35 rad (20 deg) wing sweep, the maximum lift coefficient value was 0.615. The resulting maximum wing loading of 5770 N/m^2 (121 lb/ft^2) was derived as shown on the first chart on Figure 56. The second chart indicates that the minimum 15-year life-cycle cost aircraft has a wing aspect ratio of 8.5. A check with the next two charts verified that the landing distance and approach speed of the selected design satisfied the study guidelines. The last two charts show the selected design point to be the minimum acceptable gross weight aircraft and close to the minimum acceptable block fuel consumption configuration.

Weights are summarized in Table XXV for the selected conventional aircraft shown in Figure 57. The main landing gear of this aircraft consists of four 8-wheel bogies that have a tread width of approximately 10.7 m (35 ft) and are housed in fuselage-mounted fairings. A forward-retracting 4-wheel nose gear completes the landing system. Six 312 000 N (70 200 lb) thrust engines suspended on pylons beneath the wing provide the propulsion. Acquisition and direct operating costs presented in Tables XXVI and XXVII, respectively, are in the same format and for the same guidelines as for the span-loaded aircraft.

TABLE XXV. CONVENTIONAL AIRCRAFT WEIGHT SUMMARY

	kg	lb
Wing	112 306	247 593
Horizontal Tail	6 032	13 298
Vertical Tail	3 647	8 041
Fuselage	78 422	172 892
Landing Gear	35 848	79 032
Nacelles	12 218	26 936
Propulsion	35 727	78 764
System & Equipment	20 525	45 250
Weight Empty	304 725	671 805
Operating Equipment	9 168	20 213
Operating Weight	313 893	692 019
Payload	272 155	600 000
Zero Fuel Weight	586 048	1 292 019
Fuel	195 113	430 154
Gross Weight	781 161	1 722 173

97
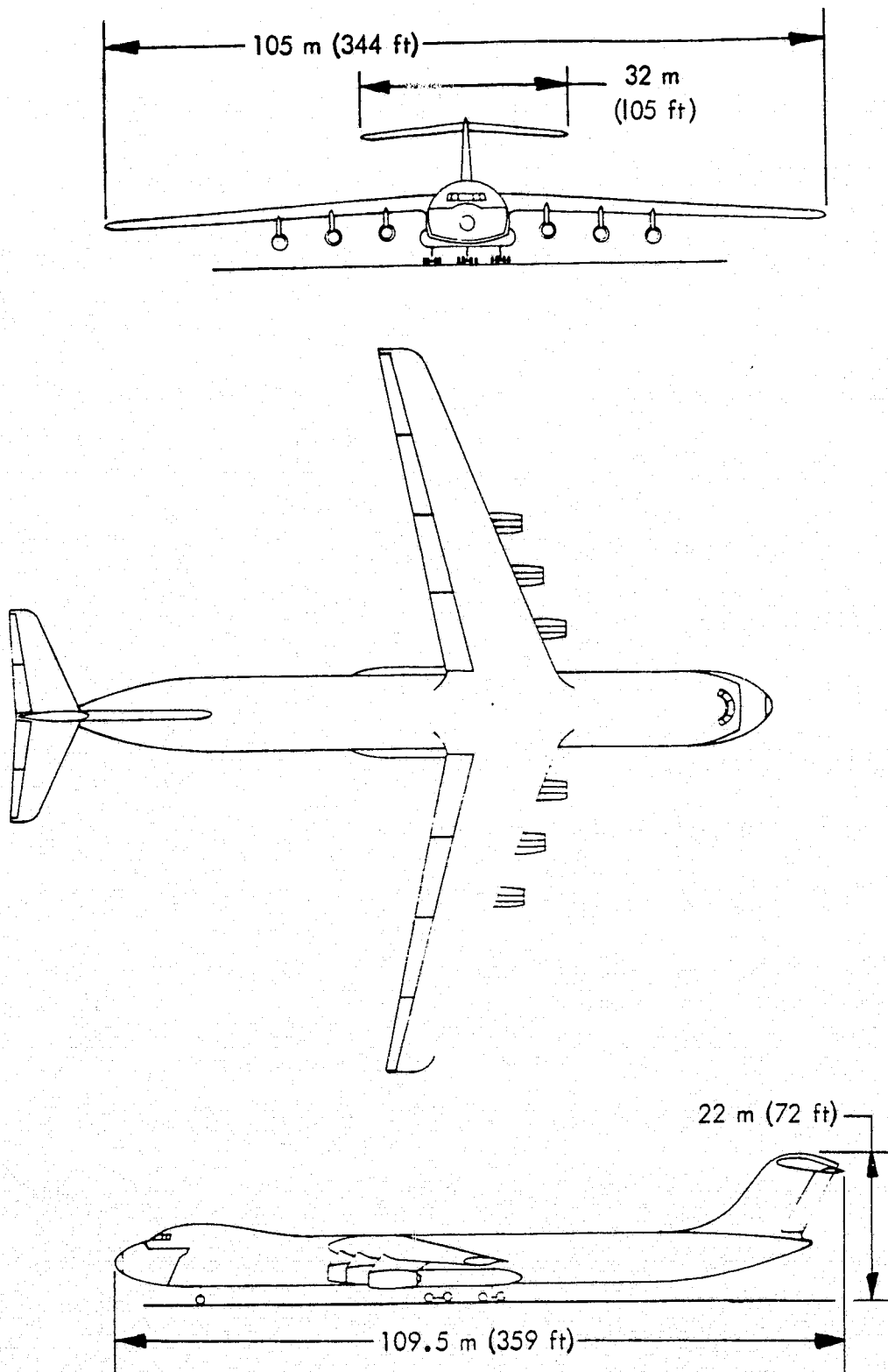
Figure 57. Conventional Aircraft Layout

TABLE XXVI. CONVENTIONAL AIRCRAFT ACQUISITION COSTS

MANUFACTURING

Wing	S 42 484 298	
Tail	2 298 546	
Body	17 170 620	
Landing Gear	1 824 969	
Flight Controls	1 151 407	
Nacelles	6 881 076	
Propulsion	151 345	
Instruments	187 158	
Hydraulics	303 750	
Electrical	337 681	
Electronics	172 615	
Furnishings	512 186	
Air Conditioning	402 289	
APU	50 590	
Final Assembly	2 189 799	
Production Flight	1 091 526	
System Integration	1 336 281	
Total Empty Manufacturing Cost	S 79 176 136	

PRODUCTION

Sustaining Engineering	S 6 214 806	
Tooling Maintenance	8 717 992	
Quality Assurance	8 931 791	
Airframe Warranty	5 143 367	
Airframe Fee	16 201 606	
Airframe Cost		124 385 698
Engine Warranty	509 899	
Engine Fee	1 284 946	11 992 832
Avionics Cost		500 000
Research & Development		19 876 831
Total Flyaway Cost		S 156 755 361

TOTAL PROGRAM RESEARCH AND DEVELOPMENT

Development Technical Data	S 74 693 014
Design Engineering	1 662 717 053
Develop Tooling	1 445 204 468
Develop Test Article	651 182 984
Flight Test	107 478 426
Special Support Equipment	19 918 137
Development Spares	332 201 376
Engine Development	0
Avionics Development	0
Total	S4 293 395 458

TABLE XXVII. CONVENTIONAL AIRCRAFT DIRECT OPERATING COSTS

Item	Cost on 5560 km (3000 n.mi.) Mission
Crew	$ 2 782
Fuel & Oil	20 074
Insurance	5 397
Aircraft Labor	1 190
Aircraft Material	6 399
Engine Labor	774
Engine Material	3 722
Maintenance Burden	3 535
Depreciation (Including Spares)	25 255
Total	$69 128
Direct Operating Cost	4.57 ¢, T - km (7.68 ¢, T - nm)

6.2 AIRCRAFT COMPARISON

Both the span-loaded aircraft and the conventional fuselage-loaded aircraft were designed for the same mission of carrying 272 155 kg (600 000 lb) of payload over a range of 5560 km (3000 n.mi.). Since the cruise speeds and altitudes were the same, both aircraft provided equal productivities in flying the design mission.

Overall dimensions of the two aircraft are similar, as noted in Table XXVIII, with the fuselage-loaded aircraft requiring more terminal area - the product of wing span and overall length. The substantial differences in values for wing thickness ratio and area reflect the different design philosophies for the two concepts. For the fuselage-loaded aircraft, the wing size is optimized for mission fuel and cruise performance. The wing of the span-loaded aircraft is sized to accommodate the cargo.

One of the major disadvantages of the span-loaded aircraft is the large gear tread width required to provide somewhat uniform support during ground operations. The 66.5 m (218 ft) tread width is incompatible with the majority of commercial airports (See Section 3.1.6, 8.0, and Appendix) and will require some redesign with attendant weight penalties.

Weights for the two aircraft are compared in Table XXIX. Similar wing weights were obtained even though the span-loaded aircraft has 34-percent more wing area and is 8-percent thicker. This benefit is the result of lighter structural requirements of the wing for the span-distributed loading concept. With most of the cargo in the wing, the

span-loaded aircraft has a relatively small fuselage. This saved considerable weight and produced a 20.8-percent lower operating weight. Due to the higher lift-to-drag ratio of the conventional aircraft, fuel savings for the span-loaded aircraft amounted to only 8.2 percent. As a final weight comparison, the gross weight of the span-loaded aircraft is 10.4 percent less than that of the conventional aircraft.

TABLE XXVIII. AIRCRAFT GEOMETRY COMPARISON

	Span-Loaded	Fuselage-Loaded
Wing		
Span, m (ft)	101 (331)	105 (344)
Sweep, rad (deg)	0.70 (40)	0.35 (20)
Thickness Ratio	0.218	0.136
Area, m^2 (ft^2)	1 725 (18 559)	1 290 (13 889)
Aspect Ratio	5.9	8.5
Overall Length, m (ft)	90.5 (297)	109.5 (359)
Maximum Height, m (ft)	24.4 (80)	22.0 (72)
Gear Tread Width, m (ft)	66.5 (218)	10.7 (35)

TABLE XXIX. AIRCRAFT WEIGHTS COMPARISON

	Span-Loaded		Fuselage-Loaded	
	kg	lb	kg	lb
Wing	109 594	241 614	112 306	247 593
Operating	248 755	548 409	313 893	692 019
Payload	272 155	600 000	272 155	600 000
Fuel	179 104	394 857	195 113	430 154
Gross	700 014	1 543 266	781 161	1 722 172

A comparison of the performance characteristics listed in Table XXX shows that the fuselage-loaded aircraft enjoys a 2 percent better lift-to-drag ratio as a result of its higher wing aspect ratio and wing loading. Field lengths correspond directly to the wing loadings. Since both aircraft were well below the 3660 m (12 000 ft) runway limit, no additional improvements in field lengths are warranted. The difference in engine thrust levels is basically due to the difference in aircraft gross weight.

Costs for the two aircraft are compared in Table XXXI. The span-loaded aircraft realizes an 8-percent savings in airframe cost due to the lighter structural weight, and

a 14.5-percent lower total aircraft cost. This benefit from the lower aircraft acquisition cost is responsible for the 11.7 percent savings in direct operating cost and life-cycle cost for the span-loaded aircraft.

TABLE XXX. AIRCRAFT PERFORMANCE COMPARISON

	Span-Loaded	Fuselage-Loaded
Cruise Lift Drag Ratio	19.66	20.05
Wing Loading, N/m^2	3 860	5 770
lb/ft^2	81	121
Engine Thrust, N	283 500	312 000
lb	63 800	70 200
FAA Field Length, m	1 830	2 780
ft	6 000	9 135

TABLE XXXI. AIRCRAFT COST COMPARISON

	Span-Loaded	Fuselage-Loaded
Unit Costs, Million $		
Engine	1.34	2.00
Airframe	123.03	144.59
Aircraft	134.08	156.58
DOC, c T-km	4.04	4.57
c T-nm	6.78	7.68
15-Year Life-Cycle Costs, Billion $	114.67	129.95

The span-loaded aircraft has an inherent manufacturing advantage which cannot be quantitatively evaluated until a detailed design is completed. Common rib structure design and material thicknesses for the majority of the wing span will reduce the complexity of manufacture considerably. This factor was not evaluated, but as a conservative estimate, a 10-percent savings in initial acquisition cost is probable.

Three-point loading at the nose and both wingtips is a disadvantage for the span-loaded aircraft because of the additional loading ramps and equipment required. Flexibility

102

of the light wing structure turns out to be a disadvantage during loading operations. Some type of support jacks, either integral with the aircraft or as ground equipment, will be required to hold the outboard wing section rigid.

In summary, the major advantages of the span-loaded aircraft relative to the fuselage-loaded aircraft for the specified mission are:

o   11.7 percent lower direct operating costs and life-cycle costs

o   20.8 percent lighter operating weight, 8.2 percent fuel savings, and 10.4 percent less gross weight

o   Ease of manufacture due to constant wing section design.

Conversely, the major disadvantages are:

o   More difficult loading and additional ground support equipment

o   Incompatible with commercial airport operation due to gear tread width

o   Requires considerably more research and development in structural design and flutter, in thick airfoil aerodynamics, and in handling qualities.

7.0 CONCLUSIONS

For the specified mission to carry a 272 155 kg (600 000 lb) payload over a 5560 km (3000 n.mi.) range, an optimum span-distributed loading aircraft was developed for initial operation in 1995. This aircraft and a competitive conventional fuselage-loaded aircraft were designed with supercritical airfoils, 60-percent levels of composite materials, and high-thrust-level engines. A comparison of these aircraft was performed to assess the technical and economic feasibility of the span-distributed loading aircraft concept. Conclusions reached as a result of the design efforts and subsequent comparison are as follows:

o The span-loaded aircraft offers weight and cost benefits relative to a conventional aircraft. The major weight advantages achieved were: 20.8 percent lighter operating weight; 8.2 percent less fuel consumption; and 10.4 percent lower takeoff gross weight. An 11.7-percent savings was obtained in both direct operating cost and 15-year life-cycle cost.

o Design of a span-loaded aircraft wing experiences more critical conditions due to structural stability than a conventional aircraft wing since minimum gage materials are used in many areas. While it is possible to save considerable structural weight with the distributed load concept, extensive analyses are required to cover all potentially critical load conditions and to assure adequate structural strength and stability. Structural material selection, the mix of materials, and the orientation of composite materials can have a significant effect on the amount of weight saved and on achieving an optimum design to satisfy the various loading conditions.

o The thickness of the wing does not automatically preclude flutter problems nor assure rigidity. With inertia loads nearly balanced by airloads in the span-distributed loading concept, minimum gage materials are used for much of the wing design, resulting in a very flexible structure that is susceptible to flutter. Through proper design layout, flutter problems can be resolved.

o Design of an adequate stability and control system poses no serious problem. The more difficult problem is to establish the handling qualities criteria pertinent to such a large aircraft. This is the subject of one of the recommendations in the next section.

o Pressurization of the entire cargo compartment results in a negligible weight penalty of 0.4 percent of the aircraft gross weight. The insignificant magnitude of this penalty is the result of the pressurization bringing the structural loads up closer to the available strength of the minimum gage materials in most areas, and of making double use of the structure for both bending and pressurization.

o Single-point loading is possible with containers not exceeding 6.1 m (20 ft) in length. For longer containers, the aircraft must be loaded through all three

105

openings - at the nose and at both wingtips. Care must be exercised during the loading to maintain the aircraft center of gravity within limits.

o   As a result of the large tread width for the main landing gear, the current span-loaded aircraft design is not compatible with existing and proposed future commercial airports. This problem could be solved by redesigning the gear and accepting some weight penalty.

o   Additional ground support equipment will be required to compensate for the wing flexibility and the height above the ground and the sweep angle of the wing cargo compartment.

8.0 RECOMMENDATIONS

Before a span-distributed loading aircraft concept can become a reality, considerable research and development effort will be required. System studies are needed to define the design requirements for the aircraft, to determine the optimum configuration characteristics, and to overcome problems uncovered in this study. Continued technology studies are required to advance the state of the art in the areas of aerodynamics, flight controls, structures, propulsion, and noise reduction. Several study recommendations in these areas must be pursued in the near term if the aircraft is to achieve an operational capability by 1995.

The span-loaded aircraft was designed for a 272 155 kg (600 000 lb) payload and used a 60-percent level of composite materials. Parametric studies are recommended to determine if these values are optimum design guidelines. By developing aircraft for payloads of 90 717 kg (200 000 lb) and 181 434 kg (400 000 lb), with all other guidelines unchanged, it is expected that the optimum design payload can be defined to minimize life-cycle cost for the specified productivity. The 60-percent level of composites was defined as optimum for a conventional passenger transport (Ref. 1). Lower weight savings are realized per unit cost for composites on a span-loaded aircraft since the wing design cannot be optimized as for a conventional aircraft. Aircraft designed for the same study guidelines but with composite levels of 0, 20, and 40 percent are expected to provide sufficient data to define the optimum composite material level to minimize life-cycle costs.

The loading analysis summarized in Figure 36 showed the effect of fuselage cargo on wing bending moments. The large moments resulting from the fuselage and outsized-equipment transport capability are responsible for sizeable structural weight and cost penalties. A study is recommended to determine if there is sufficient demand to transport outsized cargo to justify designing a span-loaded aircraft to accommodate it. While the outsized-cargo-carrying fuselage is recognized to impose penalties on the aircraft, the magnitude of these penalties is unknown. A study is recommended to determine the effect of the fuselage on optimizing the aircraft design. For a fair comparison, all other study ground rules should be maintained. With all of the cargo carried in the wing, full advantage of the distributed-loading concept can be realized and a different optimum configuration may result.

The aircraft main landing gear tread width of 66.5 m (218 ft) negates, for all practical purposes, its operation at all commercial airports in the U.S. Both the runways and taxiways at existing airports will have to be widened before they can handle the current span-loaded aircraft. Since the airlines pay for such improvements to airports, the improvement cost must be included when determining the total cost of the aircraft to the airlines – an economic disadvantage for the aircraft. The only apparent alternative, which is recommended, is to reoptimize the aircraft design subject to an airport compatible constraint on gear tread width.

107

Brief investigations have indicated that potential problem areas exist in the design and operation of on-board cargo loading and restraint systems. Both static and dynamic wing bending are areas of concern in relationship to the loading/restraint system, the wing cargo compartment structural envelope, and the effect on the cargo container. Studies are also recommended to address the problems of maintaining the cargo floor at a fixed level in the vicinity of the cargo doors, of being compatible with the multi-point loading characteristic of the airplane, and of interfacing with existing cargo docks and facilities. Part of the cargo loading problem is the height of the cargo floor above the ground. To alleviate this problem, consideration should be given to relocating the engines above the wing, thereby permitting a drop in the cargo floor height.

Considerable analytical and experimental efforts are needed to establish a data base on thick supercritical airfoils and to develop the aerodynamic characteristics of the aircraft. Studies are recommended to define the overall requirements for load alleviation, active controls, and high lift systems. A multi-segment flap system will be needed to tailor the lift distribution along the wing span. Wind-tunnel tests of the complete configuration, including the control surfaces, in both high and low-speed regimes will be required to confirm system performance evaluations.

Because of the size, weight, inertia distribution, and types of controls, current aircraft flying qualities criteria will probably not be adequate or applicable for a span-loaded aircraft. It is suggested that the C-5 criteria studies be extended to encompass the peculiarities of span-distributed loading concept configurations. Particular attention should be directed toward the high yaw and roll moments of inertia and toward the responses of the aircraft to conventional and non-conventional types of control. A preliminary analytical study is recommended to establish flying qualities criteria which would be correlated with previous large aircraft flight-test experiences. Subsequently, further validation would be recommended using ground-based simulators.

Studies are recommended to determine the effects of non-uniform cargo density and various internal load distributions on wing structural design and flutter. Thus far, only uniform cargo density and a limited number of cargo distributions have been considered in the design of the wing structure. In the area of flutter, only the zero fuel and payload case was considered. It is suggested that other potentially critical flutter cases be investigated to establish the most flutter critical fuel and cargo loading conditions. Part of the study should include a systematic investigation of the most promising passive means of increasing flutter speed and an evaluation of the benefits from active flutter-suppression concepts.

Two potential problem areas that require investigation are the result of the engine locations beneath the wing. One of these concerns the guideline which specifies an engine-ground clearance of one engine diameter to prevent foreign object ingestion and damage. Extension of the guideline to engines of the size on the span-loaded aircraft requires validation. The second area of concern is the interference drag between the

wing lower surface and the nacelle afterbody. Critical flow, including shocks and separation, may occur and result in premature drag rise. An alternative of relocating the engines above the wing, as suggested earlier, would remove these potential problems.

Noise certification and community noise analysis studies need to be performed for the aircraft consistent with recent developments in the aero-acoustic technical and regulatory fields. This study should attempt to identify the nacelle acoustic design requirements for compliance with applicable regulations anticipated for the 1990 time period. Further, the airframe noise minimum should be investigated, and the impact of applying the results from the NASA/GE quiet engine program should be assessed. Part of the end result should be nacelle acoustic designs and acoustic footprints for takeoff and landing.

REFERENCES

1. Lange, R. H., et al, "Study of the Application of Advanced Technologies to Long-Range Transport Aircraft," NASA CR-112088, Lockheed-Georgia Company, May 1972.

2. Lange, R.H., and Lassiter, L. W., "Advanced Structural Material Applications for High-Subsonic-Speed Transports," SAE Paper Number 73-0887, October 1973.

3. Lange, R.H., and Deets, D. A., "Study of an ACT Demonstrator with Substantial Performance Improvements Using Redesigned JetStar," Paper presented at NASA Symposium on Advanced Control Technology and Its Potential for Future Transport Aircraft, Los Angeles, California, July 1974.

4. Cleveland, F. A., "Size Effects in Conventional Aircraft Design," AIAA Journal of Aircraft, Volume 7, Number 6, November-December 1970.

5. Hurkamp, C. H., et al, "A Preliminary Investigation of the 'Spanloader' Advanced Heavy Logistics Aircraft Concept," ER-10497, Lockheed-Georgia Company, March 1970.

6. Sturgeon, R. F., "The Spanloader Advanced Capability Transport Concept," PDP-96, Lockheed-Georgia Company, January 1974.

7. "Technical and Economic Assessment of Span-Distributed Loading Cargo Aircraft Concepts," RFP 1-16-5603, NASA Langley Research Center, March 1975.

8. "Airport Design Standards - Airports Served by Air Carriers - Taxiways," AC 150/5335-1A, Federal Aviation Administration, Department of Transportation, May 1970.

9. Hoerner, S. F., "Fluid-Dynamic Drag," Published by the Author, 1958.

10. "Airworthiness Standards: Transport Category Airplanes," Federal Aviation Regulations, Part 25 (FAR 25), Federal Aviation Administration, 1974.

11. "Noise Standards: Aircraft Type and Airworthiness Certificate," Federal Aviation Regulations, Part 36 (FAR 36), Federal Aviation Administration, 1974.

12. "Flying Qualities of Piloted Airplanes," Military Specification MIL-F-8785B (ASG), 1969.

13. "Certification and Operations: Domestic, Flag and Supplemental Air Carriers and Commercial Operators of Large Aircraft," Federal Aviation Regulations, Part 121 (FAR 121), 1974.

14. Brewer, G. D., Moore, J. W., et al, "Study of the Application of Hydrogen Fuel to Long-Range Subsonic Transport Aircraft," NASA CR-132559, Lockheed Aircraft Corporation, 1975.

15. Sturgeon, R. F., et al, "Study of the Application of Advanced Technologies to Laminar Flow Control Systems for Subsonic Transports," NASA CR-133949, Lockheed-Georgia Company, 1976.

APPENDIX

Data for all airfields in the United States were examined to determine their suitability for a span-loaded aircraft operation. From this data review, the listing in Table XXXII was made of those sites with runways at least 61 m (200 ft) wide and 1830 m (6000 ft) long. Since the aircraft is intended for commercial operation, airports which handle only military traffic were excluded.

The study guidelines specified that the aircraft be able to operate out of 3660 m (12 000 ft) runways. The final aircraft design was found to have a standard day critical field length of 1830 m (6000 ft). On hot days, the field length would be longer, probably in the 2440 m (8000 ft) category.

The gear tread width of 66.5 m (218 ft) for the span-loaded aircraft limits its operation to those airports with runways 91.5 m (300 ft) wide. From the data in the table, there are only eight airports in the United States with runways of adequate width and at least 2440 m (8000 ft) long. Of these, only three airports qualify as gateway or commercial center airports that would use large cargo aircraft, and they are located in Walla Walla and Grant County, Washington, and in Bangor, Maine. In reality, only one of the two locations in Washington would be used due to their close proximity. Thus, the number of airports available for the practical use of a span-loaded aircraft is limited to two.

TABLE XXXII. RUNWAY CHARACTERISTICS OF POTENTIALLY APPLICABLE U. S. AIRPORTS

Airport	Length		Width	
	m	ft	m	ft
1830 - 2438 m (6000 - 8000 ft) Long Category				
Arcadiana, La.	2438	8000	61	200
Cleveland Hopkins, Ohio	1903	6242	61	200
Deland Municipal, Fla.	1832	6005	61	200
Grumman Bethpage, N. Y.	2112	6600	61	200
Hutchinson, Kan.	2134	7000	61	200
Lake City, Fla.	1903	6243	61	200
Bedford Hanscom, Mass.	2134	7000	61	200
NASA Wallops Sta., Va.	2438	8000	61	200
New Hanover Co., N. C.	2438	8000	61	200
Opa Locka, Fla.	2438	8000	61	200
Pendleton, Ore.	1919	6296	61	200
Port Isabel, Tex.	2438	8000	61	200
Sanford, Fla.	2438	8000	61	200
Shreveport, La.	2225	7300	61	200
Vero Beach, Fla.	2188	7180	61	200
Walla Walla, Wash.	2191	7188	91	300
2438 - 3048 (8000 - 10 000 ft) Long Category				
Baltimore - Wash., Md.	2880	9 450	61	200
Boeing Field Int., Wash.	3048	10 000	61	200
Boise Air Term., Ida.	2975	9 763	61	200
Bradley Int., Conn.	2896	9 500	67	220
Charleston, S.C.	2743	9 000	61	200
General Mitchell Field, Wisc.	3028	9 912	61	200
Harrisburg Int., Pa.	2900	9 510	61	200
Long Beach, Calif.	3048	10 000	61	200
Minn. - St. Paul, Minn.	3048	10 000	61	200
Mobile Aerospace, Ala.	2926	9 600	61	200
Mojave, Calif.	3008	9 870	61	200
Atlantic City NAFEC, N. J.	3048	10 000	61	200
Pocatello, Ida.	2514	8 249	91	300
Snohomish Co., Wash.	2746	9 010	61	200
Tulsa Int., Okla.	3048	10 000	61	200
3048 - 3657 m (10 000 - 12 000 ft) Long Category				
Anchorage, Alas.	3231	10 600	61	200
Bangor Int., Me.	3486	11 438	91	300
Chicago - O'Hare, Ill.	3535	11 600	61	200
Dallas-Fort Worth, Tex.	3470	11 387	61	200
Detroit-Wayne Co., Mich.	3200	10 500	61	200
Los Angeles Int., Calif.	3658	12 000	61	200
Philadelphia Int., Pa.	3200	10 500	61	200
St. Louis (Lambert), Mo.	3053	10 018	61	200
San Francisco Int., Calif.	3230	10 600	61	200
Greater than 3657 m (12 000 ft) Long Category				
Albuquerque, N. Mex.	4076	13 373	91	300
Amarillo Air Terminal, Tex.	4115	13 500	91	300
Honolulu (Hickam), Hi.	3770	12 371	61	200
Lincoln Municipal, Neb.	3932	12 900	61	200
Moses Lake (Grant Co.), Wash.	4115	13 500	91	300
Roswell, N. Mex.	3962	13 000	91	300
Salina Municipal, Kan.	4065	13 331	91	300
Yuma Int., Ariz.	4053	13 300	61	200